

**Pilus biogenesis in uropathogenic *Escherichia coli*: An
electrophysiology study on the PapC usher**

**A Dissertation Presented to
the Faculty of the Department of Biology and Biochemistry
University of Houston**

**In Partial Fulfillment of the Requirements for the Degree
Doctor of Philosophy**

**By
Owen S Mapingire
December 2012**

Pilus biogenesis in uropathogenic *Escherichia coli*:

An electrophysiology study on the PapC usher

Owen S Mappingire

APPROVED:

Dr. Anne Delcour, Chairperson

Dr. Peter Christie

Dr. Hye-Jeong Yeo

Dr. Stuart Dryer

Dr. Mark A. Smith, Dean

College of Natural Sciences and Mathematics

Acknowledgements

First of all let me start by thanking the almighty, **God**, for blessing me with this opportunity and the ability to engage successfully in this intellectual exercise. Let glory be given unto him.

This dissertation is dedicated to my parents; Robert Mapingire and Violet Abraham. They are the ones who inspired my love for study and kept me motivated through all my academic endeavors. I would not be who I am today without their long term unconditional support. I would also like thank all my family, back home in Zimbabwe, for all your thoughts and prayers throughout the last five years. Even though we have been separated by distance, I still remain as close as ever to you all. Special mention to my Grandma and Grandpa; “Mbuya Amai” and “Sekuru Baba”, you were always the stalwarts in my life since birth. Much thanks as well to my special aunt, “Mai nini Mai Blessing”. I will never forget her contributions in supporting my education and development.

I also owe a debt of gratitude to all my friends who have been my family away from home. Each and every one of you has been there for me in times of need and beyond. I say “tatenda” to the following; Gerald and Siria, Ralph and Sana, Victor, Frank, Norbert, Tinashe, Justice, Monty, and the rest of my Houston Zimbabwean family. Let me also take this opportunity to thank all the special people I’ve become friends with since my arrival in Houston, TX; Jennifer, Lucy, Guillaume, Rolf, Eylem, Heather, Kiko, Danny, and many others who have touched my life.

Lastly, let me thank my advisor, Dr Anne Delcour for recruiting me all the way from Zimbabwe and for the excellent mentorship she has given me over the last five years. Special mention also goes out to our outstanding collaborators from Stony Brook University; Dr David Thanassi and Nadine Henderson. This whole project would not have been possible without your partnership. I would also like to thank Karen Dodson and Scott Hultgren for their collaboration. To my thesis committee members; Dr Peter Christie, Dr Stuart Dryer, and Dr Hye-Jeong Yeo I am appreciative of the constructive critique and insightful advice you provided throughout all our meetings.

**Pilus biogenesis in uropathogenic *Escherichia coli*: An
electrophysiology study on the PapC usher**

An Abstract of a Dissertation

Presented to

the Faculty of the Department of Biology and Biochemistry

University of Houston

In Partial Fulfillment of the Requirements for the Degree

Doctor of Philosophy

By

Owen S Mapingire

December 2012

Abstract

Uropathogenic *Escherichia coli* are the main causal agents of urinary tract infections. Pili are bacterial surface adhesive organelles that are critical virulence factors in the successful colonization of the urinary tract by uropathogenic *E. coli*. Pili are composite in structure and are formed from the polymerization of different subunits. The chaperone/usher pathway is a bi-component secretion system that is dedicated to the biogenesis and export of pili to the cell surface. It is comprised up of a periplasmic chaperone protein and an outer membrane usher protein that functions as the site of pilus assembly and simultaneous translocation. The usher exists as a dimer, where each monomer consists of a gated β -barrel pore with several domains.

To shed insight into the mechanistic details behind pilus biogenesis we instituted the first electrophysiology study on the PapC usher channel. In this dissertation we present data on the pore properties of the PapC usher. Using planar lipid bilayer technique we found that PapC forms an ion conducting channel that is mostly in a closed state. However, the usher channel is dynamic and transiently opens to various conductance levels. A structure function relationship study was applied to investigate the roles of the α -helix, plug, N- and C-terminal domains on the usher channel behavior. Domain deletion mutants characterized using planar lipid bilayer showed the modulating effects of the α -helix, plug, N- and C-terminal domains on the usher channel behavior. In contrast to the wild type, domain deletion mutants displayed open channel behavior that was marked by frequent closing transitions. The Δ plug mutant formed a channel with an extremely large conductance indicating that the plug domain gates the usher closed and its removal

creates a large pore. Single site substitution of the D234 residue resulted in an open channel as well, indicating the D234 residue plays a role in plug displacement. Following characterization of the usher, we investigated the modulatory effect of chaperone – subunit complexes on the usher channel behavior. We attained inconclusive results and found no clear-cut discernible effect on the usher channel behavior by the chaperone subunit complexes in the various assays reported in this dissertation. However, these results set the stage for more work on the modulation of the usher by substrates.

Table of Contents

Acknowledgements.....	iii
Abstract	vi
Abbreviations.....	xi
Chapter 1: Introduction	1
1.1 Urinary tract infection and etiology.....	2
1.1.1 Uropathogenic <i>Escherichia coli</i>	3
1.1.2 Disease pathology	4
1.1.3 Host response and UPEC cell invasion.....	7
1.1.4 Type 1 and P pilus.....	9
1.2 Cell envelope of the Gram negative bacteria.....	12
1.3 Secretion systems in Gram negative bacteria	15
1.3.1 The Sec pathway.....	16
1.3.2 Type 1 Secretion System	17
1.3.3 Type 2 Secretion System	17
1.3.4 Type 3 Secretion System	18
1.3.5 Type 4 Secretion System	18
1.3.6 Type 5 Secretion System	19
1.4 Chaperone/usher pathway.....	20
1.4.1 Chaperone	21
1.4.2 Usher.....	21
1.4.3 Pilus assembly.....	23
1.5 Electrophysiology of translocons.....	28

1.6 Scope of dissertation	30
Chapter 2: Materials and methods	33
2.1 Protein expression and purification	34
2.1.1 Strains and plasmids	34
2.1.2 Fraction isolation and protein extraction	36
2.1.3 Chromatography	37
2.2 Electrophysiology experiments.....	38
2.2.1 Planar lipid bilayer.....	38
2.2.2 Patch Clamp	41
2.2.3 Data acquisition and analysis.....	44
Chapter 3: Modulating effects of the Plug, Helix, N- and C- terminal domains on the PapC usher	46
3.1 Introduction.....	47
3.2 Results.....	49
3.2.1 PapC WT and domain deletion mutants form ion conducting channels.....	49
3.2.2 PapC WT forms a closed, but dynamic channel.....	53
3.2.3 PapC Δ plug forms an open channel with extremely high conductance.....	58
3.2.4 PapC Δ helix forms a lower conductance open channel.....	62
3.2.5 The Δ N Δ C mutant is also an open channel.....	67
3.3 Discussion.....	71
Chapter 4: Site-directed cysteine substitution mutants shed insight on the mechanism of plug dislocation	77
4.1 Introduction.....	78
4.2 Results.....	82

4.2.1 PapC D234C/Y329C displays open channel behavior	82
4.2.2 Single Cys mutants reveal D234 mutation alone contributes to the D234C/Y329C open behavior.....	87
4.2.3 The P292C/S525C mutant shows a behavior similar to WT	93
4.3 Discussion.....	97
Chapter 5: Modulation of the usher channel by chaperone-subunit complexes.....	104
5.1 Introduction.....	105
5.2 Results.....	107
5.2.1 PapDG chaperone subunit complex does not display modulating effect on PapC usher channel behavior.....	107
5.2.2 Addition of PapD/G, F, E, K, A chaperone-subunit complexes does not display a modulating effect on the usher channel behavior	111
5.2.3 FimCH and FimCG chaperone – subunits do not show modulation effect on the FimD usher channel	115
5.3 Discussion.....	120
Chapter 6: Concluding remarks.....	124
References	130

List of Abbreviations

ABC: ATP binding cassette	AT: autotransporter
CTD: C-terminal domain	CU: chaperone/usher
DSC: donor strand complementation	DSE: donor strand exchange
DTT: Dithiothreitol	EM: electron microscopy
GI: gastrointestinal tract	IBC: intracellular bacterial communities
IM: inner membrane	IPTG: Isopropyl β -D-1-thiogalactopyranoside
I-V: current-voltage	Kd: dissociation constant
LB: Luria-Bertani	LPS: lipopolysaccharides
NTD: N-terminal	OM: outer membrane
OMPs: outer membrane proteins	TPS: two partner secretion
T1SS: type 1 Secretion System	T2SS: type 2 Secretion System
T3SS: type 3 Secretion System	T4SS: type 4 Secretion System
T5SS: type 5 Secretion System	UPEC: uropathogenic <i>Escherichia coli</i>
UTI: urinary tract infections	VMD: visual molecular dynamics
WT: wild type	

Chapter 1

Introduction

1.1 Urinary Tract Infections and Etiology

The human urinary tract is generally considered to be a sterile environment in normal and healthy individuals. The shear force of urine flow, coupled with an assortment of innate host immune strategies such as secreted tissue associated antibacterial molecules and immune cells, contribute to keep the urinary tract void of pathogens [1-6]. Despite this arsenal of defense strategies, urinary tract infections [7] have established themselves as one of the most common infectious diseases in humans [7]. Epidemiological studies have revealed how the disease disproportionately affects women and elderly men [8]. Women are particularly infected. In the US alone, it has been estimated that 60% of all women will experience a urinary tract infection (UTI) at least once in their lifetime, with 25% of those suffering from relapsing infections [1, 9, 10]. These infections translate into a significant economic impact, where an estimated 8 million outpatient hospital visits are made, costing in excess of \$2 billion in healthcare costs annually [11, 12].

The etiology of UTIs is characterized by a variety of bacterial pathogens. Infections have been attributed to the *Klebsiella* spp, *Proteus* spp, *Enterobacter* spp, *Citrobacter* spp, *Staphylococcus aureus*, coagulase-negative *Staphylococcus*, and *Enterococci*, but strains of the uropathogenic *Escherichia coli* (UPEC) [7] are the major etiological agent of UTIs [13]. Studies show UPEC account for up 95% of community acquired infections and are the causal agents in 50% of hospital acquired infections, with most nosocomial infections arising from urethral catheterization [10, 13, 14].

1.1.1 Uropathogenic *Escherichia coli*

UPEC strains are believed to have a gastrointestinal (GI) tract origin, where they start off as commensal *E. coli* strains that colonize the gut in the immediate aftermath from birth. These commensal *E. coli* strains have a symbiotic relationship with their host and pose no disease threat. Instead, they promote stability of the native microbial flora – preventing GI tract infection with foreign pathogens. They also regulate an array of critical host processes such as nutrition, intestinal tissue development and maturation in newborns and elicit host immune responses that impact disease susceptibility and the overall health of the GI tract [7, 15]. With time, some of these commensal *E. coli* can diverge into more pathogenic strains via horizontal gene transfer of transposons, plasmids, bacteriophages and mobile genetic elements such as pathogenicity islands. These new genes can confer virulence and the adaptive capacity to colonize new anatomical niches and cause disease [7, 16, 17]

E. coli pathogenic strains are broadly classified as either enteric/diarrheagenic *E. coli* or extraintestinal pathogenic *E. coli* [1, 7]. These broad classes are further grouped into “pathotypes”, with each pathotype representing a group of strains that share the same virulence factors and elicit similar pathogenic outcomes in their host. [18]. Examples of these diarrheagenic pathotypes that are causal agents of various enteric diseases, include enteropathogenic *E. coli*, enterohemorrhagic *E. coli*, enterotoxigenic *E. coli*, enteroaggregative *E. coli*, enteroinvasive *E. coli*, and diffusely adherent *E. coli* [19]. Most pathotypes of diarrheagenic *E. coli* are limited to their niche and it is atypical for them to cause disease outside the GI tract [19].

There are two pathotypes in the extraintestinal pathogenic *E. coli*. These are the neonatal meningitis *E. coli* and the UPEC that cause infections of the bladder and kidneys. The primary reservoir of UPEC is proposed to be within the gut. Using chromosomal restriction fragment length polymorphism (RFLP), comparison of samples of recurring UTI isolates from infected women and fecal isolates from the same individual showed similar profiles [20], thereby entailing UPEC ascend from the rectum into the urinary tract. Thus, despite the contribution of other behavioral and genetic factors [21], the principal cause for the enhanced UTI susceptibility in women is the close proximity of the female urogenitalia to the bacterial reservoirs in the rectum. In addition, compared to men, their shorter urethra provides a more conducive bridge for bowel originating pathogens to quickly ascend into the bladder before been washed out by the protective action of urine voidance [22].

1.1.2 Disease pathology

The site of infections is typically used to classify UTIs. Bladder infections are deemed as lower tract infections that lead to the cystitis syndrome. Kidney infections are considered upper tract infections and referred to as pyelonephritis. UPEC in the urine is referred to as bacteriuria and can be asymptomatic [12]. Typically patients with asymptomatic bacteriuria (ABU) do not require treatment, and the presence of these urine colonizing UPECs may prevent the incidence of more virulent UPEC [23-25]. Symptomatic and more virulent strains ascend towards the bladder and cause cystitis. In most cases, cystitis is an uncomplicated infection in normal individuals [26]. Mild symptoms accompanied with these infections include frequent urination, pain or a

burning sensation during urination, and suprapubic pain. Among normal and healthy persons, 95% of all UTIs are these uncomplicated bladder infections. Nevertheless, UPEC can further ascend into the kidneys via the ureters to cause pyelonephritis. Pyelonephritis is a more serious condition with the potential to cause irreversible kidney damage [11]. The symptoms are more severe and include chills, high fever, nausea, joint and muscle aches, and side pains. If the condition is left untreated pyelonephritis can progress into renal failure, bacteraemia and sepsis, which can result in death [19].

An understanding of why ABU infections do not progress into discernible symptoms still remains an open question. However, one important observation is the lack of adherent and hemolytic virulence factors in isolated ABU strains [7]. In one enlightening study, a strain (*E. coli* 83972) isolated from a 3-year carrier ABU patient showed that it had no ability to express functional P and type 1 fimbriae/pili [27-29]. P and type 1 pili are the adhesive extracellular organelles that mediate bacterial cell attachment to host epithelial lining in the kidney or bladder, respectively [30]. The lack of adherence capacity allows the host to rid itself of the bacteria invading its tract during urination, thus establishing P and type 1 pili as critical virulence factors in the infection of the urinary tract.

In order to colonize and persist within the urinary tract, UPEC strains must employ a variety of virulence factors that allows them to overcome highly effective host defense mechanisms [7]. UPEC isolates show evidence of high genetic diversity primarily because of specialized virulence genes that are located on mobile genetic entities termed pathogenicity islands [7, 19]. Virulence factors of UPEC can be broadly classified into two groups, the cell surface virulence factors and virulence factors that are secreted to

their site of action [31]. Surface virulence factors include the adhesive organelles called pili/fimbriae that extend from the microbial surface and mediate attachment to the host uroepithelial surface. Various types of pili such as the S-pili, Dr family adhesins, P pili, and Type 1 pili are associated with UPECs [30]. The expression and presentation of these pili to the bacterial surface is the most cardinal determinant for pathogenicity [7] and the type of pili expressed onto the microbial surface dictates the site of infection in the urinary tract.

Type 1 pili found in most UPEC isolates are ubiquitous among both pathogenic and non-pathogenic commensal *E. coli* [32]. As a result of this, earlier studies cast some doubt on the pathogenicity relevance of type 1 pili, as they found no significant difference in *fim* genes (which code for type 1 pili) frequency between virulent and avirulent strains. However, later studies portrayed a pre-eminent pathogenic role, where type 1 pili were shown to initiate attachment to uroepithelial cells and elicit host immune response that results in subsequent internalization of UPEC, transforming them from extracellular to intracellular pathogens [33]. Type 1 pili are more common than P pili and are found in most UPEC isolates [34] and are expressed in 95 % of pathogenic and commensal *E. coli*. As such, type 1 pili appear to be less restricted than P pili in the sites where they mediate infection. In fact co-expression of P and type 1 pili occurs at a higher incidence in patients with pyelonephritis than it does for patients with cystitis [35, 36]. Type 1 pili have an adhesin molecule that binds to mannose containing glycoprotein receptors on a variety of host cells [37] but mostly on bladder uroepithelial cells [33, 34]. P pili which are more restricted to pyelonephritis UPEC isolates bind to the α -D-galactopyranosyl-1-4- β -D galactopyranoside (Gal α (1-4)Gal) moieties found in

glycolipid receptors present on kidney epithelia cells [8]. Unlike with cystitis, P pili are statistically the major virulence factor associated with pyelonephritis in UPEC [38].

1.1.3 Host response and UPEC cell invasion

The acquisition of virulence genes transforms intestinal *E. coli* into highly adaptive UPEC with an arsenal of virulence factors that allows them to establish and persist in new niches such as the epithelial lining of the urethra, bladder, ureter, renal pelvis, adjoining tubules, and collecting ducts of the kidney [1, 2]. The bladder luminal surface is made up of a stratified transitional epithelium (referred to as urothelium), of three to four cell layers at varying stages of differentiation. The outermost layer is the umbrella cells/superficial facet cells, which are large cells (25-250 μm in diameter), polyhedral in shape and sometimes multinucleate. Below them is the intermediate cell layer, with cells which are 10 – 25 μm in diameter and pyriform in shape. These cell types can form one or multiple layers. At the bottom of the urothelium cross section are the basal cells which make contact with the underlying connective tissue and capillary bed. These cells are undifferentiated, small (~ 10 μm in diameter), immature and serve as precursors for the other cell layers whenever cell regeneration occurs [39]. The urothelium has a slow turnover rate with shedding and replacement of the umbrella cells via a fusion of the intermediate cells, only occurring after damage [40]. This is important in maintaining an effective barrier against pathogens, urine solute permeation, as well as maintaining mechanical flexibility to accommodate bladder expansion during urine storage. When UPEC enter the tract they bind onto host receptors on the superficial facet cells. Using mouse models of infection, electron micrographs of infected mouse bladders show the infecting bacteria adhered to the urothelial surface as single cells or in large biofilm like

colonies [6]. A long held view was that UPEC exist mainly as extracellular pathogens that elicit a robust host innate response following attachment to the luminal surface [7]. This response can include the LPS-mediated production of pro-inflammatory cytokines that recruit neutrophils into the bladder lumen and mitigate against bacterial infection. In consequence, the inflammatory host response results in the exfoliation of infected bladder epithelial cells and the production of more bactericidal compounds [2, 7]. As the bladder sheds the exfoliated and infected luminal surface cells into the urine, it rids itself of the pathogens, a strategy that potentially represents the primary host innate mechanism. However, this also exposes the underlying layers of the immature and less differentiated cells to potential infection. Regardless of this potential the extracellular pathogen status quo prevailed and was supported by some strong data.

It had been widely accepted that recurrent UTIs are the result of a re-inoculation of the urinary tract by previously infecting UPEC that originate from the GI tract reservoir [41]. This notion was supported by observations that patients with recurring UTIs (rUTIs) had an inherent immune vulnerability. One study done in 2002, found that patients with rUTIs had neutrophils with reduced antibacterial function. Furthermore, using biochemical phenotyping and genotyping, epidemiological surveys found that up to 68% of rUTIs were caused by strains identical to a prior infection strain lending credibility to the re-inoculation theory [2]. However, earlier transmission EM evidence from infected mouse bladders, had demonstrated that bladder epithelial cells can internalize UPEC. In these studies UPEC cells were observed within membrane bound vacuoles and the cytoplasm of the superficial facet cells, but this was regarded as strictly the consequence of the host defense mechanism. With time, an alternative proposal introduced the concept

of UPEC as opportunistic intracellular pathogens after observations showed that bacteria resist elimination from the host by invading deeper and underlying tissue after exfoliation has occurred. This provides them a niche to multiply, and be protected from the innate host defenses and antibiotics during treatment.

As intracellular pathogens, UPEC enter the bladder epithelial cells and become localized within membrane-bound vacuoles. If they encounter immature and undifferentiated cell layers, they can persist quiescently within these vacuoles, which are usually ensnared within actin fiber networks which make bacterial replication limited [41]. In this environment UPEC can persist for long periods without causing clinical symptoms while been protected from the host defense systems and antibiotic action. Eventually these bacteria break their dormancy, multiply and potentially appear as a recurring UTI [41]. Intracellular replication begins after release from the vacuoles into the cytoplasm. Replication occurs at a rapid rate and the pathogens form biofilm-like intracellular bacterial communities (IBCs) within the intermediate filaments of the host cytoskeletal network. These IBCs represent reservoirs of pathogens within the host that can re-infect healthy bladder epithelia and cause acute or chronic cystitis.

1.1.4 Type 1 and P pili

Both P and type 1 pili are prototypical adhesive fibrous organelles that are assembled through the chaperone/usher (CU) pathway that is utilized by many Gram negative bacteria to assemble surface associated virulence factors [42]. P and type 1 pili have a composite architecture and are built from multiple subunits expressed from the *pap* and *fim* gene operon, respectively [43] (See Fig 1.1).

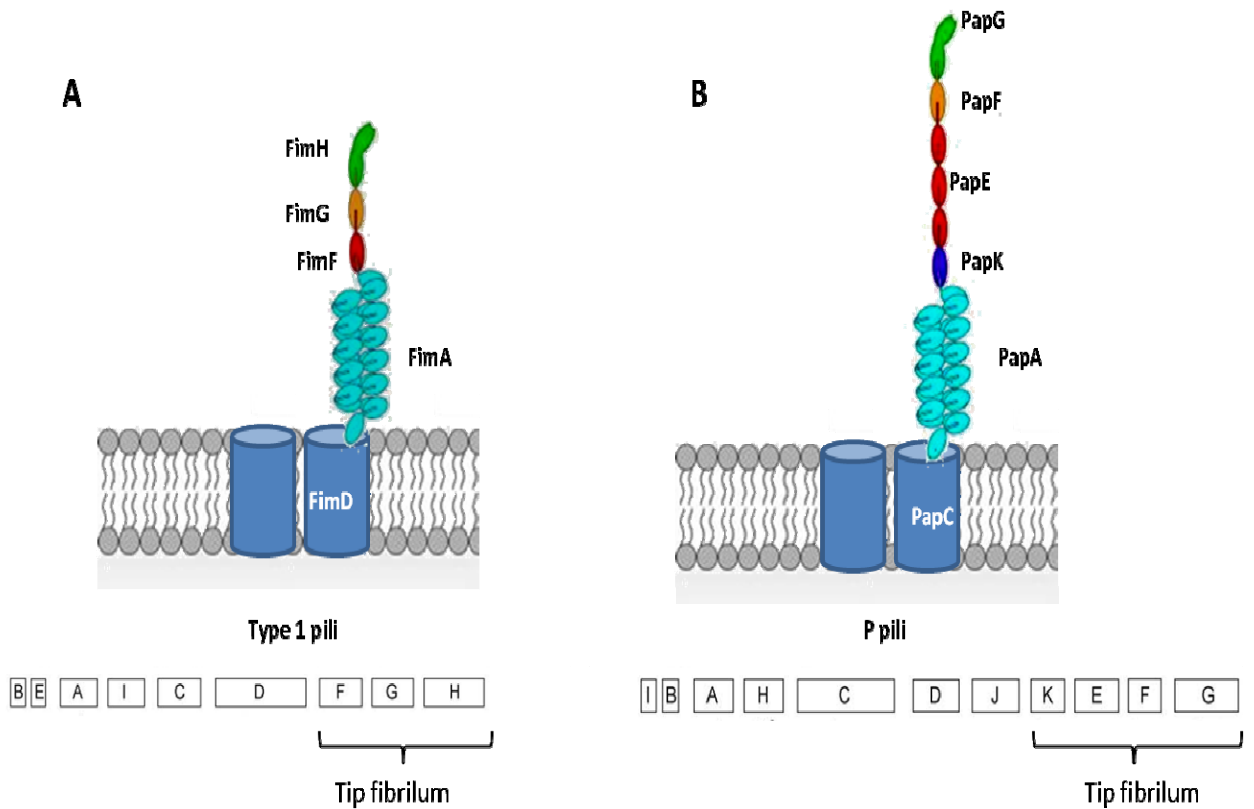


Fig 1.1 Architecture of the type 1 and P pili surface organelles. Adapted from [44-46]. Schematic of (A) Type 1 pilus and (B) P pilus. The cartoon shows the composite structure of pili and the arrangement of the different subunits for each type of pili. The lower panel in (A) is the *fim* gene cluster. B and E code for regulatory proteins. A, is the major pilus rod; C, periplasmic chaperone; D, outer membrane usher; F and G, tip fibrillum components and H is the adhesin. The lower panel in (B) is the *pap* gene cluster. I and B code for regulatory proteins; A, major pilus rod subunit; H, rod terminator; C, outer membrane usher; D, periplasmic chaperone; K, adaptor protein; E, is the major tip fibrillum component; F, adaptor protein and G, adhesin.

The general morphology of these organelles consists of a major rigid pilus rod that is anchored to the bacterial outer membrane and a flexible tip fibrillum that is distally linked to the rod [44]. These two pili types, which are expressed in UPEC are closely related and have been used as model systems to study mechanisms of pilus biogenesis by the CU pathway.

The *pap* (pilus associated with pyelonephritis) gene cluster encodes for regulatory proteins, a chaperone, usher, and the pili subunits [44]. These pili are composed of six different structural proteins that are linked to form a heteropolymeric fiber that is arranged into a distinct rod and tip (See Fig 1.1). The rod measures between 5 – 7 μm in length with a 8.2 nm thickness. The tip fibrillum is thinner, and has thickness of 2 nm with a length of ~22 - 58 nm [47]. The rod is a rigid helical structure formed from repeating PapA subunits (~1000 copies), tightly wound in a right handed twist with a pitch of 2.5 nm and 3.3 subunits per turn [43, 48]. PapA is terminated by the PapH subunit that anchors the pili to the bacterial outer membrane [49, 50]. The tip fibrillum is comprised of several copies of PapE subunits that arrange into an open helical conformation and is connected to the rod via the adaptor subunit, PapK. The PapG adhesin subunit is at the distal end of the tip and is linked to the PapE fibrillum by the adaptor subunit PapF [47, 51, 52]. The PapG adhesin confers recognition of host cells and mediates binding to Gal α (1-4)Gal moieties found in the kidney glycolipids [51].

The type 1 pili share a common structural arrangement with P pili. Type 1 pili are encoded by the *fim* gene cluster and through the action of the tip adhesin FimH, bind to mannose residues in host bladder uroepithelia leading to the development of cystitis [53]. The type 1 pilus also consists of a rigid helical rod that is formed by repeating FimA

subunits and has dimensions similar to the P pilus rod. This rod is connected to a shorter tip fibrillum, ~10 – 19 nm in length [54] that is made up of the FimF and FimG subunits. Multiple copies of FimH form the major part of the fibrillum and the adaptor subunit FimG links the fibrillum to the FimH adhesin subunit.

1.2 Cell envelope of the Gram negative bacteria

The Gram stain which was developed by Christian Gram over a 100 years ago, designates all bacterial species into two large groups, Gram positive or Gram negative [55]. Gram positive bacterial cells can retain the stain, while Gram negative cannot. The stain differentiates the two groups based on the structural composition of the cell envelope. Within the Gram negative bacteria group is the large family of rod shaped Gram negative bacteria called *Enterobacteriaceae*. This family comprises most of the enteric bacteria such as *E. coli*. *E.coli* and other Gram negative bacteria utilize their cell envelope as an effective barrier to detergents such as bile acids found in the gut [55]. The Gram negative cell envelope is arranged into three distinct layers, the outer membrane, inner membrane and a periplasmic space with a single layer of peptidoglycan that delimits the two membranes.

The inner membrane (IM) is a phospholipid bilayer that is akin to cytoplasmic membranes found in eukaryotic cells and intracellular organelles like mitochondrion. It is mostly comprised of phosphatidylethanolamine and phosphatidylglycerol. However, phosphatidylserine and cardiolipin can occur in smaller amounts. The inner membrane is also imbedded with α -helical proteins that participate in transport, signal transduction, ATP formation, secretion, and lipid biosynthesis [55].

The periplasmic space is an aqueous compartment that separates the IM and the outer membrane and makes up ~10% of the cell volume. It houses a three-dimensional mesh-like network of a single peptidoglycan layer. Peptidoglycan is made up of polymers of N-acetyl glucosamine-N-actyl muramic that are cross linked by penta - peptide side chains. The peptidoglycan layer contributes to the cell shape and prevents lysis in hypotonic environments. The periplasm environment is densely packed with proteins and is more viscous than the bacterial cytosol. Proteins that are localized in the periplasm, include chaperones, periplasmic binding proteins (PBPs) that function as receptors for a diverse range of ligands, including carbohydrates, amino acids, anions, metal ions, dipeptides, and oligopeptides [56, 57]. Other important proteins found in the periplasm include proteases such DegP, which act as quality control molecules that degrade misfolded proteins [58]. Disulphide isomerases are also localized in the periplasm and ensure proper folding of proteins by catalyzing disulphide bond formation.

The outer membrane (OM) is the outermost layer of the Gram negative cell envelope. It is a unique feature that distinguishes Gram negative from Gram positive bacteria. The OM has an asymmetric architecture with a thinner inner leaflet composed of phospholipids and a thicker outer leaflet made up of lipopolysaccharides (LPS) [59]. The OM forms an effective selectively permeable barrier that is essential to the survival of *E. coli* [55, 60]. Permeation occurs through channel forming proteins that permit the entry of necessary nutrients into the cell, extrude waste products and translocate proteins (toxins and virulence factors) across the OM.

The OM has lipoproteins in the inner leaflet and β -barrel proteins that traverse the OM and are known as outer membrane proteins (OMPs). Lipoproteins are non-transmembrane proteins and protrude towards the periplasm. They are hydrophilic proteins that are anchored to the membrane by a lipid moiety which is attached to a N-terminal cysteine residue within the protein [61]. They can be localized either to the IM or the OM and play a diverse range of roles in cellular processes such as substrate transport, biogenesis, drug efflux, and maintenance of surface structures [62, 63].

The LPS that makes up the outer most layer of the OM, is composed of molecules built from three basic units. Each molecule consists of lipid A, a core oligosaccharide that is partitioned into an inner and outer region, and an O-antigen polysaccharide of variable length [64]. Lipid A has a diglucosamine diphosphate head group and between four to six acyl chains. The hydrophobic acyl chains anchor the LPS into the OM and the rest of the LPS distally extend into the extra-cellular milieu. The inner core oligosaccharide is characterized by a base component that connects to lipid A. This is usually 3-deoxy-D-manno-oct-2-ulosonic acid (Kdo). The rest of the inner core is made up of other Kdo sugars, heptoses, and phosphates. The outer region of the core oligosaccharide is made up of a three residue hexose chain of either D-glucose, D-mannose, or D-galactose. The first and third hexose residues link to the inner core and the O-antigen, respectively [65, 66]. The outer most domain of the LPS is the O-antigen [64]. It is a polysaccharide formed by 1 to 40 repeating units with 2 to 8 monosaccharides each. The O-antigen together with the flagella protein H, form the basis of serotype classification of *E. coli* strains.

LPS contributes the most to the permeation barrier properties of the OM. Saturated acyl chains result in a densely packed non-fluid environment that is difficult for hydrophilic molecules to penetrate. In the presence of divalent cations, LPS attract to each other and augment the dense packing of the OM outer leaflet. The O-antigen of the LPS confers its immunogenic properties that elicit response from the innate host defense systems. LPS is also recognized as an endotoxin that has been implicated in endotoxic septicemia attributed to Gram negative bacteria [64].

1.3 Secretion systems in Gram negative bacteria

Gram negative bacteria secrete a multitude of exoproteins that have a diverse range of function. These proteins can play roles in cytotoxicity, taxis, nutrient acquisition, drug efflux, adhesion, and other numerous functions [67]. Since proteins are synthesized in the cytoplasm, protein export to the surface or the extra-cellular environment must overcome two barriers, the IM and OM. Gram negative bacteria have evolved specialized secretion systems that are broadly categorized into two groups based on their utilization of the Sec pathway. Therefore secretion systems can be categorized as either Sec dependent or Sec independent. Sec dependent pathways rely on the Sec translocase to move proteins across the IM and into the periplasm, before a dedicated OM transport apparatus completes the delivery across the OM. Sec independent pathways lack this periplasm intermediate stage and, instead they export proteins in a single step, moving their cargo directly from the cytoplasm to the extracellular surface [67]. There are several types of secretions systems that have been characterized and brief descriptions of some well studied systems are given below.

1.3.1 The Sec pathway

The outer membrane is imbedded with a large number of integral transmembrane proteins. These proteins have a diverse array of functions and can be translocons of toxins and adhesins, enzymes, environmental signal receptors, ligand gated channels, and specific or non-specific channels [55]. Most of these proteins adopt a β -barrel structure, with a noted exception being the *E. coli* polysaccharide translocon, Wza, that forms α -helical barrels [68]. All of these proteins are synthesized in the cytoplasm and are exported across the IM as unfolded proteins by the Sec pathway. Thus the Sec pathway plays an important role in outer membrane protein biogenesis. All outer membrane proteins (OMPs) are synthesized as pre-proteins with a N-terminal signal sequence that targets them for translocation across the IM through the Sec pathway. The Sec system is comprised of an integral membrane heterotrimeric translocase (SecYEG), an ATPase (SecA) that interacts with SecYEG and a cytoplasmic chaperone (SecB) [69, 70]. When pre-proteins are synthesized they bind to the SecB chaperone and avoid premature folding and aggregation. This is important because the SecYEG can only translocate unfolded polypeptides across the IM. SecB shuttles the pre-protein to the translocation apparatus where ATP hydrolysis by SecA provides energy for the unfolded polypeptide to move through the SecYEG conduit. During the secretion process the signal sequence is removed through the proteolytic action of the signal peptidase [71]. Once the mature OMPs reach the periplasm they are bound to periplasmic chaperones which serve to prevent them from misfolding and aggregation during their passage through the periplasm.

1.3.2 Type 1 Secretion System

The Type 1 Secretion System (T1SS) is a Sec-independent pathway that is comprised of three structural components that oligomerize to form a continuous conduit that spans the IM to the OM [72], allowing for direct export of proteins from the cytoplasm to the extracellular environment [67]. Typical substrates for T1SS include proteases, lipases, and toxins [73]. A well studied T1SS prototype that secretes the α -hemolysin toxin (HylA) in pathogenic *E. coli* strains is comprised of an IM ABC translocase (HylB) and an OM β -barrel pore, TolC. Bridging these two membrane proteins is the periplasmic membrane fusion protein, HylD [74, 75].

1.3.3 Type 2 Secretion System

The Type 2 Secretion System (T2SS) is a Sec-dependent pathway used by many Gram negative bacteria to translocate protein substrates from the periplasm to the extracellular environment. It is closely related to the type IV pilus and is comprised of 12 – 15 proteins that build up the transport apparatus [76]. Translocation across the OM is performed by a multimeric secretin complex, generically referred to as Protein D. D proteins share a conserved C-terminal domain that forms an integral OM translocation channel and adopts a β -barrel conformation. The N-terminal domain extends into the periplasm and functions in substrate recognition and potentially gates the formed C-terminal pore [77].

1.3.4 Type 3 Secretion System

The Type 3 Secretion System (T3SS) is also a Sec-independent pathway that is used by pathogenic Gram negative bacteria to inject effectors into host cells. It is comprised of a multi component needle-like transport apparatus or injectosome that spans the entire bacterial cell envelope and the host eukaryotic cell membrane. T3SS is a contact dependent pathway which can directly deliver cytotoxins from the bacterial cytoplasm into the host cytosol [78]. The architecture of the T3SS consists of a basal body that spans the entire width of the cell envelope. The basal body anchors the needle complex that protrudes from the OM towards the host cell membrane. The needle complex is built from the bottom up and when contact is made with a host cell membrane, it secretes proteins that imbed into the host cell membrane and form a channel for effectors during infection.

1.3.5 Type 4 Secretion System

Type 4 Secretion Systems (T4SS) are mostly Sec-independent and export protein and DNA substrates across the cell envelope in a process that is dependent on contact with a recipient cell [79]. A well studied and representative system is the VirB/VirD4 T4SS system found in *Agrobacterium tumefaciens*. The translocation machinery is comprised of 1VirD4 and 11 VirB subunits that assemble to into a gated channel for DNA substrate transfer into a recipient cell or a conjugative pilus that makes contact with a recipient cell prior to plasmid or DNA transfer [80]. Other accessory proteins include ATPases and nucleoside triphosphatases that provide energy for the recruitment and transfer of protein

and DNA substrate into the translocation machinery. Based on the crystal structure of a homologous *E. coli* system, T4SS forms a large chamber from 14 copies of VirB7, VirB9 and VirB10 [80, 81]. The chamber spans the width of the cell envelope and is divided into two partitions, the inner layer that is closest to the IM and an outer layer, closest to the OM. The chamber core complex is proposed to function as a scaffold for an internal translocation channel or as the assembly site for the conjugative pilus. Pilin substrates are suggested to pass through the core chamber and build a nascent pilus on the bacterial surface. The outer membrane pore of the chamber complex is proposed to be made from the VirB10 protein. VirB10 spans the OM and is made from an assembly of two adjoined helix bundles that arrange to form a pore with a 32 Å diameter. This pore diameter is sufficient for passage of DNA and unfolded substrates, but not large macromolecules like the conjugative pilus. It is suggested that a gating mechanism that involves conformational changes in the helix bundle arrangement might occur to create a larger translocation pore [80, 81].

1.3.6 Type 5 Secretion System

The Type 5 Secretion Systems are generally split into two families, the autotransporters (AT) and the two partner secretion (TPS) systems. The hallmark of the AT system is that substrates can mediate their own translocation across the OM. The AT secretes virulence factors that have diverse pathogenic functions. AT substrates are synthesized in the cytoplasm as one large multidomain pre-protein that has an N-terminal Sec signal sequence, a middle passenger domain and a C-terminal domain that forms the translocation channel. After passage across the IM, the Sec signal sequence is cleaved

off, and the C-terminal domain inserts into the OM as a β -barrel pore and initiates translocation the passenger domain to the surface of the cell. The passenger domain either stays on the surface or gets cleaved and released to the extracellular environment [67, 82-84]. TPS systems share a similar mechanism as AT, but have two separate polypeptides that play the role of the transporter and passenger. Transporter proteins are generically referred to as TpsB proteins and their cognate substrates are TpsA proteins. TpsB proteins are predicted to fold into β -barrels upon insertion into the OM. A well studied prototypical system is the FHA/FhaC system found in *Bordetella pertussis*. FHA is the filamentous haemagglutinin and is the TpsA protein, while FhaC is the TpsB protein. FhaC forms a 16 stranded β -barrel and acts as the OM translocon to FHA [85].

More details on the channel properties and electrophysiology of the OM translocons found in the various secretion systems are given in Section 1.5

1.4 Chaperone/usher pathway

The chaperone/usher (CU) pathway is a conserved secretion system among the terminal secretory pathways that are dedicated to the assembly and translocation of adhesive virulence organelles on the Gram negative bacterial surface [42]. The pathway is a bi-component system comprised of a periplasmic chaperone and an OM protein, the usher, whose involvement is critical in the secretion of pili across the OM. The CU pathway is responsible for the assembly of two prototypical surface organelles, the P and type 1 pili.

1.4.1 Chaperone

Pilus subunits are exported across the IM of Gram negative bacteria as unfolded polypeptides through the Sec pathway. They remain bound to the membrane until they interact with the chaperone. The PapD chaperone facilitates the proper folding and caps the subunits interactive surface, thus preventing premature subunit-subunit interactions in the periplasm [86]. The crystal structure of PapD reveals that it has two domains that arrange to form a boomerang shape [87]. Each domain has a similar β -strand structure formed by two anti-parallel β -pleated sheets that have an overall topology similar to the immunoglobulin (Ig) fold. Each of the pilus subunits also shares this same Ig-fold. However, they lack the seventh carboxyl terminal β -strand present in the Ig-fold, which leaves a deep groove that exposes the hydrophobic core of the subunit. This feature forms the basis of the interaction between the chaperone and pilus subunits, where the chaperone complements the incomplete and unstable pili subunit by donating a β -strand into the subunit groove. This process is referred to as donor strand complementation (DSC) and leads to the formation of chaperone – subunit complexes in the periplasm. In the absence of PapD, pilus subunits accumulate and aggregate in the periplasm before degradation by the protease DegP.

1.4.2 Usher

The usher protein serves a dual function in pilus biogenesis. It is the site of subunit assembly into a mature and functional pilus, as well as being the translocation channel for

the secretion of the mature pilus onto the surface of the bacterial cell. Initial evidence of the usher's pore forming property came from liposome swelling assays using PapC proteoliposomes [88]. Liposome swelling assays represent a widely used approach to investigate the pore properties of bacterial general diffusion porins [89]. In this study, swelling rates were found to be 20 times lower than those for OmpF, which suggested that PapC existed in a closed state [90]. This supported a widely held view that having a huge open pore in the OM would be deleterious to the cell by allowing passive entry of toxic solutes or exit of critical periplasmic proteins. Nevertheless, swelling rates increased fivefold after the addition of lipopolysaccharides to the liposomes, indicating that PapC is destabilized in a non-native environment. Thus, understanding the mechanistic details behind the usher's activity becomes critical to the understanding of pilus biogenesis. In 2008 this effort was significantly advanced by the elucidation of the PapC crystal structure by Remaut *et al* [45].

In this study, the authors crystallized a truncated usher (resid 130 – 640), missing the periplasmic N- and C-terminal domains. The crystal structure showed the usher to exist in the dimer form as two asymmetric pores lined up side by side. Each monomer is made up of a 24-strand transmembrane β -barrel wall (residues 146 – 635) that measures 45 Å in height, with inner diameter dimensions of 45 Å by 25 Å (See Fig 1.2). Occluding this huge pore is the plug domain (residues 257 – 332), which has a six stranded β -sandwich fold formed from a loop sequence between the β 6 and β 7 strands. Holding the plug in place is an inwardly folding β 5-6 hairpin that dips away from the barrel wall into the channel lumen. The luminal segment of the hairpin is crowned off from the extracellular side by a

downward dipping α -helix domain (residues 448-465). It is believed that a collection of charged residues on the barrel wall, hairpin, α -helix and plug loop form an intricate electrostatic interaction network that clutches the plug in a lateral position within the channel lumen. In fact, there are eight residues that are located on the plug, the β 5–6 hairpin, the α -helix domains and the barrel wall, and interact as a set of four residues that link the plug to the other domains. The first set is the network that links the plug to the hairpin and barrel wall. These residues are Glu361 (barrel wall), Lys339 (barrel wall), Asp234 (hairpin) and Arg303 (plug). The second quartet of residues is Arg237 (hairpin), Glu467 (helix), Arg305 (plug) and Asp323 (plug) (See Fig 1.3).

1.4.3 Pilus assembly

Pilus assembly proceeds within the usher through a top down addition of pili subunits following an ordered recruitment of different chaperone subunit complexes [91]. Once recruited to the usher, pili subunits polymerize into a nascent fiber by employing donor strand exchange (DSE). DSE follows the same principle involved in DSC. With the exception of the adhesin subunit, pili subunits have a long N-terminal extension (Nte) that complements the Ig-fold of the preceding subunit. The Nte of the incoming subunit inserts into the hydrophobic groove of the preceding subunit, replacing the G1 strand of the chaperone and thus dissociating the chaperone-subunit complex [92, 93]. DSE occurs independently of any cellular energy source [94]. The process is potentially driven by the energy differences between the chaperone-subunit complex conformation and subunit-subunit interaction.

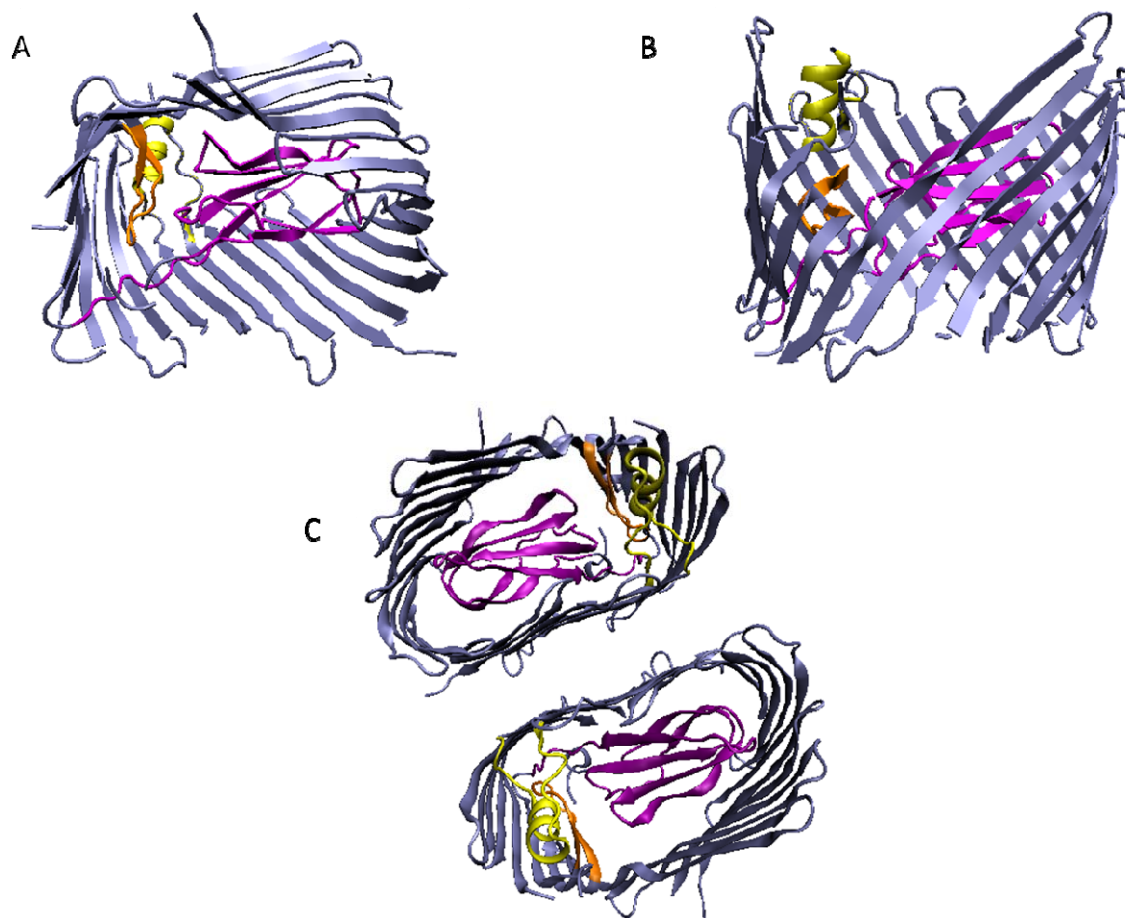


Fig 1.2 Molecular representation of the PapC usher. (A) View of the monomer from the periplasm side. (B) View of the monomer from across the OM. (C) View of the dimer from the extracellular side. Domains are color coded as follows, β -barrel wall, ice blue; α -helix, yellow; β 5-6 hairpin, orange and the plug domain, purple. The images were generated using VMD and pdb file 2VQI.

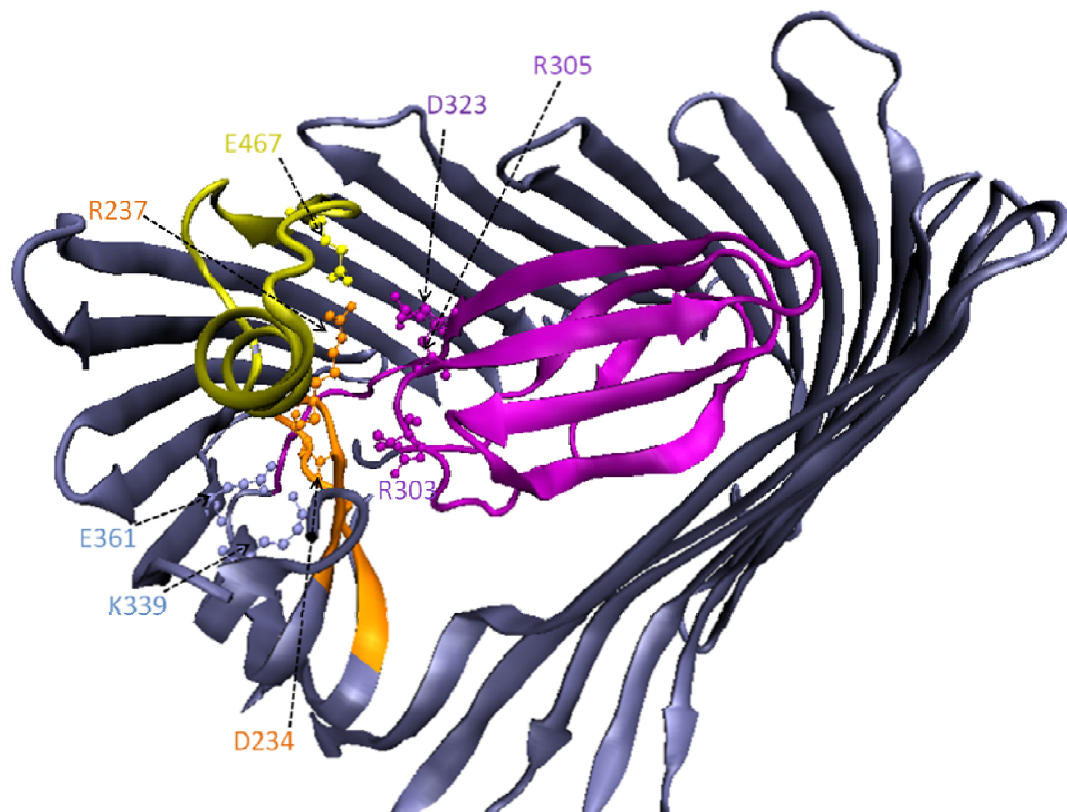


Fig 1.3 Molecular representation of residues forming a network of electrostatic interactions that hold the plug of PapC in place. Residues are shown in stick and ball format and colored according to their domain location. Domains are color coded as follows, β -barrel wall, blue; α -helix, yellow; β 5-6 hairpin, orange and the plug domain, purple. The image was generated from an extracellular side view using VMD and pdb file 2VQI.

In order to form functional pili with the right order of subunit arrangement, the recruitment of chaperone- subunit complexes follows an ordered sequence that is driven by the differential affinity of the complexes to the usher [91]. The usher discriminately recruits chaperone-subunits based on the final position of the subunit in the mature pilus [91, 95, 96]. Recruitment occurs on the periplasm side, where the N-terminal domain (NTD) of the usher is the initial site of chaperone-subunit binding [97-99]. After initial N-terminal targeting, the chaperone-subunit complex is shuttled to the C-terminal domains, CTD1 and CTD2. The adhesin subunit is recruited first, an outcome guaranteed by having the highest chaperone – subunit the affinity to the usher [91].

It is proposed that PapC exists in a resting inactive state and the binding of the first chaperone – subunit complex primes the usher ready for pilus biogenesis [45, 100]. As such one of the consequential events after usher activation is the displacement of the plug domain in only one of the pores, creating a pore large for the passage of folded pilus subunits [45]. The plug displaces to the periplasm side and is suggested to form a complex with the NTD [101]. PapDG bound to the NTD-Plug is turned over to the CTDs through an allosteric destabilization that frees up the NTD-Plug complex for subsequent chaperone-subunit recruitment. When the next incoming chaperone subunit is recruited it is also turned over to the CTDs, where the incoming subunit links with the docked adhesin subunit through DSE and frees up the chaperone from the preceding subunit. This release of the chaperone from the complex after DSE could also be aided by competitive interaction of the plug with the chaperone [101].

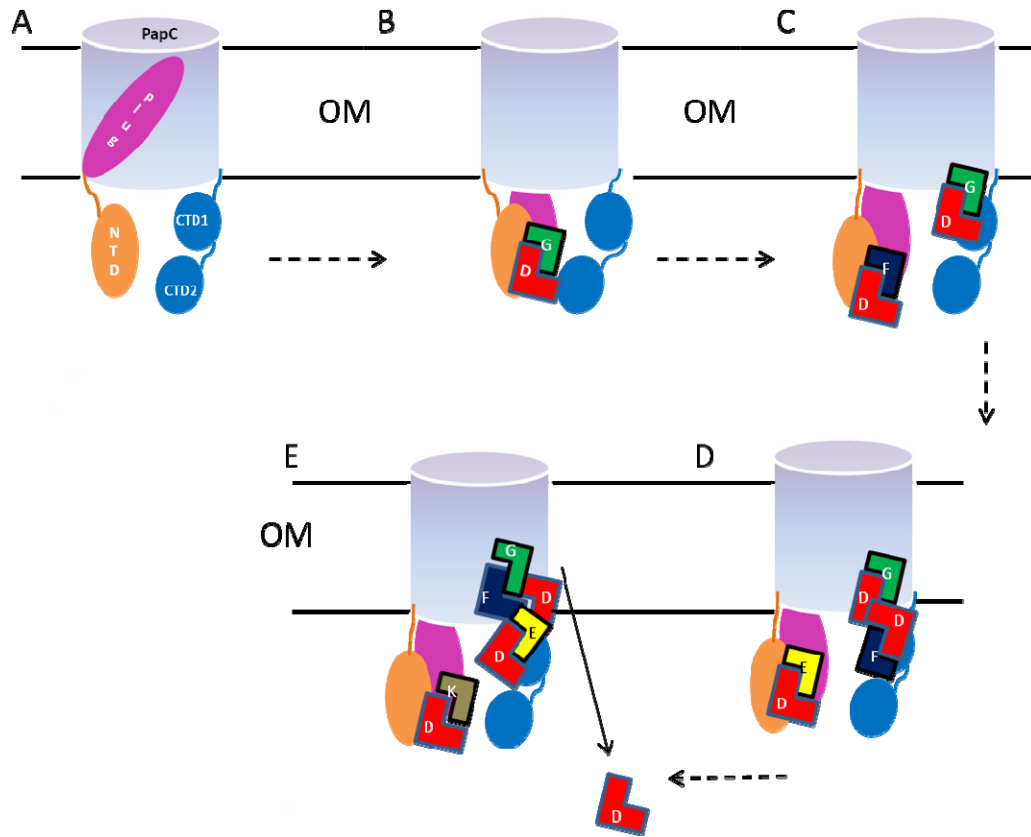


Fig 1.4 CU pathway pilus biogenesis model. (A) PapC channel in its resting state with the plug domain occluding the channel lumen (B) PapDG complex binds to the NTD. This triggers plug displacement and the plug positions on the periplasm side, adjacent to the NTD. (C) The NTD hands over the DG complex to the CTDs and the DG complex begins entry into the pore. Meanwhile the free NTD recruits the next chaperone subunit complex. (D) The PapDF complex is shuttled to the CTD, with the incoming subunit complex interacting with the preceding subunit. (E) Donor strand exchange occurs between PapG and PapF and releases the chaperone initially bound to PapG. Successive steps in this process lead to the assembly of the nascent pilus. The dashed arrows represent the time order of events. Adapted from [101].

1.5 Electrophysiology of translocons

Electrophysiology is one of the canonical techniques used to study properties of pore forming proteins. Although other technique such as swelling assays and dye leakage assays are also widely used to demonstrate the transport function of pore forming proteins, electrophysiology offers the unique perspective of a real-time single-molecule analysis. With the combination of a structure – function relationship study, the mechanistic details behind pore function can be elucidated. The technique is based on the monitoring of electrical current patterns generated from the movement of ions through the protein conduit under investigation. Each pore forming protein can generate a signature current pattern that can reveal among others, the open probability of a pore, dimensions of the pore and the intrinsic modulatory factors that participate in the transport activity of the pore. By introducing various experimental conditions, the effect of various physical and chemical parameters on pore function can be investigated as well.

In Gram negative bacteria, the technique has been extensively used to study the general diffusion porins. Electrophysiology has helped enhance our understanding of bacterial porin permeation at a molecular level [65]. These type of studies have now been extended to outer membrane translocons from various secretion systems that export large folded protein substrates. In most cases these translocons form gated channels and electrophysiology has become a useful tool to decipher the pore properties and the gating mechanism of these translocons.

One such example is found with the T5SS translocons, FhaC and HMW1B that transport protein-surface virulence factors. HMW1B is the outer membrane transporter in a TPS system, with HMW1 adhesin being the transported exoprotein [102] found in *Haemophilus influenzae*. FhaC is also an outer membrane transporter for the filamentous hemagglutinin (FHA) in *Bordetella pertussis*. These two translocons have been studied using electrophysiology and shown to form ion conducting channels that share similar traits [84, 103]. HMW1B formed a channel with a low open probability but with high dynamic behavior. Although it was mostly in a closed state, it was capable of opening to a high conductance which was comparable to that of FHAC.

Another example of a closed OM translocon is the T1SS TolC channel-tunnel found in pathogenic *E. coli* and responsible for the secretion of hemolysin. The TolC channel-tunnel is a trimeric complex resulting in an OM β -barrel channel domain that is constitutively open. Within the periplasm, the complex extends inwards; into to a tunnel formed from α -helix domains that arrange to form a ring like structure. The tunnel spans the periplasm and its diameter tapers into a constricted aperture at the mid-length region, thereby closing the tunnel shut. Substrate gating is thought to open up the tunnel through induced conformational changes of the helices that widen the constricted aperture. Studies of TolC in electrophysiology have revealed that TolC forms an ion conducting channel with a low conductance of 80 pS. The channel can adopt up to three substates that were initially mistaken to be the activity of one or more monomers. Using electrophysiology it has also been shown that small peptides can enter the channel and

lower the conductance of TolC. This indicated a potential binding site for the peptides, thus further affirming the role of TolC as a polypeptide translocation channel [75].

In the T2SS, the secretin PulD from *Klebsiella oxytoca* has also been studied using electrophysiology. PulD is an OM multimeric transporter that secretes pullulanase, a cell surface lipoprotein with glucanase exoenzyme activity. PulD forms a large gated channel comprised of 10-14 subunits that are arranged into a ring like structure with a central pore that allows passage of folded protein substrates. PulD reconstituted in liposomes has been reported to form channels with a low conductance and low open probability. However, following voltage activation, the channels became dynamic and had frequent opening transitions with a higher dwell time and conductance. These transient openings were attributed to voltage dependent minor displacements of domains in the protein complex. Displacements result in short lived openings of a channel that rather prefers to stay in a closed conformation [77].

1.6 Scope of the dissertation

PapC belongs to a class of outer membrane transporters that translocate folded macromolecular substrates to the bacterial cell surface. It also functions as the platform for pilus subunit polymerization into a nascent pilus. Therefore, it is necessary that this occluded translocon forms a pore large enough to fit its cognate substrate. Indeed, it is postulated that during pilus biogenesis there is a gating conformational change that dislocates the plug from the channel lumen, resulting in a large pore sufficient to allow passage and assembly of the nascent pilus [45]. Based on the crystal structure and

liposome swelling assay data, it has been accepted that PapC exists in a closed low activity state, thereby inviting questions on the gating mechanism of the usher.

The PapC protein structure reveals a complex protein with multiple domains whose roles in pilus biogenesis remain partially understood. Proposed models give prominence to the periplasm sided N- and C-termini as platforms for substrate recruitment to the usher. There is growing evidence that upon substrate activation the plug domain is displaced from the channel lumen in preparation for pilus assembly and pilus passage through the pore. However, the molecular details behind such a large scale conformational change are still not known. Pilus biogenesis models strongly suggest that binding of the chaperone-adhesin complex to the N-terminal is the molecular cue that induces plug displacement and thus forming the foundation of our current knowledge on the gating mechanism of the usher. In order to unravel the mechanistic details of pilus biogenesis and the gating mechanism of the usher, an understanding of the functional roles of all the domains in this complex protein needs to be constructed. By initiating an electrophysiology study a unique real time single molecule analysis of the usher protein can be done.

In this study we undertook the first electrophysiology study on the PapC usher. Presented in this dissertation are data from the novel electrophysiological characterization of the usher in a planar lipid bilayer assay. The channel signature and the basal activity of the WT usher will be presented and the channel forming properties of the usher described. From current pilus biogenesis models, it is strongly suggested that the usher exists as twin pore complex, but only one pore appears to be involved in translocation. Due to this, the functional significance of the dimer has been questioned [104]. Using our

alternative electrophysiology assay more evidence to support the dimer organization shall be presented.

Following the characterization of the WT usher, we initiated a structure function relationship study to investigate the roles of the α -helix, plug, N- and C-terminal domains on the usher channel properties. The signature channel behavior of the domain deletion mutants; Δ helix, Δ plug, Δ N Δ C shall be presented and their modulating effect on the usher described. A comparison of these mutant channels to the WT shall be presented and more insight on the functional roles of the α -helix, plug, N- and C-terminals will be provided. Site directed mutagenesis on the usher was done to investigate the effect of the D234 residue on channel behavior. Channel behavior of this mutant channel shall be presented and a proposal on the significance of D234 in channel gating will be made. In addition, we present data on investigations into the modulation of the usher by chaperone-subunit complexes.

Chapter 2

Materials and methods

2.1 Protein Expression and Purification

All the *papC*, *papDG*, *fimD*, *fimCH* plasmid construction, protein expression and purification work was performed by Nadine Henderson in the David Thanassi lab. Expression and purification of PapF, PapE, and PapK in complex with the chaperone PapD was done by Karen Dodson from the Scott Hultgren lab. In both cases, purified protein samples in solution were frozen or iced and sent to our lab using overnight courier for electrophysiological study. PapC and FimD proteins were either frozen or iced before transportation. FimCH and PapDG complexes were frozen before transportation. The complexes PapDK, PapDF, and PapDE were iced before they were sent to our lab. A brief description of the purification strategies are given later.

2.1.1 Strains and Plasmids

a) PapC WT and mutants

The *E.coli* strain DH5 α [105] was used as the host strain for the construction of plasmids encoding wild type PapC and various PapC site directed and domain deletion mutants. The *E.coli* BL21(DE3)omp8 strain [106] was used as the host strain for protein expression. This strain lacks OM porins OmpF, OmpC, OmpA, and LamB, and is used to prevent porin contamination in electrophysiology experiments. Plasmid pDG2 confers ampicillin resistance and is arabinose inducible, and harbors the *papC* sequence linked to a thrombin cleavable C-terminus His-tag [88, 107]. It was used to express wild type PapC and construct the *papC* mutant plasmids. The mutant plasmids were pNH281 - (PapC Δ Plug), pNH269 – (PapC Δ Helix). Plasmid pNH270 coding PapC Δ N Δ C was derived

from pDG2-Pap₁₃₀₋₆₄₀ [45, 108]. The following plasmids were developed for the single or double cysteine substitution mutants: pNH366 – (PapC P292C/S525C), pNH257 – (PapC D234C/Y329C), pNH254 – PapC D234C, pNH261 – (PapC Y329C). Mutations were engineered through site-directed ligase independent mutagenesis (SLIM) [109] or by using the QuickChange Site-Directed Mutagenesis kit (Stratagene) [108].

Disulphide bond (S-S) bond prediction programs, “Disulphide by Design” and “MODIP” [110, 111] were used to predict sites where S-S bonds might form following substitution of double cysteines at the appropriate residues. S-S bond formation was verified by use of a fluorescent probe, Oregon Green 488 Maleimide (Life Technologies), to assay for free sulphydryls [112].

b) FimD

Expression of FimD was done in *E.coli* strain BL21(DE3)omp8, using plasmid pNH213, which is derived from pETS4 and contains *fimD* with a thrombin cleavable His-tag at the C-terminus end [113]. This plasmid is IPTG inducible and confers ampicillin resistance. With the exception of IPTG induction, bacterial growth conditions were similar to those for PapC protein expression.

c) Chaperone-subunit complexes

Protein expression of the PapDG chaperone-subunit complex was done in *E.coli* strain Turner co-transformed with plasmids, pHJ9210 and pTN17. Plasmid pHJ9210 encodes the *papD* chaperone with a C-terminal His-tag, while also conferring

spectinomycin resistance and is arabinose inducible [114]. Plasmid pTN17 encodes the *papG* adhesin, carries an ampicillin resistance gene and is IPTG inducible [91]. To express the other chaperone-subunit complexes, *E.coli* strain Turner was also co-transformed with the same *papD* plasmid and another plasmid encoding either of the remaining pilin subunit genes, *papF*, *papH*, *papK*, or *papA*.

The expression of the FimCH chaperone-subunit complex protein expression was also done in *E.coli* strain Turner transformed with plasmids pETS1000 and pHJ20. Plasmid pETS1000 encodes an arabinose inducible *fimC* with a C-terminal His-tag, while also conferring spectinomycin resistance gene [113]. Plasmid pHJ20 encodes an IPTG inducible *fimH* adhesin and confers ampicillin resistance [54].

2.1.2 Fraction isolation and protein extraction

a) PapC proteins and FimD

To isolate OM fractions with PapC usher or mutants, *E.coli* strain BL21omp8 was transformed with the appropriate plasmid carrying the desired *papC* construct and grown in LB medium supplemented with 100 µg/ml ampicillin at 37°C with aeration and induced with 0.1% L-arabinose. Protein extraction was done according to published procedures [108]. In brief, cells were grown to mid log phase, harvested, and lysed by French Press at 14000 p.s.i. Cell debris was subsequently removed by centrifugation and the supernatant collected for OM fraction extraction. An OM fraction was obtained by treating the supernatant with 10% Sarkosyl, which solubilized the cytoplasm membrane.

The usher was solubilized overnight from the OM fraction in 1% Dodecyl-maltopyranoside and further purified by chromatography.

To isolate OM fractions with FimD usher, *E.coli* strain BL21(DE3)omp8/pNH213 was grown overnight in LB medium supplemented with 100 µg/ml ampicillin and induced with 100 µM IPTG. The extraction and purification of FimD usher generally followed the same protocol as for the PapC usher.

b) Chaperone subunit complexes

Briefly, cultures were grown overnight in LB with antibiotics, spectinomycin and ampicillin, as well as IPTG and arabinose to induce expression. Spheroplasts were prepared from the resuspended bacteria, and a periplasmic fraction was isolated by centrifugation of the spheroplasts, dialysis and further purification by passage through a non-protein binding syringe filter.

2.1.3 Chromatography

His-tagged usher proteins were purified by affinity chromatography on a HisTrap column (GE Healthcare) using an Akta fast protein liquid chromatography system (GE Healthcare). Usher proteins were eluted by applying an imidazole step gradient. After dialysis to remove the imidazole, tag removal was performed by incubating the His-tagged usher with 1.5 units of thrombin/mg of usher protein and allowing for overnight digestion at room temperature. The thrombin cleaved usher was further subjected to another run on a His-Trap column, and PapC/FimD came out in the flow through. After

concentration of the flow through fraction on a Millipore Ultrafree centrifugal concentrator (with a molecular mass cut off – 50kDa), it was further purified by gel filtration on a HiLoad 16/60 Superdex 200 prep grade gel filtration column (GE Healthcare). A peak fraction containing PapC/FimD usher was collected from the column, concentrated and stored. His-tagged chaperone-subunit complexes were also generally purified from periplasmic extracts using the same His-trap strategy in usher purification, but with an additional Resource S cation exchange column run to remove excess His-tagged chaperone and ensure 1:1 purified chaperone subunit complex stoichiometry.

Protein concentration determination was done by Bicinchonnic acid (BCA) protein quantification assay (Pierce).

2.2 Electrophysiology experiments

The characterization of purified PapC, FimD, and PapC mutants was performed using mostly the planar lipid bilayer technique. The patch clamp technique was used for the experiments on the modulation of the usher by chaperone-subunit complexes.

2.2.1 Planar lipid bilayer

a) Planar lipid bilayer set up

A customized set up was used for all planar lipid bilayer experiments (Fig 2.1). This set up was made up of two adjoined 3 ml Teflon chambers. These were separated by a 10 μm thick PTFE film (Goodfellow) with a 100 μm hole punctured in the middle using an

electrical arc generated from a High Frequency Spark Tester PPM MK3 (Buckleys Ltd.) The hole was pre-treated by adding a drop of 5% hexadecane (TCI) dissolved in pentane (HPLC High purity solvent grade from Burdick & Jackson) to create a hydrophobic surface. 1.5 ml of buffer solution (See Table 2.1) was added on each side before two silver chloride electrodes were lowered into designated conduits of the two chambers and became submerged in solution. The electrodes were connected to the CV-4B headstage, of an Axopatch 1-D amplifier (Axon Instruments). The amplifier was further connected to an analog/digital converter (ITC-18 Computer Interface – Instrutech) and an oscilloscope. The measuring electrode was placed on the intended side of protein addition and referred to as the *cis* side. The ground electrode was placed on the *trans* side.

b) Formation of a single lipid bilayer

On both sides of the chamber, 5 μ l of a 5 mg/ml azolectin (1,2-Diacyl-*sn*-glycero-3-phosphocholine Type II-S, Sigma-Aldrich) dissolved in pentane were added onto the surface of the buffer solution. A 5-10 minutes wait was observed to allow solvent evaporation and formation of a lipid monolayer on each side. A planar lipid bilayer was formed over the punctured hole using the principle of lipid monolayer apposition [115]. With the use of 1 ml syringes the level of solution was lowered and raised on one side or both sides of the teflon film until an increase in resistance was observed on the oscilloscope. A stable bilayer was confirmed by a stationary line on or near the 0 pA current level on the oscilloscope.

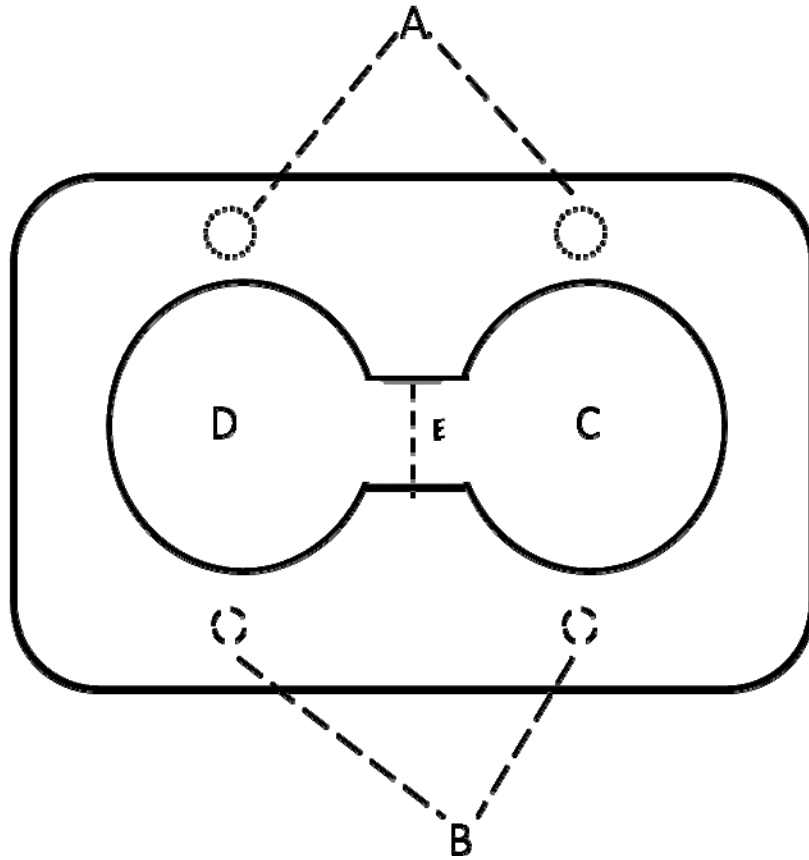


Fig 2.1 Planar lipid bilayer chamber. Shown is a general design of the planar lipid bilayer chambers used in this electrophysiology study. (A) The two designated crevices where electrodes are placed. (B) The two designated crevices where syringe tubes are placed. (C) and (D) are the two sides of the bilayer where ionic solutions are added. (E) The two sides are separated by a teflon film with an aperture in the middle (not shown).

c) Channel recordings

Purified protein in detergent was added on the *cis* side. A range of 0.01-10 µg of protein was added under different experiment conditions followed by gentle stirring with a magnetic stir bar on the *cis* side. Voltage was applied and protein insertion into the bilayer (and resulting pore activity) monitored for up to 10 mins after the voltage was applied. If no insertion or activity was observed within this time period, the bilayer was broken using the zap trigger on the amplifier and a new one formed.

In some of the modulation experiments, chaperone-subunit complexes were added on the *cis* side only or both *cis/trans*, after recordings of the basal activity were acquired.

2.2.2 Patch Clamp

a) Protein reconstitution into liposomes

Reconstitution was done in accordance with a published protocol [116]. A sample of 100 mg of soybean phospholipids (1,2-Diacyl-*sn*-glycero-3-phosphocholine Type II-S, Sigma-Aldrich) was added to 10 ml of 5 mM Tris Buffer and sonicated with a probe sonicator (Fisher Scientific 550 Sonic Dismembrator) for 5-8 mins on ice or until the lipids were fully solubilized. An aliquot of 500 µl was taken and mixed with purified protein to achieve the desired protein: lipid ratio. Typical protein: lipid ratios ranged from 1:100 – 1:500 (w/w). This protein – lipid mixture was incubated at room temperature and rotated for 1hr. Following incubation, 20 mg of Biobeads (SM2-BioRad) were added to the solution and mixture was incubated with rotation at room temperature for an

additional 3hrs. The beads were then removed and the suspension centrifuged at 320,000 g for 15 min. The acquired pellet of reconstituted liposomes was resuspended in 50 μ l MOPS buffer and 3 separate drops of equal volume of the total suspension were aliquoted onto a microscope glass slide. The slide was placed in a dessicator and incubated at 4°C for up to 4hrs to allow dehydration. After the drops dried, an appropriate volume of buffer A was added onto each lipid film to obtain a final lipid concentration of 90 mg/ml. The slide was then placed in a glass Petri dish with a wet filter paper pad at the base to create a humid environment and kept overnight at 4°C, to allow rehydration and formation of large multilamellar liposomes.

b) Patch Clamp of proteoliposomes

From any one drop of the overnight proteoliposome suspension, a 5 μ l aliquot was added in the patch clamp bath filled with buffer B. Buffer B contains magnesium which collapsed the giant liposomes, and with time, unilamellar bulging blisters that appear transparent under a phase contrast microscope emerged from the liposomes [116]. With the PapC and FimD ushers, appearance of these blisters ranged from 15 min – 60 min after addition into the bath. A glass capillary tube (Drummond Scientific) was heated and pulled using a pipette puller (Sutter Instrument) to form a micropipette. The pipette was filled with buffer A and a measuring electrode introduced into the pipette such that it was in contact with the buffer solution at the tip end. The measuring electrode and the reference electrode dipping into the bath solution were both connected to the CV-4 headstage of an Axopatch 1D amplifier (Axon Instruments) and oscilloscope (Fig 2.2).

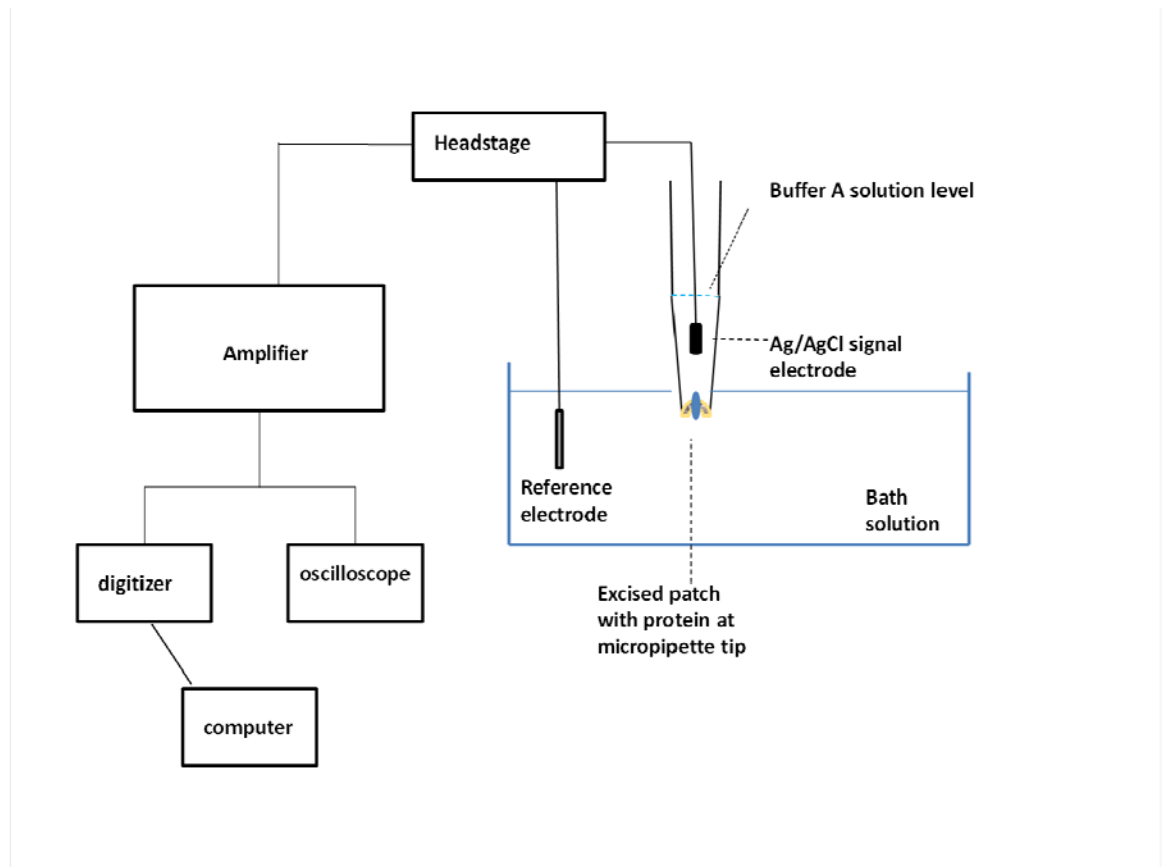


Fig 2.2 Schematic of the Patch Clamp set up. Shown is the general organization of the patch clamp set up and circuit. At the micropipette tip end is an excised membrane patch with reconstituted protein (marked in blue) in a single lipid bilayer. The bath solution can be exchanged through gentle perfusion and substrate added on the bath solution side for the chaperone subunit complex modulation experiments. In some experiments chaperone subunit complexes were also added together with buffer A on the pipette solution side.

The open pipette resistance was 10 M Ω . Once a suitable blister was spotted, the pipette was manipulated to the bottom of the bath where the liposomes settle, and brought into close contact with the blister before suction was applied to form a tight seal between patch pipette and blister membrane. A membrane patch with a good seal was considered to have a resistance ≥ 1 G Ω and such a patch was excised by a brief exposure in air, before being lowered back into the bath. Patch excision breaks any lipid multilayer and ensured that only a single phospholipid bilayer membrane patch was present at the pipette tip. Each patch was verified for pore activity by applying a steady voltage and monitoring the current signal. If activity was detected, buffer B was exchanged for buffer A through gentle perfusion to achieve symmetric conditions of pipette and bath solutions. During recordings the pipette was submerged slightly in the bath solution to limit noise.

2.2.3 Data acquisition and analysis

Current signal recordings were acquired under voltage clamp mode using the Axopatch -1D or Axopatch 200B amplifier. Data was filtered by a low pass Bessel filter at 1 KHz or 500 Hz, and digitized with an ITC-18 A/D converter (Instrutech at 0.1 msec or 1.25 msec sampling intervals, respectively). Current traces were analyzed using pClamp (Axon Instruments) and represented with Sigma Plot software. Single channel currents were obtained either by amplitude histograms using pClamp or from individual events. Conductance (g) was attained from current (pA) / voltage (mV) plots and the slope of curve used as a measure of (g) and given in pS. Conductance was also calculated using Ohms law, with $(g) = I/V$.

Name	KCl	pH	CaCl₂	MgCl₂	K-EDTA	Hepes	MES	Tris	MOPS
Buffer A	150	7.2	0.01	-	0.1	5	-	-	-
Buffer B	150	7.2	0.01	5	0.1	5	-	-	-
Buffer I	1000	4.0	-	-	-	-	5	-	-
Buffer T	1000	7.2	-	-	-	5	-	-	-
Tris	-	7.2	-	-	-	-	-	5	-
MOPS	-	7.2	-	-	-	-	-	-	10

Table 2.1 Electrophysiology buffers and solutions. The table lists concentrations in mM. Solutions were filtered with a 0.2µm filter and stored at 4 °C until usage.

Chapter 3

Modulating effects of the plug, helix, N-, and C-terminal domains on the PapC usher.

Published in: Mapingire, O.S *et al.* **J Biol Chem**, 2009

3.1 Introduction

The chaperone/usher pathway is the dedicated protein secretion system utilized by uropathogenic *E.coli* to assemble and secrete pili fibers onto the cell surface. Pili are heteropolymers in structure and are critical virulence factors that mediate attachment to host cells, contribute to host defenses evasion and the initiation and persistence of infection [44, 117]. The CU pathway is a bi-component system made up of a periplasmic chaperone, PapD, and an outer membrane pore forming usher, PapC [88, 118, 119]. The usher protein functions as the site of ordered pilus subunit assembly and simultaneously translocates the nascent pilus across the OM onto the bacterial cell surface [91, 96]. PapC and PapD are both encoded from the *pap* gene cluster, which also comprises the structural genes for the rest of the pili subunits. In the absence of the usher, pilus subunits accumulate in the periplasm and no assembled pili are secreted to the cell surface [53, 119]. As such understanding the mechanistic details involved in the usher's dual function of pilus biogenesis and translocation remains an important open challenge, with the precise details of these processes not yet fully elucidated.

Initially, PapC was shown to form an outer membrane channel using liposome swelling assays. Although these experiments revealed relatively slow swelling rates when PapC was reconstituted in artificial lipid bilayers, they indeed provided evidence for the transport function of PapC and its existence as a channel [88]. Following the revelation of the usher crystal structure, more questions arose on how this translocation channel forms a conduit for its protein cargo. The crystal structure, which was acquired from the truncated transmembrane segment of the mature protein (residues 130-640), revealed that

PapC exists as a twin pore. Each monomer is a complex structure with several domains. The pore is comprised of a 24 strand β -barrel wall that spans the width of the OM. Within the β -barrel wall is a β -strand sandwich fold plug domain (residues 257-332) that completely occludes the channel lumen, preventing passive entry of solutes or leakage of periplasmic proteins. Holding this plug domain in place is an inwardly folding β 5-6 hairpin and a downward dipping α -helix domain. Located at the periplasmic side are the N- and C-terminal globular domains which are not shown in the crystal structure (See chapter 1) [45]. These two globular domains coordinate the ordered recruitment of chaperone-subunit complexes to the usher based on their differential affinity to the usher. The highest affinity resides with the PapDG complex, which guarantees that the adhesin subunit is recruited first in the top down assembly of the pilus [91, 95, 97]. Suggested models of pilus biogenesis allude the initial targeting of the chaperone-adhesin complex to the usher N-terminus as the catalyst in the activation of the usher from a resting state to a secretion competent state. This activation culminates into a significant conformational change that displaces the plug into the periplasm [97, 100]. Plug displacement frees up the pore to create a conduit with dimensions large enough to accommodate the pilus rod [45]. Thus, to shed insight on the molecular details involved pilus biogenesis and translocation; we instituted an electrophysiology study to investigate the pore properties of the usher channel.

As one of the canonical methods to study channels in general, electrophysiology is a useful tool that can provide time resolved traits of a channel's behavior. Although the technique is based on the generation of a current signal from the flux of ions through a

membrane reconstituted protein conduit, when combined with a structure – function relationship study, the functional roles of specific structural entities of a pore forming protein can be established. As a dedicated translocon, the function of PapC is not to conduct ions. However, its channel properties and roles of its various domains can be revealed through electrophysiological assay of the usher channel and engineered usher mutants. In this chapter we probed the channel properties of the PapC usher and the domain deletion mutants PapC Δ plug, PapC Δ helix, and PapC Δ N Δ C (Fig 3.1). Comparison of PapC WT channel properties and its mutant proteins was done to determine the role of the various domains in modulating the channel behavior of the usher.

3.2 Results

3.2.1 PapC WT and domain deletion mutants form ion conducting channels

The planar lipid bilayer technique was used to characterize the PapC usher channel and its domain deletion mutant channels. Proteins were added to the bilayer chamber on the *cis* side and inserted into the lipid bilayer to form ion conducting channels that had signature patterns of current fluctuation under voltage clamp conditions.

A summary of the attained representative current signal recordings is shown in Fig 3.2. Each construct had a distinct kinetic character that was reproducible over different experiments. The PapC channels showed dynamic behavior, with frequent opening and closing transitions. The channels had clearly discernible and reproducible signature kinetics, with each construct distinct from the other.

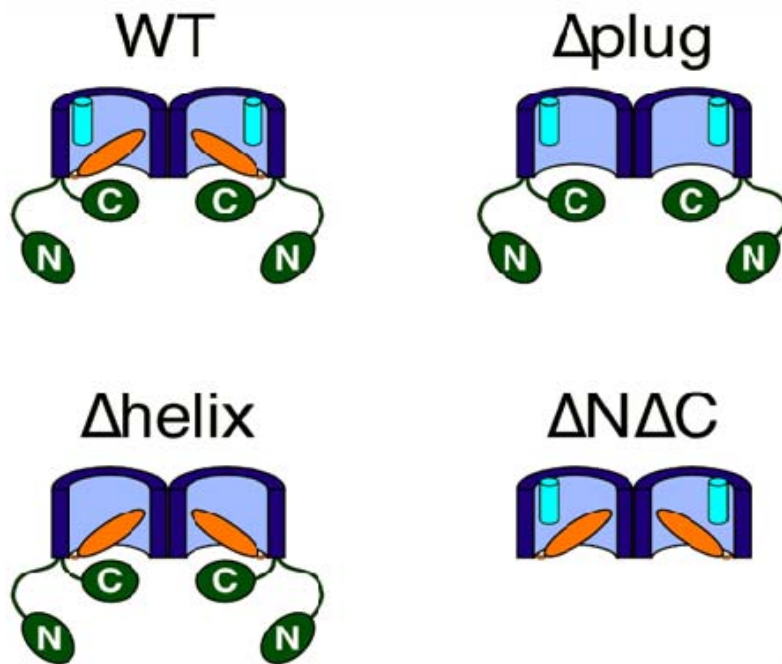


Fig 3.1 Cartoon representation of the WT and PapC domain deletion mutants. The domains are color coded as follows; β -barrel, blue; plug domain, orange; α -helix, aqua; N- and C- terminal domains, green. This image was constructed by D. Thanassi and published in [108].

This gave us confidence that the current signal patterns attained were genuine and not an artefactual effect stemming from lipid bilayer disturbance or noise. Nevertheless, all the PapC channels did exhibit a common aversion to insertion into the bilayer. Compared to the general diffusion porin, OmpF, which readily inserts within minutes after addition to the chamber, PapC channels were difficult to insert into the lipid bilayer. This was despite gentle stirring which usually aids insertions. Repeated attempts to get the proteins to insert were necessary because PapC did not insert within the standard 10 min wait period. β -barrel proteins like porins generally easily insert into the bilayer. Therefore the reluctance of PapC to insert might be due to the large and complex structure. PapC is a large dimer of two 24-stranded β -barrels and each has two large globular N- and C- domains. Interestingly, low reconstitution of PapC in artificial bilayers has been observed in liposome swelling assays as well. Swelling rates only improved after addition of lipopolysaccharides (LPS) to the lipids during the reconstitution process [88]. To counter the low insertion rates, comparatively large amounts of protein were added into the bilayer chamber. The amount of PapC proteins added to the chamber ranged from 0.01 to 7 μ g. This is almost 7000 times more than the amounts used with OmpF, where \sim 1 ng of protein is enough to generate insertions. Because the WT channel has a low open probability we cannot determine the number of channels that insert into the bilayer. With open channels such as the domain deletion mutants studied here it is possible to analyze the channel kinetics and determine the number of channels inserted. A more detailed description of the WT PapC and its domain deletion mutants' channel activity is given in the text to follow.

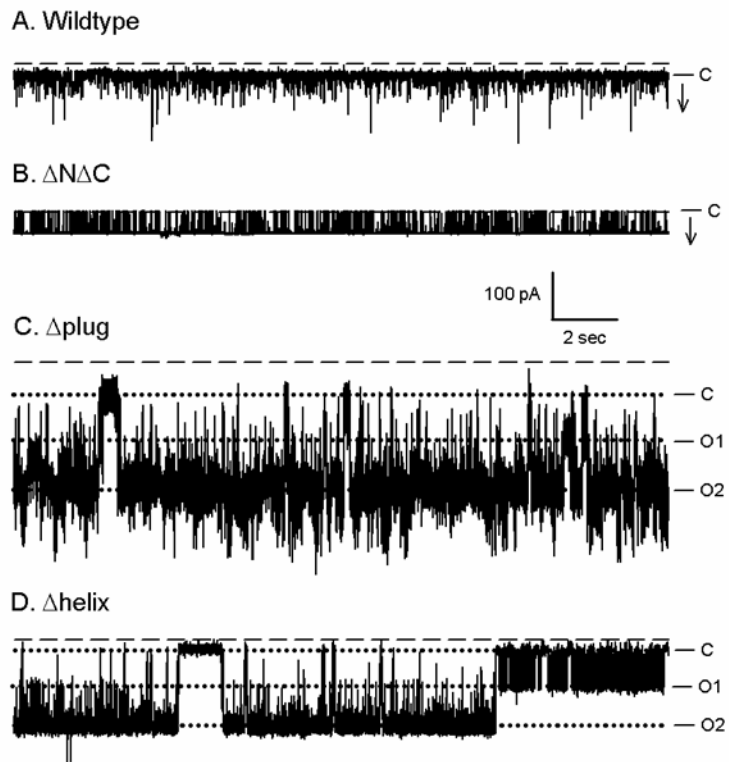


Fig 3.2 Signature channel kinetics of the WT PapC and the mutant channels. Representative 20 sec traces of channel recordings were acquired in 1M KCl with a voltage of -30 mV applied. The closed level is labeled as C; the downward deflections indicated by the arrow represent channel openings. The $\Delta plug$ channel is open with a signal that dwells mostly at a high conductance level marked as O2. A lower conductance level was also observed and is marked O1. O1 and O2 are also marked in the $\Delta helix$ channel. The zero current level is displayed as the dashed line.

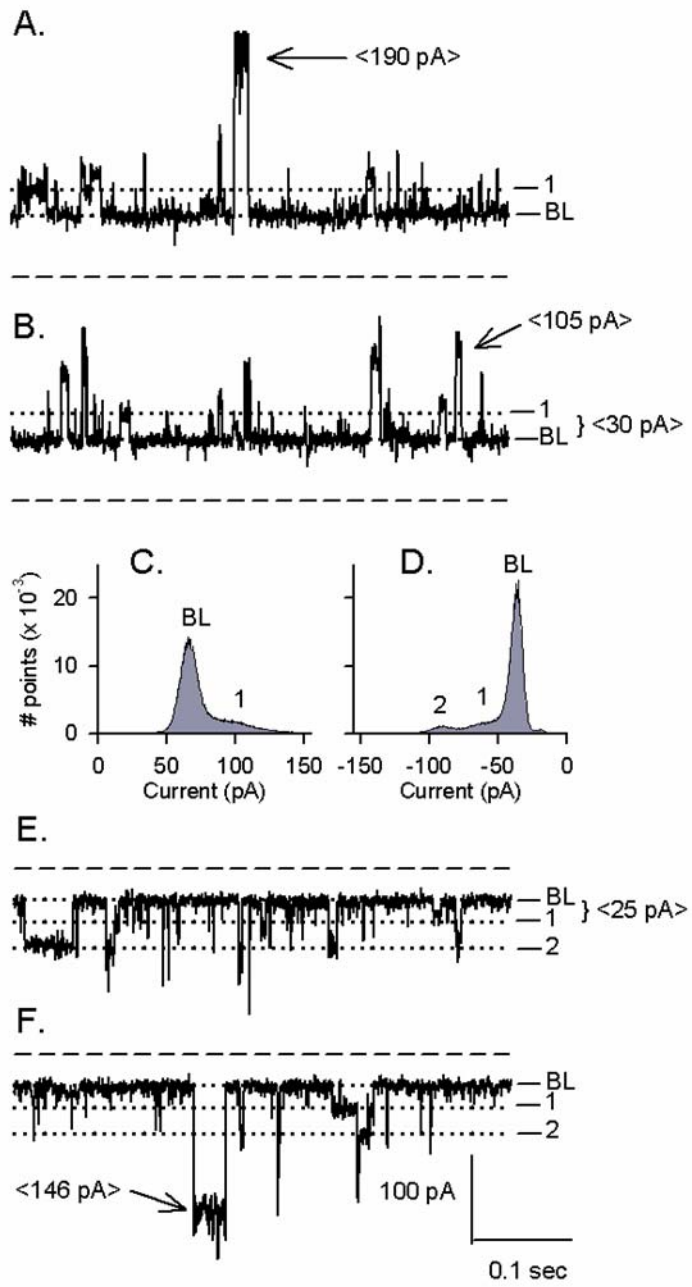
3.2.2 PapC WT forms a closed, but dynamic channel.

From a set of more than 50 experiments, we observed that the WT PapC channel forms an ion conducting channel that is mostly closed. This channel is highly dynamic with rich kinetic behavior marked by frequent and short lived opening transitions to higher current levels. In Fig 3.2 a 20 sec trace of the WT is shown. The trace shows a clear baseline or closed level marked as “C”, that is nearest to the zero current level. The channel activity is punctuated by opening transitions that appear as downward current deflections at negative voltage. A more detailed depiction of these opening transitions is shown in Fig 3.3.

This figure shows both positive and negative voltage recordings of WT PapC at an expanded time scale and gives a better resolution of the WT opening events. These recordings were acquired from the same inserted channel and current signal recordings attained with either a +50 or -50 mV voltage applied. The WT usher channel opens frequently to various current levels. The size of these opening events is variable and random. Size of the events was determined as the difference in current from the closed level baseline and the height of the square top event. In Figs 3.3A, B, and F, high current level openings are shown. These openings measure up to 190 pA, 105 pA, and 146 pA, respectively. The events are genuine and exhibit the canonical square top that is characteristic for channel gating transitions. Smaller events are imbedded within the traces and can be as low as 30 pA or 25 pA, as shown in Figs 3.3B and E, respectively. These levels marked by the dotted line labelled 1 in Figs 3.3A, B, E, and F are prominent but appear not to have other levels which are integer multiples of them. These low current

Fig 3.3 Basal activity of PapC WT. Representative 0.5 sec traces acquired in 1M KCl with a voltage of +50mV (**A** and **B**) and -50mV (**E** and **F**) applied, show the details of the behavior of the WT. The channel dwells mostly at level (BL) nearest to the zero current level (displayed as the dashed line). Upward and downward deflections represent channel opening events at positive and negative voltage respectively. These events are variable in size and duration. Numbers in brackets are the current sizes of selected events measured from the BL and given in pA. Amplitude histograms (**C** and **D**) were generated from 1 min recordings of the +50 and -50mV traces shown above. The plots show peaks that correspond to the closed level (BL) and the prominent open levels labeled 1 and 2.

PapC WT



events are abundant enough to appear as peaks in an amplitude histogram plot, but other various levels are also present but are not frequent or dwell at the same level long enough to yield peaks in an amplitude histogram plot. The negative voltage recording showed peaks that correspond to closed level (BL), the 55 pA level, and the 95 pA level. These are labeled as BL, 1, and 2 in the histogram shown in Fig 3.3D. The positive voltage recording showed peaks at the closed (BL) level and the 100 pA level. These are labeled BL and 1 in the plot in Fig 3.3C. The peaks from the amplitude histogram plots represent the most frequent or prolonged opening events in a given trace. However, by visual inspection of the trace, openings to other various current levels are imbedded within the trace. Thus, there is great diversity in the size of the opening events such that it makes it impossible to construct a I/V relationship, as there is no one particular level you can track or monitor after voltage change. The sizes of the transitions appear not to follow a consistent reproducible trend and different size ranges of opening events can be observed in different experiments.

The diversity is not limited to the size of openings only but extends to the overall behavior of PapC channels. An example of the diversity of PapC behavior is shown in Fig 3.4. In Fig 3.4A we observe a closed behavior with a channel kinetics pattern that is consistent throughout the duration of the recording. In Fig 3.4B the channel begins with low sized opening transitions and then shifts to larger sized transitions towards the end of the recording. In Fig 3.4C the channel had closed behavior and then the current signal shifted to a prolonged open level, and then shifted back to the closed level (BL) and retained the typical closed channel kinetics for the rest of the trace.

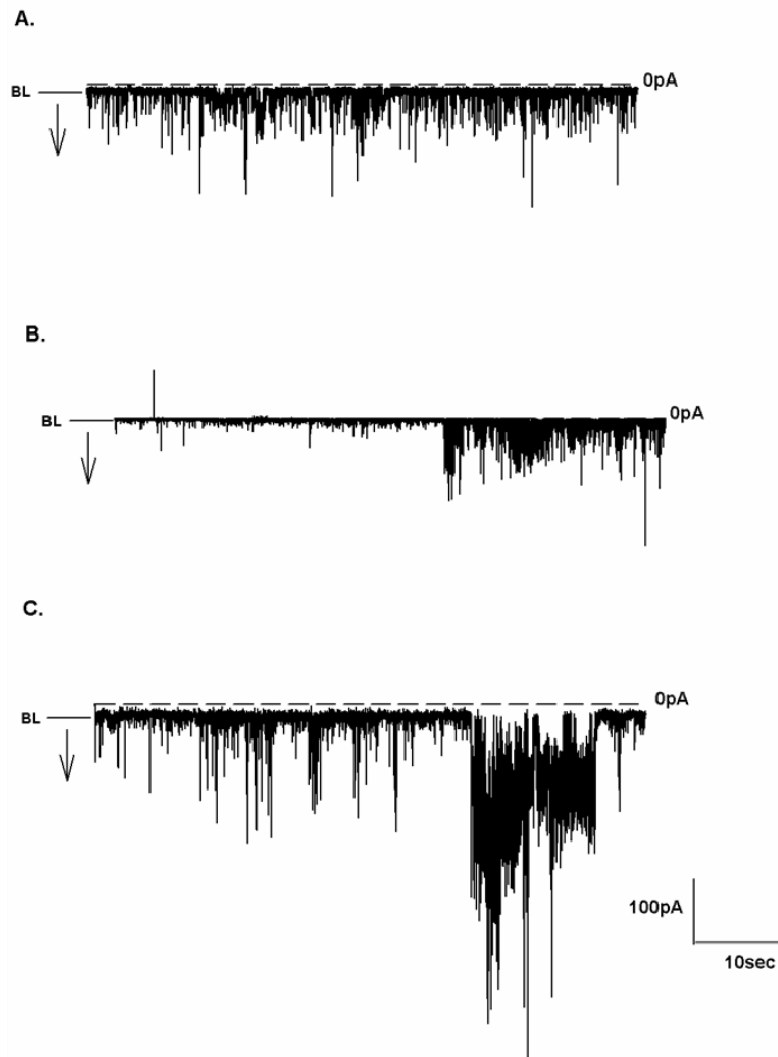


Fig 3.4 The diversity of PapC behavior. 1 min recordings attained from three different experiments in 1M KCl with a -50 mV voltage applied show the different types of behavior PapC can attain. (A) The channel displays a consistent closed channel behavior over the whole duration of the recording. (B) Shows the kinetics shifting from low sized opening transitions to larger sized opening transitions towards the end of the recording. (C) Shows a channel that starts closed at the beginning of the recording and then opens for a prolonged duration and before shifting back to the closed level (BL).

Due to this, it has not been possible to do a quantitative analysis of the channel kinetics, which would be based on the identification of a single channel open current level. Nevertheless, the closed level baseline with opening transitions of various sizes is the simple reliable definition of the PapC WT behavior. Another salient feature of the WT PapC behavior is the lack of voltage polarity dependence. We found no qualitative difference in the channel kinetics of the negative or positive voltage. Also important, is the presence of a leak in the WT recordings. A leak is the difference in current between the closed level baseline and the zero current level and is highly variable between experiments. In Fig 3.3A the channel recording shown has a relatively large leak at 70 pA, but in some experiments the leak can be small or completely absent. Leaks are common in the planar lipid bilayer following channel insertion, but they are usually measuring up to a few pA.

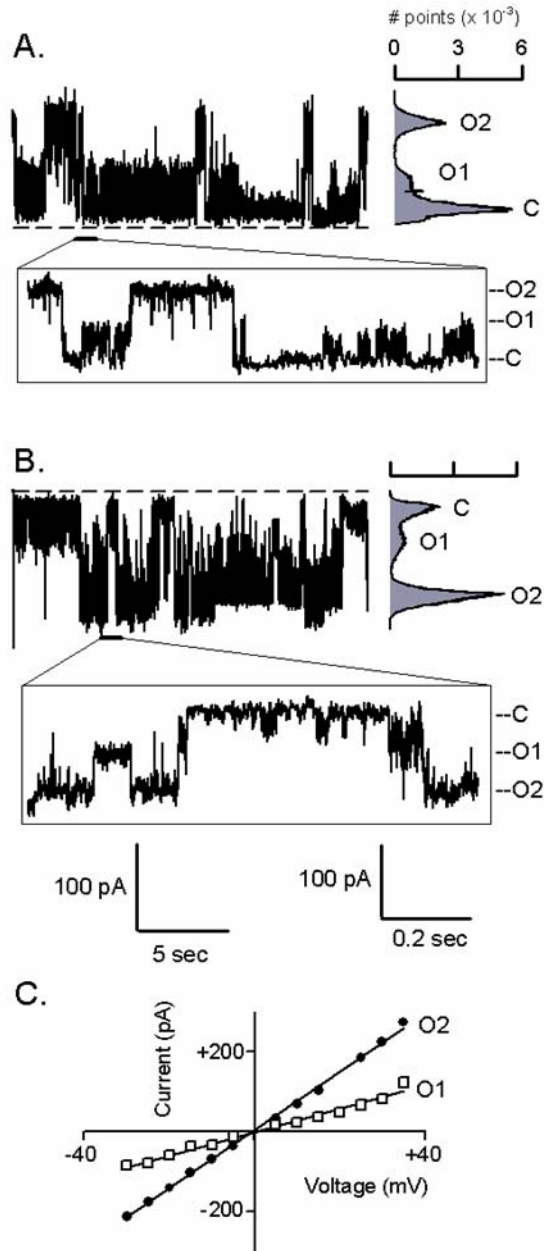
3.2.3 PapC Δ plug forms an open channel with extremely high conductance.

The plug domain occludes the channel lumen of the PapC usher. This maintains the channel in a closed state preventing leakage of critical periplasmic proteins or passive entry of harmful solutes into the cell, which could have a deleterious effect to cell. It has been proposed that, following the activation of the resting usher by the chaperone – adhesin subunit complex, plug displacement occurs creating a large open pore, that is 45 x 25 Å in dimensions, and provides a conduit for the translocation of the nascent pilus [45]. Therefore, we hypothesized that deleting the plug would yield a gaping pore with open channel behavior. The Δ plug mutant was engineered and its electrophysiological signature investigated using the planar lipid bilayer technique.

From a set of 9 experiments, we found that in sharp contrast to the WT, PapC Δ plug exhibited open channel behavior with an extremely high conductance open state. Unlike the WT, Δ plug had a well defined open level baseline at the highest conductance level labeled as “O2” in Figs 3.5A and B. The channel was not a gaping pore, but had a dynamic kinetic pattern, with transitions to two lower conductance states “O1” and the closed level “C” nearest to the zero current level. The current signal dwelled at these three conductive states, which was confirmed with the amplitude histogram plot analysis. In Figs 3.5A and B, the plots on the right side of the each top trace, show three peaks that correspond to the O2, O1, and C levels. In the negative voltage trace, the highest peak was O2, which showed that the current signal dwelled mostly at this highest conductance state. The positive voltage trace does show the major peak as the closed level, suggesting a potential preference to openness in negative voltage. However, this observation was not a consistent trend. Expanded time scale traces at the bottom of each top trace in Fig 3.5A and B give better clarity to the three prominent levels, with O2 been the highest conductance level and O1 been a lower conductance. It is important to note that these recordings were acquired with a low voltage of +15 or -15mV applied because higher voltage generated overwhelming current levels that saturated the amplifier. However, this observation was not a consistent trend. Expanded time scale traces at the bottom of each top trace in Fig 3.5A and B give better clarity to the three prominent levels, with O2 been the highest conductance level and O1 been a lower conductance. It is important to note that these recordings were acquired with a low voltage of +15 or -15mV applied because higher voltage generated overwhelming current levels that saturated the amplifier.

Fig 3.5 *PapC* Δ plug forms an open channel with an extremely high conductance. Representative current traces of 20 sec recordings in 1M KCl with a +15mV (**A**) and -15mV (**B**) applied. The current signal dwells mostly at three prominent levels; C, the closed level, O2 the highest conductance level and O1 a lower conductance level. Amplitude histogram peaks at positive voltage show the current signal dwells mostly at the C level, but the channel opens to O2 and O1 levels. At negative voltage the amplitude histogram peaks show the current signal dwells mostly at the O2 level, and transits to the O1 and C levels. Expanded time scale of the upper traces in A and B display the O2, O1 and C levels. The scale bar at the left side is for the 20 sec upper traces in A and B, and the scale bar at the right side is for the expanded time scale traces of the both A and B. (**C**) Current – voltage relationship generated from the same experiments shown in A and B. The conductance was calculated as the slope of the regression line on each curve. O2 was calculated to be 7,300 pS and O1 ~ 3,000 pS.

Δ plug



The conductance of the O2 and O1 levels were attained through a current – voltage relationship plot, shown in Fig 3.5C. Unlike the WT, an I-V plot was possible because of the well defined levels O2 and O1. The conductance for O2 and O1 was calculated to be 7, 330 pS and 2, 950 pS, respectively. We observed transitions that shifted in multiple of the monomer. Transitions either shift from the C to O1, O1 to O2, C to O2, or in the opposite order; O2 to O1, O1 to C, or O2 to C. We believe we have separate channel entities within a bilayer and because we are confident PapC Δ plug inserts into the bilayer as dimer, the two conductance levels O2 and O1 represent open states of the dimer and monomer, respectively. By that notion, we believe only a single channel insertion occurs and the activity we observe is from a single pore forming protein.

To give perspective to the extremely high conductance of the Δ plug, we observed that even at a low potential of 15mV, the amplifier struggled to clamp the voltage due to the high amount of current passing. Recordings had to be done for 30 sec at most in order to acquire recordings with the normal signal to noise ratio. Higher voltages above 40mV led to the deterioration of the bilayer and increased channel noise due to the overwhelming current. As a note for comparison, an OmpF monomer conductance is 1400 pS in the same conditions. Therefore deleting the plug creates a huge conduit in the usher channel.

3.2.4 PapC Δ helix forms a lower conductance open channel

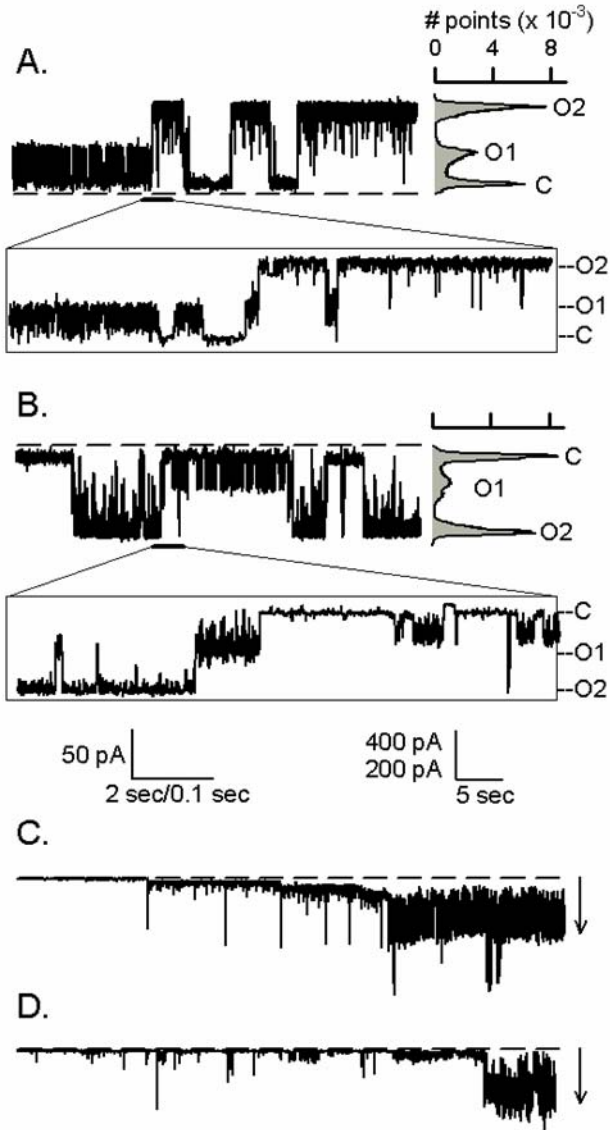
The α -helix is an inward dipping domain located at the extracellular side of the PapC usher. It caps the gap left in the β -barrel wall by the inward folding β 5-6 hairpin. Based on the crystal structure of PapC, specific residues on the α -helix, β 5-6 hairpin and the

barrel wall are part of an electrostatic network of interactions that is believed to hold the plug domain in place [45]. This network of residues is a potential point of structural strain that if disrupted could affect the dislocation of the plug from the channel lumen. As such we sought to investigate the effect of deleting the helix domain on the channel kinetics of PapC.

A Δ helix mutant was engineered and characterized using the planar lipid bilayer technique. We found that unlike the WT, but akin to the Δ plug mutant, the Δ helix mutant formed an open channel. From the recordings attained from 8 different experiments, the data split between traces that showed open behavior from the onset (Figs 3.6A and B) and traces that started with a low activity that later progressed into the open Δ plug-like behavior (Figs 3.6C and D). In the traces that showed Δ plug-like behavior from the onset, well defined open state levels were present. These are shown in Figs 3.6A and B, where the three major current signal levels are marked as O2, O1, and the closed level C. These levels also correspond to the peaks shown in the amplitude histograms on the right side of the upper panel traces in Fig 3.6A and B. Conductance levels of the O2 and O1 levels were measured to be 5,800 pS and 2,500 pS respectively. These two levels were also attributed to be the outcome of dimer and monomer open state activity. The conductance measurements recorded for the Δ helix were comparatively lower than the Δ plug conductance despite the channel exhibiting similar open channel kinetics.

Fig 3.6 *PapC* Δ helix displays Δ plug-like behavior but with a lower conductance. (A) and (B) Current traces obtained at +15mV A and -15mV, show the open behavior that is similar to the Δ plug mutant. In these traces the channel is already in the open mode from the onset of the recording. The current signal in these traces dwells mostly at three levels as shown by the amplitude histograms in A and B. The peaks from the histogram plots correspond to; the closed level C, O1 and the highest conductance level O2. Recordings were acquired in 1M KCl for 30 sec. (C) and (D) are traces that show the delayed opening of the channel. The channel starts off in a closed and low active state before bursting into a open dynamic state. These recordings were attained at -50mV. The left scale bar is for traces A and B. The right scale bar is for C and D. The current scale for C is 400 pA and that of D is 200 pA.

Δ helix



We attribute the open behavior to the displacement of the plug due to the α -helix domain deletion. Hence, the α -helix domain plays a role in the stabilization of the plug within the channel lumen. However, deletion of the α -helix domain does not result in a gaping pore. Instead, there is partial displacement of the plug that creates a more open conduit for ion flux that is still obstructed by the presence of the partially dislocated plug. This would explain the lower conductance of the Δ helix channel compared to the Δ plug mutant. The second set of recordings shown in Figs 3.6C and D, displayed the pattern of a progressive opening to the Δ plug-like open channel kinetics. In these traces, the channels start off in the closed channel mode with the closed baseline nearest to the zero current level, reminiscent of the WT behavior. Over time these channels convert to an open state through a downward shift of the current signal from a closed level baseline to a higher conductance level at negative voltage. This shift to an open state is permanent and not reversible in this set of recordings acquired for the Δ helix mutant.

Our data suggest two scenarios that might be splitting our Δ helix recordings into two sets. In the recordings that show open behavior from the onset, the plug is already partially displaced and removed from its position in the channel lumen. In contrast, in the traces that progressively shift to the open state, the plug is still in position at the beginning of the recording. With voltage been applied the plug partially dislocates over time and the channel attains the open state condition. We did not observe any consistent dependence with time or voltage in the onset of the Δ plug-like open state activity in the Δ helix. The partial plug displacement appears to be random and follows no apparent trend in the recordings acquired within this second Δ helix data set.

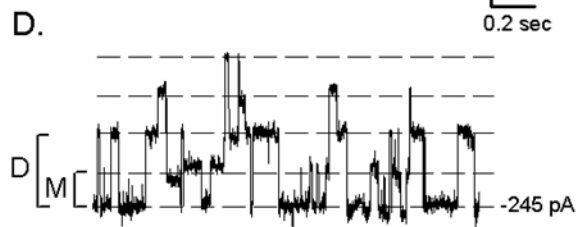
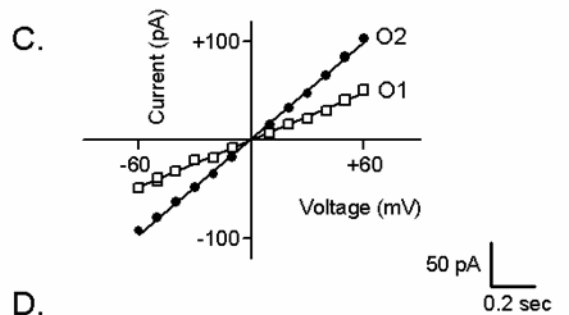
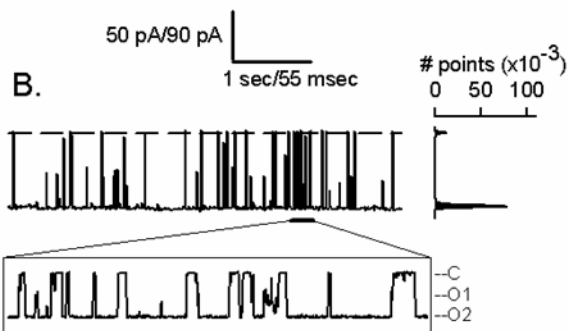
3.2.5 The $\Delta N\Delta C$ mutant is also an open channel

The N- and C-terminal domains are located on the periplasm side of the usher channel. These are globular domains that are responsible for the ordered recruitment of the chaperone-subunits complexes to the usher and are critical in the overall pilus biogenesis process [91, 101]. In proposed models, the N-terminal is thought to be the initial site of binding for the chaperone-subunits and also interacts with the displaced plug domain after recruitment of the chaperone-adhesin subunit complex. The C-terminal is structurally homologous to the plug domain [120] and might also additionally block the channel on the periplasm side prior to the onset of chaperone – subunit recruitment. We sought out to test the effect of deleting these two domains on the usher channel's basal activity.

A double deletion mutant of the N- and C-terminal domains was engineered and characterized using planar lipid bilayer technique. Although PapC and its mutants exhibit a general reluctance to insert into the bilayer, the $\Delta N\Delta C$ mutant stood out in this regard. Reproducible recordings were attained from 5 different experiments, with one experiment yielding a single dimer insertion. In other recordings, multiple channels of the $\Delta N\Delta C$ were inserted into the bilayer. A recording of the single dimer is shown in Figs 3.7A and Fig 3.7B, while Fig 3.7D shows a representative trace of the multiple channels recording. The single dimer recording displayed a channel that is mostly in an open state with a prominent baseline at the highest conductance state, marked as O2 in Figs 3.7A and B. It was also highly dynamic with closing transitions to a lower conductance level O1 or to the closed level C.

Fig 3.7 PapC $\Delta N\Delta C$ is an open channel. Representative 5 sec traces of a single dimer are shown in (A) +50mV and (B) -50mV. The channel is mostly in an open state (marked as O2), with frequent short lived transitions representing closing transitions to a lower conductance state (marked as O1) or the closed level C. The dashed line represents the zero current level. (C) Current – voltage relationship of the dimer (O2) and monomer (O1) current levels. The conductance was calculated to be 1,612 pS and 799 pS for O2 and O1, respectively. (D) Representative trace of a recording from multiple dimeric channels. The trace shows the combined channel kinetics of three dimers with well defined transitions of ~800pS (monomer, M) or ~1,600 pS (dimer, D).

$\Delta N \Delta C$



Amplitude histogram plots at the right side of the upper traces in Fig 3.7A and B show a major peak that corresponds to the O2 level. A small peak that corresponds to the closed level is also present. Events to the O1 level were either too short or infrequent to yield a peak in the histograms. However, the expanded time scale trace in Figs 3.7B (lower trace), shows the presence of this O1 level. In addition to being in a mostly open state, the Δ NAC channel also had rich dynamic behavior with closing transitions from O2 to the closed level. Due to the presence of the well defined O1 and O2 levels, an I-V plot was utilized to determine the conductance at these two levels. From the I-V plot in Fig 3.7C the conductance was calculated to be 799 pS and 1,612 pS for the O1 and O2 levels, respectively. These conductances were comparatively lower than those of the Δ plug and the Δ helix mutant. In fact, the O1 conductance was within range of the smaller events observed in the WT which were between 500 – 600 pS (See Fig 3.3B and F). Interestingly, the O1 and O2 level conductances were a near multiple of two of each other, strongly suggesting these to be monomer and dimer open state levels, respectively. This integer multiples of event current size is further illustrated in Fig 3.7D which displays the recordings attained from multiple channels in the bilayer. The recording, attained at -50mV shows the highest current level at -245 pA, which implies the channels inserted in the bilayer are in a similar open state as observed in the single dimer recording. There is an array of well defined events that are either 800pS in size (which corresponds to the monomer events size in the single dimer recording) or multiples of the monomer events. Of note, is the absence of the large (2500 – 3800 pS) single step WT opening events indicating occasional plug dislocation does not occur in the absence of the

N- and C-termini domains. This multiple channel kinetics behavior was also reproducible over the few experiments done. Thus deleting the N- and C-terminals yields a dynamic channel that is open but with a lower conductance compared to the Δ plug and Δ helix mutants.

3.3 Discussion

Using electrophysiology, we sought to characterize the basal activity of PapC WT and its domain deletion mutants. By comparing the kinetic signatures of the WT to the mutants, the role of the respective domains in the modulation of the usher channel activity could be established and shed more insight on their function in pilus biogenesis.

The WT PapC was able to insert into the lipid bilayer and form ion conducting channels, albeit at comparatively low insertions rates. We attribute the low rates of insertion to the size and complex structural organization of the PapC usher. Although we cannot determine the number of channels that inserted into the bilayer per given experiment we assume recordings were acquired from a single channel insertions. We have reasoned that if multiple channels had inserted the occasional high conductance (~3800 pS) events seen in the WT would be a composite of the low conductance (~500 pS) events. If we had multiple channels, we would observe a stepwise shift to the high conductance level, because it would be improbable that several channels would gate in precise synchrony and transition to the high conductance level in one step. However, we have no direct evidence to support our single channel insertion assumption with the WT. The channel itself is mostly in a leaky closed state with a baseline nearest to the zero

current level that is marked by opening transitions to various conductance states. The size of these opening events varied from as low as 500 pS to as high as 3800 pS. These occasional short-lived high conductance events match the size range of the open states in the Δ plug or Δ helix mutants suggesting these could be the result of occasional plug displacement in the WT channel. The ability to form an ion conducting channel with rich kinetic behavior raises the question of how ions can pass through the channel. The PapC lumen is occluded by the plug domain. PapC is in a low conductive state, which explains the leaks observed between the closed level baseline and the zero current level. On looking at the PapC structure we found that while the plug completely shuts the pore, small intrinsic water-filled channels exist at the interface of the barrel wall and the plug. These are shown in Fig 3.8 and are marked in red circles. We propose these small intrinsic channels as the routes for ion flux and the dynamic behavior of the opening and closing transitions is due to the transient interruption of ion flow by the random jiggling of the plug within the pore. We attempted to test this explanation by “plugging” one of the intrinsic channels with a bulkier residue, through a tryptophan or tyrosine substitution on residue A290. The two mutants A290W and A290Y were characterized in planar lipid bilayer and looked similar to the WT channel (data not shown). We attributed this outcome to the presence of other remaining intrinsic channels that could still provide ion flux routes. The observed dynamic behavior in the WT and all the deletion mutants implies that the plug alone is not responsible for this interruption of ion flow. In the Δ plug mutant, the open channel still had the dynamic traits with rich kinetics of opening and closing transitions.

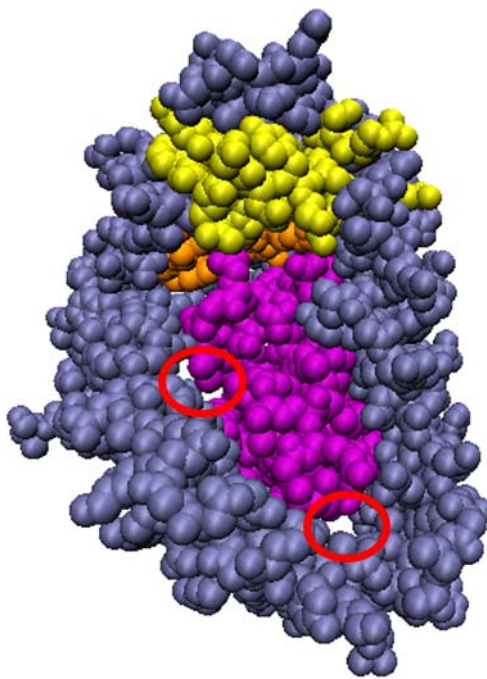


Fig 3.8 *Space-filling representation of the PapC monomer. The image shows the intrinsic water channels, encircled in red. Domains are color coded as follows: β -barrel wall, ice blue; α -helix, yellow; β 5-6 hairpin, orange and the plug domain, purple. The image was generated from an extracellular side view using VMD and pdb file 2VQI.*

In the absence of the plug, we attribute this to the interruption of ion flow by the N- and C-terminal domains on the periplasmic side. These domains are possibly also dynamic and their movements could translate into the gating pattern observed in the Δ plug channel. Thus the basal activity of the WT is modulated by 1) jiggling of the plug within the pore that interrupts the flow of ions within the intrinsic water channels and/or interruption of ion flow by movements of the N- and C-termini on the periplasmic end 2) the occasional displacement of the plug which results in the high conductance Δ plug-like opening events. To comprehensively test this it would have been ideal to obtain a mutant lacking both the plug and the N- and C-terminal domains (Δ N Δ C Δ plug). Unfortunately this triple mutant did not express well and appeared not to fold properly in the OM [108].

The high conductance Δ plug-like events are absent in the Δ N Δ C mutant. Despite the Δ N Δ C mutant forming an open channel, its conductance levels are markedly lower than the Δ plug mutant. The large Δ plug-like events are seen in the WT and to some extent the Δ helix mutant. If these openings are a function of plug displacement then their absence in the Δ N Δ C mutant might indicate a role for these globular domains in promoting the displacement of the plug. It has been shown that during pilus biogenesis the plug interacts with the N- terminal domain following dislocation from the channel lumen [101]. In addition, there is strong structural homology between the plug and the C-terminal domain. Because the Δ N Δ C mutant forms an open channel when its periplasmic globular domains are absent, the C- terminal and even the N-terminal domain might be further blocking ion flow through the intrinsic channels from the periplasmic side.

The Δ helix mutant showed an open channel behavior. This mutant still had the plug present but showed behavior akin to the Δ plug mutant, albeit with a lower conductance. We attribute the open behavior to the partial displacement of the plug as a result of a structural strain introduced by the deletion of the α -helix domain. Residues on the α -helix are believed to form part of a network of electrostatic interactions that hold the plug in place. The lower conductance is a result of the pore still being occluded by the partially displaced plug which does not create the open pore found in the Δ plug mutant.

Our study of the Δ plug revealed a channel with an extremely large conductance of $\sim 3,000$ pS. This confirmed that indeed the plug gates the channel shut. The conductance was well within expectation for a $45 \times 25 \text{ \AA}$ translocation pore. The size of the pore is significant in the movement of folded protein substrates. Other functionally analogous pore forming proteins such as the oligomeric secretins XcpQ from *Pseudomonas aeruginosa* and YscC from *Yersinia enterocolitica* form large conductance channels as well ($\sim 3,000 - 10,000$ pS) [121, 122]. In these cases EM studies provide evidence of an oligomer of 12 - 14 subunits that arrange into a ring-like structure with a central pore large enough to translocate folded protein substrates [123]. Therefore, despite the functional similarity, the closed low conductance state of PapC does not compare well with these secretins. However there are other translocons that have been shown to have conductances within the WT PapC range. A case in point is found in PulD, the outer membrane protein secretin of the type 2 secretion system. PulD is reported to be closed like PapC with some small voltage dependent openings of ~ 200 pS in a 400/100 mM KCl gradient. These openings were interpreted to be the result of movements by the proteins

domains [77]. There are also other translocons that are smaller in structure and form channels from a single polypeptide for the transport of unfolded substrates. Examples of these are HMW1B and FhaC translocons of the two-partner secretion systems in *Haemophilus influenzae* and *Bordetella pertussis*, respectively. A conductance of 1,400 pS has been reported for HMW1B [103] and 1,200 pS reported for FhaC [84].

In summary our study revealed that PapC forms a twin pore with movement of ions through the intrinsic water channels at the interface of the barrel wall and the plug. There is evidence for a substantial dynamic flexibility within the whole protein, with domains seemingly capable of movement. The plug deletion mutant has an extremely large conductance in accordance with the estimated pore dimensions and its function of translocating folded protein substrates. The N- and C-terminal domains potentially occlude the pore on the periplasmic side and play a role in supporting plug displacement. The α -helix domain plays a role in stabilizing the plug in place within the channel lumen. These data and the characterization of the basal activity set the stage for more a functional assay that tests the modulating effect of chaperone – substrate on the usher channel.

Chapter 4

**Site-directed cysteine substitution mutants shed insight
on the mechanism of plug dislocation**

4.1 Introduction

The PapC usher forms part of a bi-component secretion system that is dedicated to the recruitment, in-situ polymerization and translocation of pilus subunits across the outer membrane, onto the extracellular surface [44, 88, 124]. While the role of the chaperone, PapD has been elucidated fairly well, the mechanistic details of how the usher performs its dual function remain an open challenge. This has been intensified with the revelation of the crystal structure of the usher translocation domain that showed the unique structural features of a large corked up channel [45]. The plug occupies the channel lumen and is comprised of a six stranded β -sandwich fold that is uniquely inserted within a loop adjoining the β 6 and β 7 strands. Holding the plug in place is an inward folding β 5-6 hairpin that folds away from the barrel wall into the channel lumen. The luminal segment of the hairpin is crowned off from the extracellular side by an inward dipping α -helix domain (residues 448-465). It is believed a collection of charged residues on the barrel wall, hairpin, α -helix, and plug loop form an intricate electrostatic interaction network that clutch the plug in a lateral position within the channel lumen (Fig 4.1). The function of the usher is to act as a conduit for the nascent pilus fiber during translocation and to catalyze the polymerization of subunits. Subunits enter the pore and polymerize using DSE [93, 125]. In the absence of ATP or proton motive force, DSE [94] provides the energy for the growing pilus to transcend through the channel in an upright orientation [104].

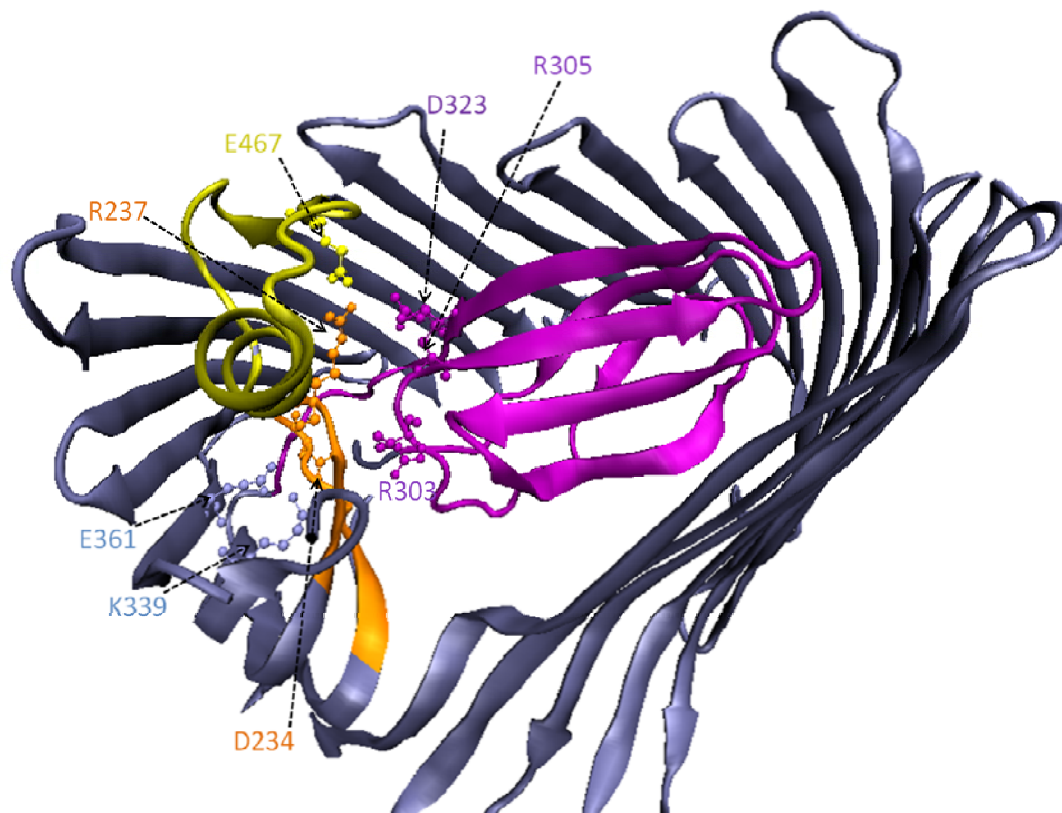


Fig 4.1 Molecular representation of residues forming a network of electrostatic interactions that hold the plug of PapC in place. Residues are shown in stick and ball format and colored according to their domain location. Domains are color coded as follows, β -barrel wall, blue; α -helix, yellow; β 5-6 hairpin, orange and the plug domain, purple. The image was generated from an extracellular view using VMD and pdb file 2VQI.

This would require that a sufficient gaping pore be present for subunits to pass through the usher and the precise plug dislocation and repositioning details would impact the eventual size of the translocation pore. Although different subunits can bind to the N-termini of the usher, plug displacement and pilus biogenesis are thought to be triggered by the chaperone-adhesin complex (PapDG) activation of the usher. By binding to the N-terminal, the usher becomes activated and primed for pilus biogenesis which requires an unobstructed pore [91, 113]. Crystal structure data have also shown a complete dislocation of the plug from the channel lumen and its repositioning on the periplasmic side. Using the Fim usher system, a complex of the translocating usher bound to its substrate, FimD:FimC:FimH showed the plug repositioned on the periplasm side [100]. Contrastingly, it has been predicted that combined with possible β 5-6 and α -helix conformational changes, the plug could displace in an alternative outward orientation and still create a translocation pore of a considerable size [45]. However, displacement to the periplasmic side creates a more complete open pore of 45 Å x 25 Å [45]. More recently, affinity binding assays have shown that in addition to the N- and C-termini, the plug domain can also bind to pili subunits [101]. Considering the strong structural homology between the plug and C-terminal domain [120], it has been speculated that subsequent to displacement, the plug has an aiding role in the periplasmic sided recruitment and shuttling of chaperone-subunits. Therefore, furthering our understanding of how plug displacement is elicited and what controls the directional movement of the plug would be valuable to understanding the mechanism of pilus biogenesis.

In its inactivated non-translocating form the usher pore is closed shut. This supports a widely held view that having a huge open pore would allow passive entry of toxic solutes or exit of critical periplasmic proteins. Evidence for this closed form exists from the usher crystal structure that shows the pore completely occluded by the plug and through our own work on the electrophysiology of PapC [108] (See chapter 3). Using the planar lipid bilayer technique we revealed that, characteristic of a closed channel, PapC is mostly in a leaky low conductance state. Its behavior was characterized by frequent opening transitions from a closed state baseline to various conductance levels. Since PapC WT is an occluded channel, ion influx through the channel was attributed to the small intrinsic water “channels” at the barrel wall and plug domain interface. The highly frequent transitions were also suggested to be the result of a combination of the plug randomly jiggling within the pore and/or movement of the periplasmic globular domains that interrupted ion flow. In addition to this, we found that deletion of the plug resulted in an open channel that had an extremely high conductance, further reinforcing the notion that the plug occludes and shuts the channel lumen. Another important feature was the presence of short lived and infrequent transitions to an extreme high conductance level. The conductance of these events was similar to that of a PapC Δ plug or Δ helix mutant. This indicated that the plug was capable of undergoing transient displacement. From characterization of the domain deletion mutants, we also found that there was an innate dynamic flexibility within the whole PapC protein, with domains capable of movement and having a modulating effect on the usher (See chapter 3)

We hypothesized that tethering the plug would suppress movement of the plug and affect the size and frequency of the opening transitions. In this study, we characterized engineered double cysteine mutants which were highly predicted to form S-S bonds. These mutants were used to test the effect of tethering the plug domain and potentially locking it in one position. The planar lipid bilayer technique was used to characterize these mutants and compare their signature channel behavior to that of the WT. Ensuing, we found that site directed substitution of the D234 residue resulted in a more open channel that was reminiscent of the Δ plug and Δ helix mutants. This suggests the D234 residue is directly involved or contributes to the gating of the translocation pore.

4.2 Results

4.2.1 PapC D234C/Y329C displays open channel behavior.

To test the effect of tethering the plug to the barrel wall, S-S bond prediction programs “Disulphide by Design” and MODIP were used to predict sites within the usher where S-S bonds might form spontaneously following double cysteine substitutions at the appropriate residues. From a generated list of potential sites, D234 and Y329 residues were predicted the best candidates to form a S-S bond. A double cys mutant, D234C/Y329C was engineered and S-S bond formation was verified by a free sulphydryl assay [112]. This mutant has a Cys substitution on the D234 residue located on the β 5-6 hairpin loop that adjoins the two β -strands. The other mutation was on the Y329 residue, located on the loop connecting the β 6 strand to the plug’s β -strand sandwich fold. The putative S-S bond thus tethers the plug to the hairpin (See Fig 4.2).

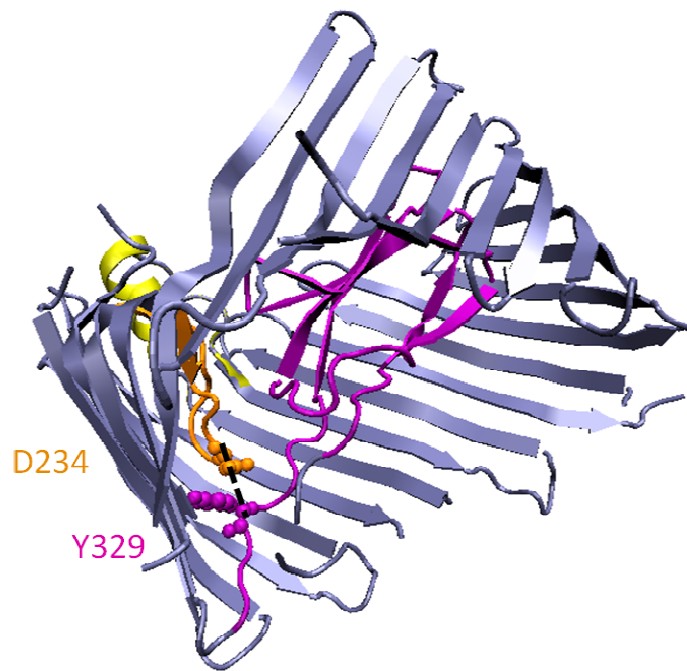
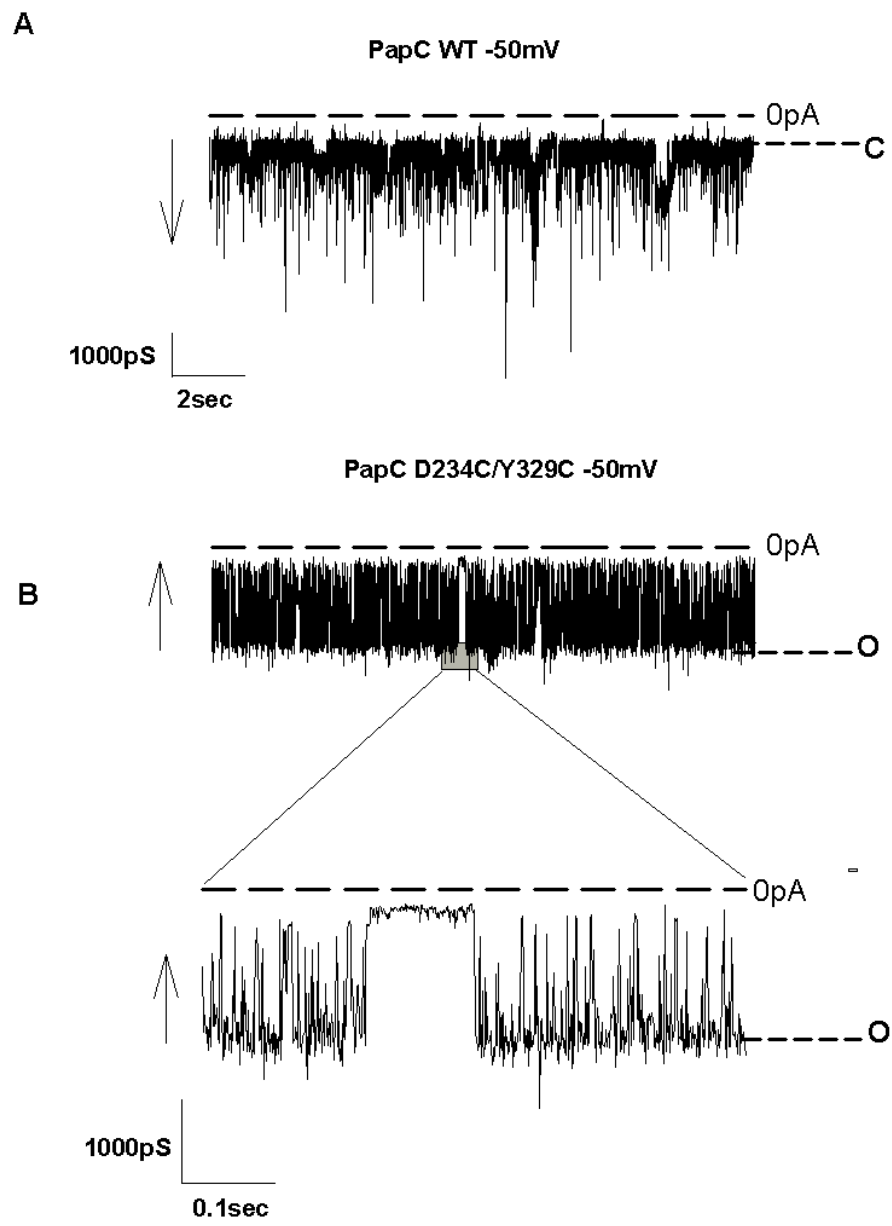


Fig 4.2 *Molecular representation of the D234C/Y329C putative S-S bond. Residues are shown as spheres and colored according to their domain location. The putative S-S bond is the black dashed line between resid D234 and Y329. The bond tethers the plug to the hairpin. Domains are color coded as follows; β -barrel wall, blue; α -helix, yellow; β 5-6 hairpin, orange and the plug domain – purple. The image was generated from a tilted periplasm side view.*

The purified D234C/Y329C protein was characterized using the planar lipid bilayer technique and channel current recordings acquired in buffer T solution, with a -50 mV voltage applied under voltage clamp conditions. Signature behaviors of the D234C/Y329C and the WT were analyzed and compared. Our prediction was that tethering of the plug would suppress plug movement and in turn reduce the rich kinetic behavior of PapC. We also anticipated that the occasional dislocation of the plug out of the pore that was observed in the WT would be diminished. However, in contrast to the WT, D234C/Y329C formed a largely open channel. Its behavior was marked by a well defined open conductance level labeled as “O” in Fig 4.3B and represents the full open state that is furthest from the zero current level. Closed channels like the WT usually dwell at a baseline that is nearest to the zero current level and have downward current signal fluctuations at negative voltage that represent openings. A conductance of ~980 pS was measured at this level using the event detection tool on pClamp. The trace also shows rich kinetic behavior, with frequent closing transitions from the open level “O” to a closed level near the zero current line. This is well displayed in the upper trace of Fig 4.3B, which shows the high density of the fast transitions in a 10 sec recording. A better resolution of these transitions is displayed on the lower trace at an expanded time scale of a short segment of the 10 sec trace. Even at an extended time scale of just 0.3 sec, we can still observe these highly abundant short lived transitions. Unlike in other open PapC deletion mutants such as the Δ plug and Δ N Δ C, no other consistent conductance levels were discernible from our analysis. These levels can occur as multiples of one another and are reasoned to be the result of the monomer or dimer activity.

Fig 4.3 D234C/Y329C forms an open channel. *A. A 10sec representative trace of the WT behavior. WT is a closed channel that dwells mostly at the lowest conductance level marked by the dashed line “C” that is nearest to the zero current level. The trace shown here has rich kinetic behavior with downward deflections, as shown by the arrow. These deflections represent opening transitions to various higher conductance levels. B. The upper panel shows a 10 sec recording from the D234C/Y329C mutant. The trace shows an open channel that dwells mostly at the highest conductance level marked by the dashed line “O”. It has rich kinetics with upward frequent and short-lived closing transitions. The lower panel shows an expanded segment of the upper trace and shows better detail of the closing transitions that go from the “O” level towards the zero current level. All current recordings were acquired in Buffer T conditions with a voltage of -50mV applied.*

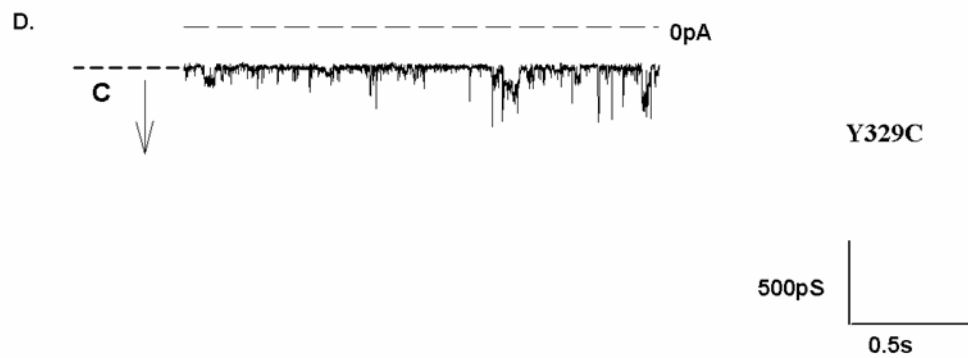
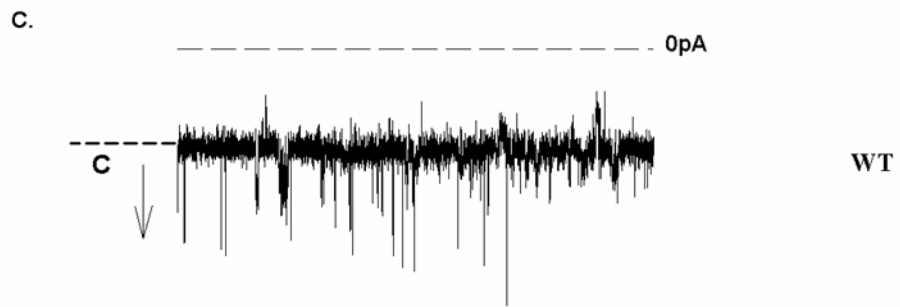
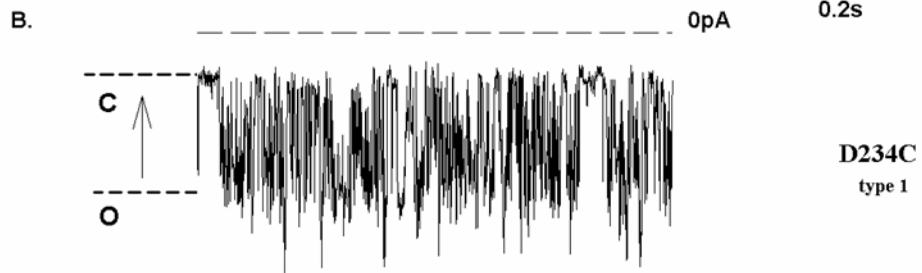
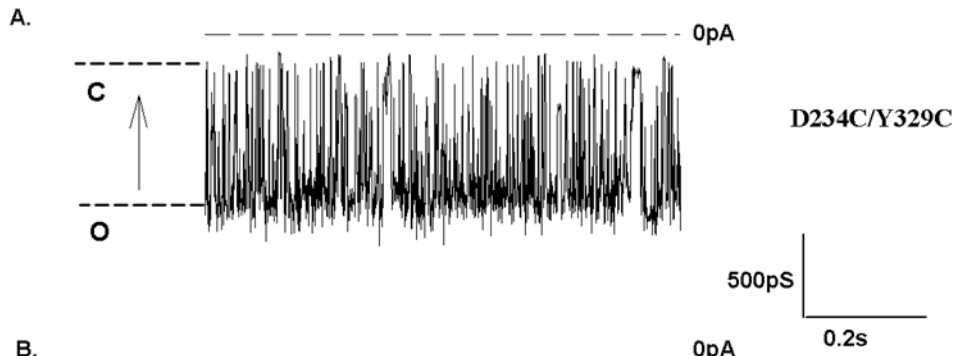


Compared to other PapC domain deletion mutants, the conductance of D234C/Y329C was the lowest for a PapC open channel (See chapter 3). The Δ plug has its highest conductance at 7330 pS, the Δ N Δ C at 1612 pS and the Δ helix at 5800 pS [108]. The conductance of the D234C/Y329C is also lower than that of an OmpF monomer (~1400 pS) in the same conditions [126]. Therefore, the overall behavior of this double cys mutant in electrophysiology presented a low conductance PapC open channel. This was unexpected and led us to probe if tethering the plug alone, was the reason for a comparatively low conductance open channel. We tried to investigate if this open phenotype could be reversed by removing the disulphide bond in-situ through DTT treatment of the D234C/Y329C protein. After treating the D234C/Y329C mutant with DTT we were not able to get the mutant to insert into the bilayer. PapC has two native cysteines in the N-terminal and C-terminal domains and DTT treatment might be causing misfolding of the protein or disintegration of the tertiary structure.

4.2.2 Single Cys mutants reveal D234 mutation alone contributes to the D234C/Y329C open behavior

To probe whether the open behavior of the D234C/Y329C mutant was due to the tethering of the plug or the site directed mutations, the single D234C and Y329C mutants were engineered. With only a single cys substitution in each mutant, any phenotypic traits observed would be attributable to the single mutation alone. Purified protein of each mutant was used for electrophysiological characterization using the planar lipid bilayer technique and current signal recordings acquired in buffer T with a -50 mV voltage applied.

Fig 4.4 Single cys mutants reveal that the D234 mutation causes an open channel behavior. Shown are representative traces of the current recordings acquired for the D234C/Y329C, D234C, WT and Y239C in buffer T and a -50 mV voltage applied. **A.** Trace of the D234C/Y329C mutant. This is an open channel with the highest conductance level marked by the dashed line labeled “O”. The channel is dynamic and characterized by frequent closing transitions to a closed level marked by the dashed line “C”. The arrow represents upward current deflections at negative voltage. **B.** Trace of the D234C single cys mutant. This is an open channel with the highest conductance level marked by the dashed line labeled “O”. The channel is dynamic and characterized by frequent closing transitions to a closed level marked by the dashed line “C”. The arrow represents upward current deflections at negative voltage. The shown trace represents one type of D234C behavior that is similar to the D234C/Y329C shown in **A.** **C.** Trace of the WT channel. This recording is a sample of the various WT channel kinetics, but is representative in being a closed channel with a baseline nearest to the zero current level, marked by the dashed line “C”. Downward current signal deflections, shown by the arrow, represent channel opening transitions to various higher conductance levels. **D.** Trace of the single cys mutant Y329C. The recording shows that the mutant is a closed channel similar to WT. It has a baseline marked with the dashed line “C” that is nearest to the zero current level. Opening transitions from this baseline are shown as downward current signal deflections as pointed by the arrow direction. The upper scale bar applies to **A, B and C** traces. The lower scale bar applies to the trace in **D.**

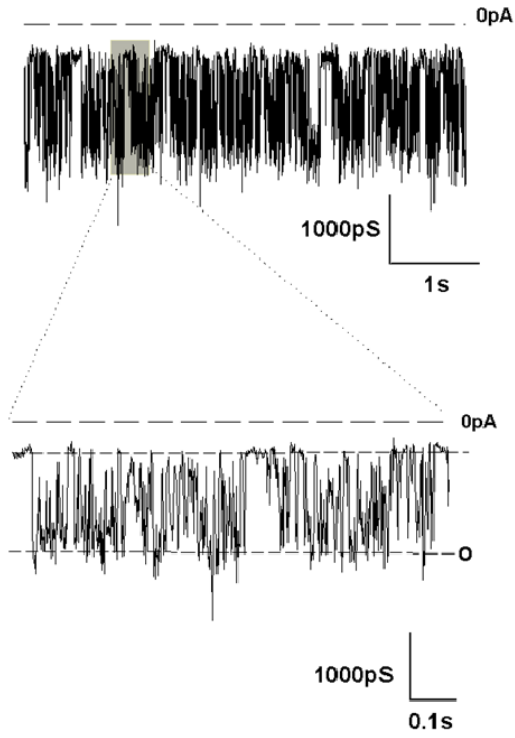


Like the double cys mutant, D234C displayed an open channel behavior. Two open channel behavior types were observed and distributed near equal in seven of nine experiments. In the first open type, the current signal dwells mostly at the highest conductance level marked “O” that is shown in Figs 4.4B and 4.5A. Open type-1 behavior shown in Fig 4.4B was remarkably similar to the current trace of D234C/Y329C shown in Fig 4.4A. Like the double cys mutant, D234C open type-1 exhibited traits of a highly dynamic channel. Its trace was marked by frequent and fast upward closing transitions from the highest conductance level “O” to a closed level “C” nearest the zero current level. The conductance for level “O” was measured using the event detection tool on pClamp and approximated to be 940 pS, which was strikingly close to the conductance measured for the “O” level in the D234C/Y329C mutant. Like in the D234C/Y239C mutant, there were no discernible substate levels in the open type-1 behavior of D234C. The second open type behavior of D234C is shown in Fig 4.5B. The trace dwells at two major conductance levels labeled as O2 and O1 on the expanded trace of trace type-2 behavior in Fig 4.5B. A conductance of ~480 pS and ~250 pS was measured for each level, respectively. Because these levels are multiples of one another and because transitions occur from one level to the other, they could be the result of monomer and dimer activity as previously suggested for the PapC $\Delta N\Delta C$ and $\Delta plug$ mutants [108]. Compared to type-1 D234C open behavior, the frequency of closing events and conductance were noticeably lower. In a few experiments, open channel behavior akin to type-2 had an even lower conductance than the one shown in Fig 4.5. Thus type-1 represents a more open and dynamic channel behavior than the type-2.

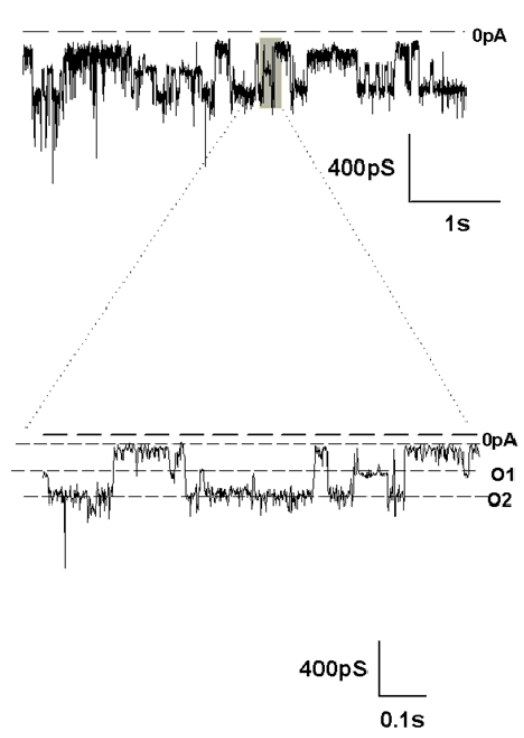
Fig 4.5. D234C has two open type behaviors. (A) Type 1 is an open behavior that is marked by frequent and short lived closing transitions from the highest conductance level “O”. This is shown in detail in the lower trace which is an expanded segment of the upper 4 sec trace. The hallmark of type-1 is the higher conductance of ~ 980 pS for the “O” level, relative to type-2, and the abundant closing events. D234C type-1 open channel behavior and conductance are similar to those of the D234C/Y329C mutant.

(B) Type-2 behavior is characterized by two open levels “O1” and “O2”, shown in better detail in the expanded segment of the upper 4sec trace. “O2” represents the highest conductance level and was measured to be ~ 480 pS, while “O1” was ~ 250 pS. The hallmarks of type-2 open channel behavior is the lower conductance and fewer closing transitions when compared to type-1 behavior.

A *type 1*



B *type 2*



Based on the similarity of the open type 1 behavior of D234C to D234C/Y329C, the single mutation to the D234 residue was the apparent cause of the open behavior in the plug tethered D234C/Y329C mutant. To further verify this explanation, the Y329C single cys mutant was also characterized under the same conditions as the D234C. Its behavior was distinctly different from the D234C or D234C/Y329C. Unlike the two, the Y329C channel was mostly closed and more comparable to the WT trace shown in fig 4.4C. The trace shown in fig 4.4D dwells mostly at a closed level nearest to the zero current level, labeled C. It is less dynamic with fewer opening transitions compared to the D234C/Y329C or D234C. Although some of these opening events reach a conductance greater or equal to 500 pS (Fig 4.4D), they have a short dwell time at this higher conductance level. Therefore based on this contrasting closed behavior, the mutation of the Y329 residue does not affect nor contribute to the open behavior of the D234C/Y329C.

4.2.3 The P292C/S525C mutant shows a behavior similar to WT

After observing that the D234C/Y329C mutant was an open channel whose behavior was dictated by the mutation to the D234 residue, we sought to test the effect of tethering the plug at a different location. Another double cys mutant, P292C/S525C, which was also predicted to form a S-S bond, was engineered and characterized. This mutant tethers the plug to the barrel wall at a location away from the electrostatic interaction network (See Fig 4.1 and Fig 4.6). The mutated residues are not known or speculated to play a gating role on the usher and presented an opportunity to study the effects of tethering the plug to the barrel wall.

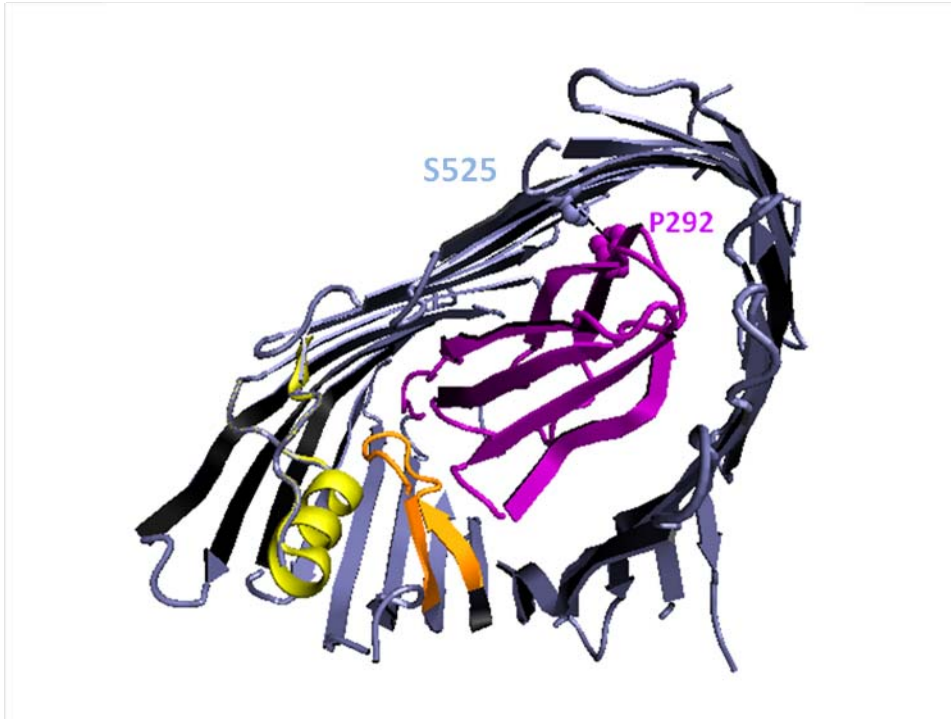
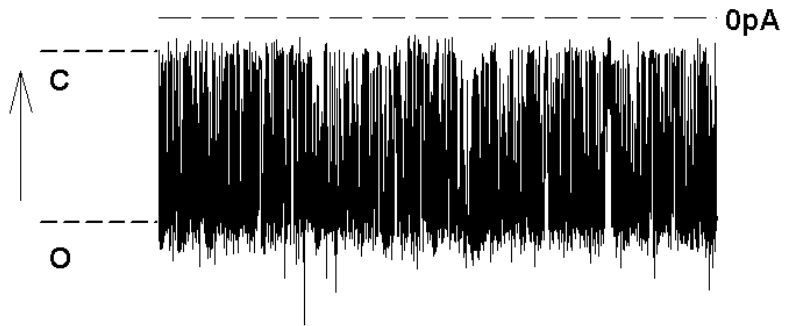


Fig 4.6 Molecular representation of PapC with the P292 and S525 residues highlighted. The bond is represented by the dashed black line and the mutated residues are displayed as blue (S525) and purple (P292) spheres. Domains are color coded as follows; β -barrel wall, blue, α -helix, yellow; β 5-6 hairpin, orange and the plug domain, purple. The image was generated from an extracellular view.

Fig 4.7 P292C/S525C is a closed channel similar to WT. All current recordings were acquired in Buffer T conditions with a -50mV voltage applied. **(A).** Trace of the D234C/Y329C mutant. This is an open channel with the highest conductance level marked by the dashed line labeled "O". The channel is dynamic and characterized by frequent closing transitions to a closed level marked by the dashed line "C". The arrow represents upward current deflections (closings) at negative voltage. **(B).** Trace of the P292C/S525C mutant. The channel is closed, reminiscent of the WT. It dwells mostly at a closed level "C" that is nearest to zero current level, with downward current deflections that represent opening events to various conductance levels. **(C).** An example of the WT behavior. The displayed trace shows a WT channel that dwells mostly at closed level "C", nearest to the zero current level. Downward deflections represent opening events from the "C" level to various conductance levels. Note that trace B was acquired at 100 μ sec sampling intervals, while trace A and C were acquired at 1.25 μ sec sampling intervals.

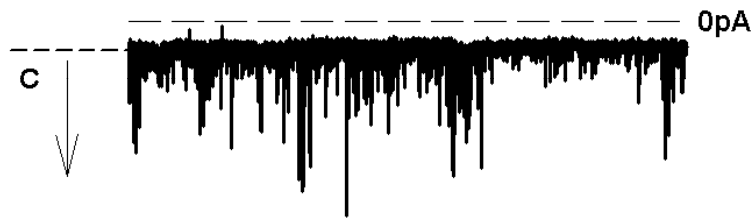
A.

D234C/Y329C



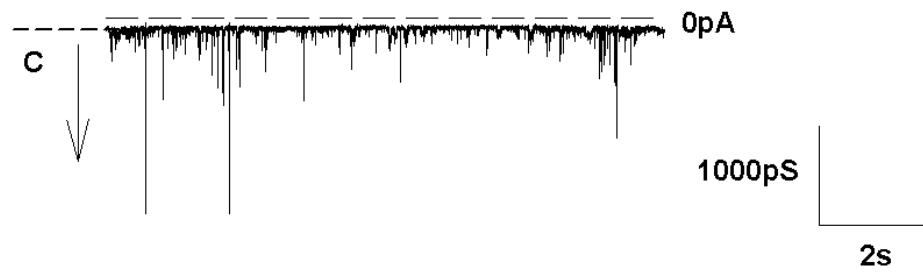
B.

P292C/S525C



C.

WT



We worked with the initial rationale for the D234C/Y329C mutant, that tethering of the plug could suppress the dynamics of the plug and affect channel kinetics. A purified sample of P292C/S525C was obtained and characterized using planar lipid bilayer. Unlike the open D234C/Y329C channel, P292C/S525C is a closed channel with a general behavior reminiscent of the WT. Current recordings acquired from the P292C/S525C mutant show a channel that dwells mostly at a closed level nearest to the zero current level. Similar to the WT, the P292C/S525C mutant trace is marked by frequent, random and short-lived opening transitions to various higher conductance levels (Fig 4.7). The rich kinetic behavior of the WT appears not to be suppressed in the P292C/S525C mutant. Rather the mutant displays the same kinetic features as the WT. This suggests that, despite the plug been putatively tethered to the wall it remains dynamic and still contributing to the kinetics of this mutant channel. It is important to note that the experiments were done on a sample treated with copper phenantroline. Copper phenantroline is an oxidizing agent that catalyzes S-S bond formation [127]. As a control, we performed some experiments on a sample not treated with copper phenantroline. We found no discernible qualitative difference between the recordings attained from copper phenantroline treated and non-treated P292C/S525C protein (data not shown).

4.3 Discussion

In this study, one aim was to probe the effect of tethering the plug on channel behavior. It was envisioned that tethering the plug would lock the plug in one position or orientation and impede its movement. From a previous study [108] we found that: 1) PapC is a dynamic channel with frequent opening events, 2) the whole PapC protein has

intrinsic flexibility, with domains that are capable of moving and blocking ion flux, 3) the opening events in PapC have a range of conductance levels, with some that are as high as the conductance levels observed in the domain deletion mutants, Δ plug and Δ helix, 4) these randomly occurring high conductance opening events were reasoned to be the result of the plug transiently dislocating out of the pore, and 5) the PapC pore is occluded by the plug but still remains an ion conducting channel. The potential routes for ion flux were reasoned to be the “water channels” at the barrel wall and plug interface. However, PapC is a highly dynamic protein and the opening transitions were postulated to be the action of the plug randomly “jiggling” within the pore and interrupting ion flow in these “water channels”. All of these observations point towards a highly dynamic plug that exerts its influence on the overall kinetics of the usher channel. Therefore, we hypothesized that by “locking up the plug”, the kinetics of the channel could be affected. This was expected to translate into a channel that was not only closed, but also less dynamic. With the plug tethered, the prediction was that the rich kinetic behavior of the WT would be suppressed. Furthermore, we anticipated that the transient high conductance opening events that emanate from the occasional displacement of the plug would also disappear from the channel kinetics signature.

However, our data revealed the opposite. It appears tethering the plug does not to suppress the rich kinetic behavior of PapC. Although there is a variation in the frequency and duration of the opening transitions among different experiments (Fig 4.3A, 4.4C and 4.7C), the closed channel with a baseline nearest to the zero current level and marked by opening transitions is a consistent hallmark among all WT recordings. Based on this

closed channel hallmark, a qualitative approach was adopted in comparing WT and mutant current recordings. From the two double cys mutants data, the effect of tethering the plug on channel kinetics depends on the location S-S bond or mutation site. The P292C/S525C mutant appeared similar to the WT. It had the hallmark closed channel behavior with frequent opening transitions (Fig 4.7). Due to the inherent variation in the WT as alluded to earlier, it was not possible to quantify and compare the frequency of opening events between the two channels. Nevertheless, looking at the P292C/S525C mutant alone, it is clear it remains a dynamic channel. Thus, disproving that locking up the plug would suppress its movement. It cannot be ruled out that a single S-S bond might not be enough to suppress the dynamics of the plug. Perhaps multiple S-S bonds would be required to sufficiently lock-in such a huge protein domain with effort made to avoid the residue sites that form the network of electrostatic interactions.

The open channel phenotype of the D234C/Y329C double cys mutant was evidently different from the WT (See Fig 4.3). The D234C/Y329C behavior was marked by an open level “O” which had the highest conductance level and with closing transitions from the “O” level towards the zero current level. The open channel behavior of this putatively plug tethered mutant was reminiscent of the domain deletion mutants, PapC Δ plug and PapC Δ helix, that exhibited open channel behavior featuring high conductance levels. The high conductance in the PapC Δ plug mutant was explained as the result of a gaping pore after deletion of the plug. For the PapC Δ helix mutant, the open behavior was postulated to be the result of partial plug dislocation after the deletion of the α -helix domain which plays a role in holding the plug in place [108]. This would also explain the

lower conductance relative to the Δ plug mutant. Therefore it was important to establish if the open channel behavior of D234C/Y329C was the result of the S-S bond introduced or the mere mutation of residues in or near the network of charged residues that interact and hold the plug in place [45]. This was done by characterizing the two single cys mutants, D234C and Y329C.

These two single cys mutants exhibited two distinctly different behaviors and served as effective controls to the double cys mutant D234C/Y329C. The Y329C mutant showed a channel behavior that was generally similar to the WT (Fig 4.4D). In contrast, the D234C displayed channel behavior similar to the double cys mutant, D234C/Y329C. The conductance of the “O” level was also nearly the same, with \sim 940 pS for D234C and \sim 980 pS measured for the D234C/Y329C mutant. Thus the combination of these similar observations implied that the open behavior of the double cys mutant was due to the single mutation on the D234 residue. The D234 residue forms part of constellation of charged residues that are proposed to interact and form a network of electrostatic interactions that hold the plug in a lateral position within the pore [45]. In fact, there are eight residues that are located on the plug, the β 5–6 hairpin, the α -helix domains and the barrel wall and interact in specific ways to link the plug to the other domains. The first set of interactions is the network that links the plug to the hairpin and barrel wall. These residues are, Glu361 (barrel wall), Lys339 (barrel wall), Asp234 (hairpin), and Arg303 (plug). The second set of interactions links the plug to the α -helix domain [45] and involve Arg237 (hairpin), Glu467 (helix), Arg305 (plug), and Asp323 (plug). The D234 residue is in the first network that links the plug to the hairpin and the barrel wall. Based

on crystal structure data D234 resides right at the center of the first interactive network (See Fig 4.8). This negatively charged residue can potentially interact with two positively charged residues, Arg303 located on the plug domain and Lys339 located on the barrel wall. Therefore it is reasonable to speculate that a single mutation to the D234 was enough to disrupt this intricate network of interactions and allow the plug to partially dislocate. A deletion of the α -helix domain resulted in an open channel which we attributed to the disruption of the network of interactions that hold the plug in place. Because the D234C mutant has a much lower conductance than the Δ helix, the single mutation to the D234 site potentially resulted in a disruption to the electrostatic interactions that was not sufficient to cause plug displacement to the extent an α -helix deletion does. Nevertheless, the D234 residue is critical in the gating of the channel and plays a role in plug displacement. Our results with the D234C highlight the relevance of the network of electrostatic interactions in channel gating and plug displacement. To test this hypothesis further, alanine scanning mutagenesis on the remainder of the interacting residues could reveal if indeed all of these residues are important in gating the usher. We could learn if there is potential for redundancy since most of the interacting residues are still capable of interacting with other oppositely charged residues. The D234 residue bridges the interaction between the barrel wall and the plug. It is at the center of the axis of interaction with K339 and R303, on either side.

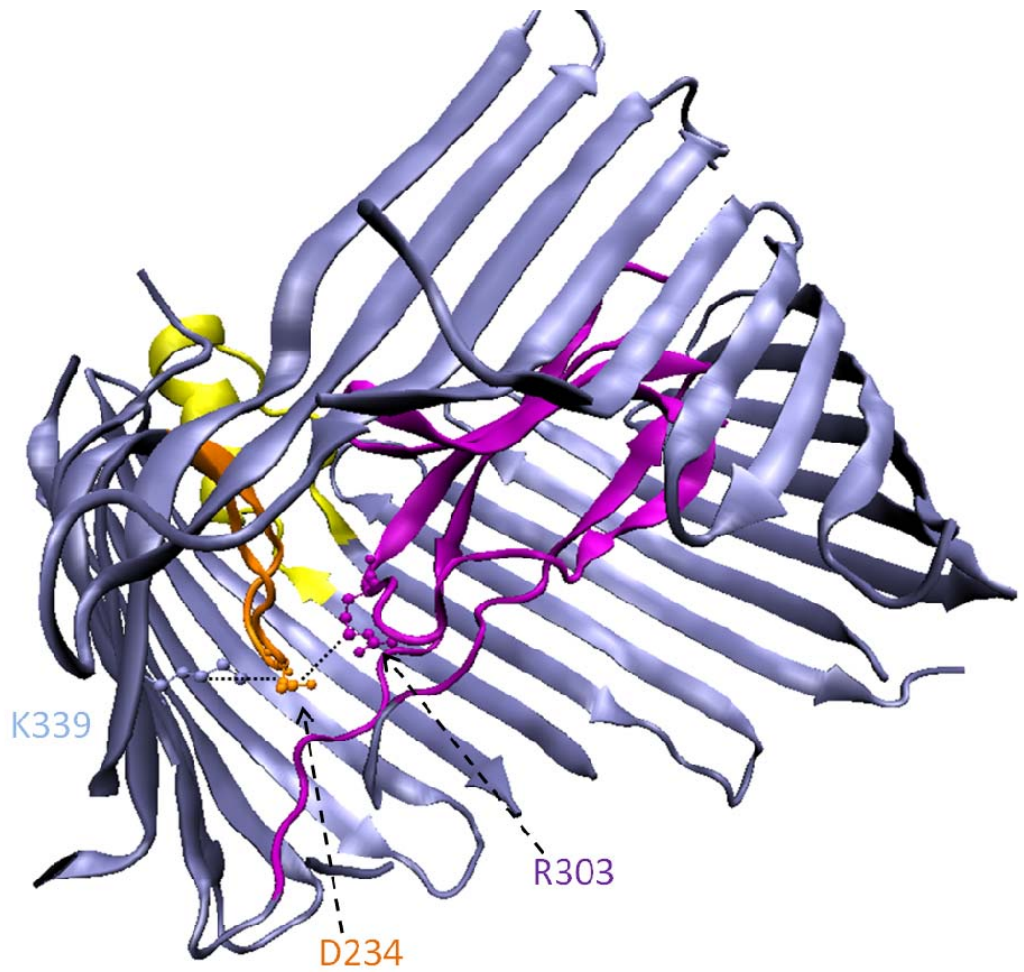


Fig 4.8 Molecular representation of some of the electrostatic interactions that hold the plug in place. D234, K339 and R303 are shown in the ball and stick format. Residues are color coded according to their domain location. The dashed black lines represent the possible electrostatic interactions between the three residues. The image was generated from a tilted side view.

Because of its unique position, it would be informative to investigate a double mutation on K339 and R303 and explore the importance of D234 to this network. It is possible that single mutations to sites that are not right at the epicenter of interaction might not yield an open phenotype. However, a focused effort on mutating this network will reveal the “molecular lock” that clutches the plug in place.

Chapter 5

Modulation of the usher channel by chaperone – subunit complexes

5.1 Introduction

One of the remaining challenges in understanding the mechanism of pilus biogenesis is mapping out the precise events involved in the chaperone-subunit complex induced activation of the usher. Activation of the usher results in conformational changes in the resting closed usher channel that thrust it into a prepared state for pilus biogenesis [113]. Pilus assembly occurs in a top down manner, with the ordered recruitment of subunits to the usher ensuring the building of functional pili, where the adhesin subunit is positioned at the tip of the nascent fiber [97]. This ordered recruitment of pili subunits is coordinated by the differential affinity of the chaperone-subunit complexes to the usher, with the adhesin complex, PapDG having the highest affinity to the usher [91, 97] and ensuring PapDG is incorporated first into the pilus, followed by the rest of the tip fibrillum and the rod structural components recruited last (See table 5.1).

The PapC periplasmic N-terminal globular domain (residues 1-125) has long been thought as the initial binding region for the chaperone-subunit complexes, with the C-terminal also capable of binding chaperone-subunits and providing the platform for DSE to occur between incorporated subunit and the incoming chaperone – subunit [45, 97, 98, 128, 129]. Although PapDG is the first one to bind, PapDF and PapDK have been shown to be capable initiators of pilus biogenesis, however the usher discriminates in favor of PapDG to ensure formation of functional pili [91, 95].

Following binding of the first adhesin complex to the NTD, the plug domain is believed to dislocate from the pore and position in the periplasm where data suggest it

forms a plug-NTD complex that recruits and shuttles subsequent chaperone-subunits to the C-terminal domains [45, 100, 101]. This would indicate a further role for the plug and thus making plug repositioning a major outcome of chaperone – subunit induced pilus biogenesis initiation/activation. Questions still remain on the active state of PapC prior to pili biogenesis. PapC is believed to be in an already active state and primed up for pilus biogenesis, in contrast to FimD which has strict requirement for the adhesin subunit to initiate pilus biogenesis [91, 113]. Thus with PapC, it remains unclear if and how activation of the usher occurs, prior to the necessary conformational changes required to cause plug displacement out of the pore.

In light of the plug domain's channel gating role [45, 108], electrophysiology offers a unique approach to explore the hypothesis that gating from the usher closed state to a pilus biogenesis competent open state is modulated by chaperone-subunit substrates interaction with the periplasmic globular domains. By using channel kinetics as an assay, we can determine the basal activity of the usher and compare it with its activity post substrate addition. This approach allows a real time *in vitro* single molecule analysis of the effect of various chaperone-subunits on the usher and assessment of which chaperone-subunit complex(es) activates the usher. The expectation was that, since PapC has a closed channel signature behavior, any substrate induced conformational changes or domain movements would translate into marked differences in the channel character and its kinetics. With the integration of electrophysiology data acquired from the structure – relationship studies on PapC domain deletion mutants, we can predict the chaperone-subunits involved in usher activation and subsequent plug displacement. Thus the scope

of our effort was focused on finding chaperone-subunit complexes that had a modulating effect on the electrophysiological behavior of the usher.

5.2 Results

5.2.1 PapDG chaperone-subunit complex does not display modulating effect on PapC usher channel behavior

In order to find out which subunits modulate the usher channel behavior we acquired purified chaperone-subunit complexes in solution. These complexes were purified in a 1:1 stoichiometric ratio and verified to be bound together (See chapter 2). The first complex to be tested was PapDG, a complex of the chaperone and the adhesin subunit. PapDG is the first complex to bind to the usher NTD and CTD [129] and has the highest affinity to the usher. Since this complex has been shown to interact with the usher in various in-vitro assays, we hypothesized this complex had the highest probability of causing in-situ modulation of the PapC usher behavior in an electrophysiological assay.

The planar lipid bilayer technique was used to test the effect of PapDG on the usher. Channel recordings of the WT usher were attained using the planar lipid bilayer channel recording protocol (See chapter 2). This was used as the basal activity control, prior to addition of the chaperone-subunit complex substrate. To recreate more physiological conditions, 150 mM KCl ionic solution was used instead of 1M KCl solution, which was used for most of the characterization work on PapC WT and mutants. With the channel still inserted into the lipid bilayer, PapDG complex was added to bilayer chamber on the

Chaperone-subunit complex	K_d (nM)
PapDG	56-90
PapDF	670
PapDE	1300
PapDA	1500

Table 5.1 Chaperone-subunit complex K_d. The final concentration of each subunit complex in the bilayer chamber was equal or above the K_d listed above [91, 113].

cis side only. Careful consideration was made to ensure that the overall PapDG concentration in the chamber was equal or above the PapDG K_d of 56 – 90 nM [91, 113]. Channel recordings of the lipid bilayer reconstituted usher, with the chaperone-subunit complex added into the chamber were then attained for up to 60 mins and compared to the basal activity control recordings attained before substrate addition. A qualitative approach was applied in comparing the recordings with the general channel kinetics pattern being the main criterion of analysis.

From a total of 21 trials we found no overall change in the usher channel signature kinetics before and after substrate addition. In 150 mM KCl conditions the WT control still exhibited the hallmark PapC closed channel behavior as observed in 1M conditions. The channel behavior was marked by a prominent baseline at the zero current level with frequent downward current deflections to various current levels representing channel opening transitions at negative voltage (See Fig 5.1A). Despite the reduction in the buffer solution ionic strength, a strong current signal was attained and the rich kinetic behavior of PapC WT in 1M KCl maintained in these lower ionic strength conditions. This behavior appeared to be generally retained even after addition of PapDG substrate. Recordings were attained in 5 – 10 min intervals for up to 60 min after chaperone – subunit complex addition and a representative trace is shown in Fig 5.1B. After addition of PapDG on the *cis* side only there was no difference in the overall signature behavior of the WT or its channel kinetics. In fact, both traces in Fig 5.1A and 5.1B look similar in general character.

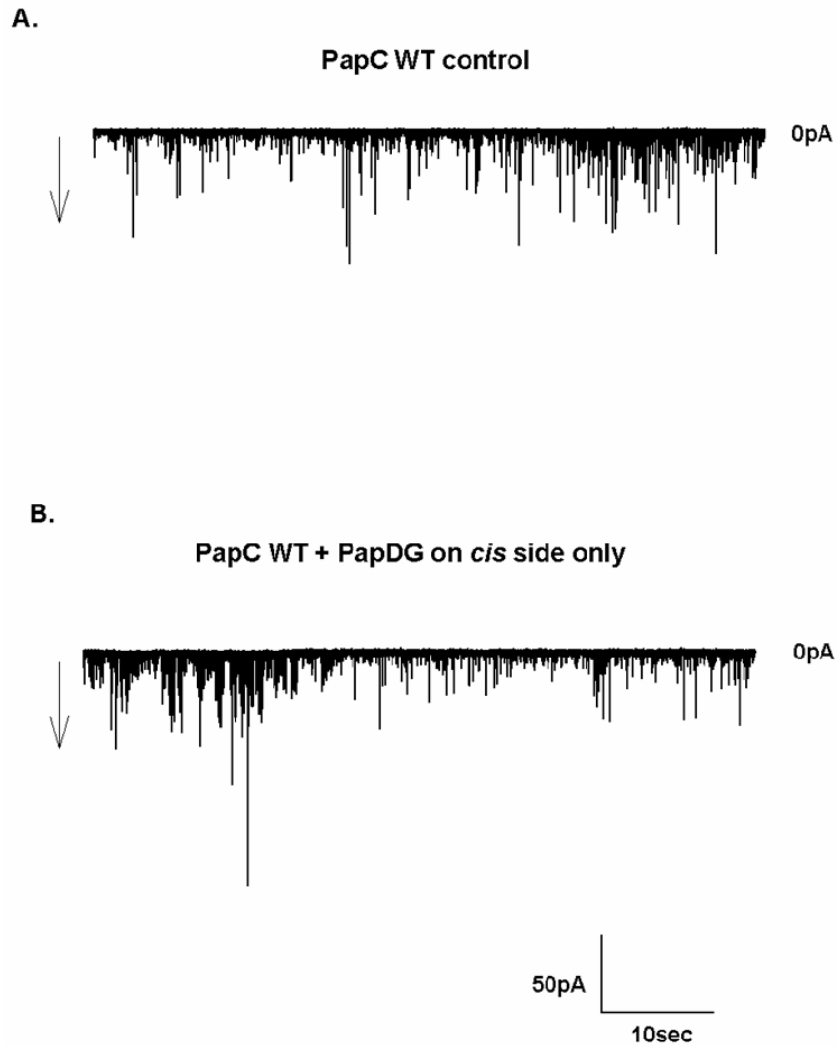


Fig 5.1 *PapDG* addition does not show a modulating effect on *PapC* usher channel. Shown are representative traces before and after substrate addition from one selected experiment. **A.** Current recording of an inserted *PapC* WT channel before *PapDG* addition. The downward arrow shows the direction of opening events at negative voltage. **B.** Current recording of *PapC* channel after addition of *PapDG* complex on the *cis* side. All recordings were acquired in 150mM KCl with a voltage of -50mV applied.

Although we do not have direct evidence to demonstrate the orientation of the usher when it reconstitutes into the lipid bilayer, we support the idea that the usher inserts into the planar lipid bilayer with the extracellular side first. We propose this offers a more energetically favorable orientation for entry into the bilayer, which leaves the periplasmic sided globular domains exposed on the *cis* side. This was our premise for adding PapDG on the *cis* side only where the N- and C- terminal domains are exposed. However, to rule out the possibility of chaperone – subunit complex binding and modulation been affected by channel orientation within the bilayer, PapDG substrate was added to both sides of the chamber. In these experiments channel recordings acquired before and after PapDG addition to both *cis* and *trans* sides showed no difference in the overall signature behavior or kinetics. The traces acquired before and after substrate addition show the same closed channel behavior with a major baseline nearest the zero current level, and marked by frequent downward opening transitions to various current levels at negative voltage (See Fig 5.2A and 5.2B). This allowed us to rule out orientation as a factor in the modulation of the usher by PapDG in our assay.

5.2.2 Addition of PapDG, F,E,K,and A chaperone – subunit complexes does not display a modulating effect on the usher channel behavior

With the highest affinity chaperone-subunit complex not showing a modulating effect on the PapC channel behavior, we sought to explore the possibility of the other pili chaperone-subunit complexes having an effect on the usher channel electrophysiology signature. In addition to PapDG, PapK, and PapF tip subunits have been shown to act as alternative initiators of non-functional pili in the absence of the PapG [95]. After PapDG,

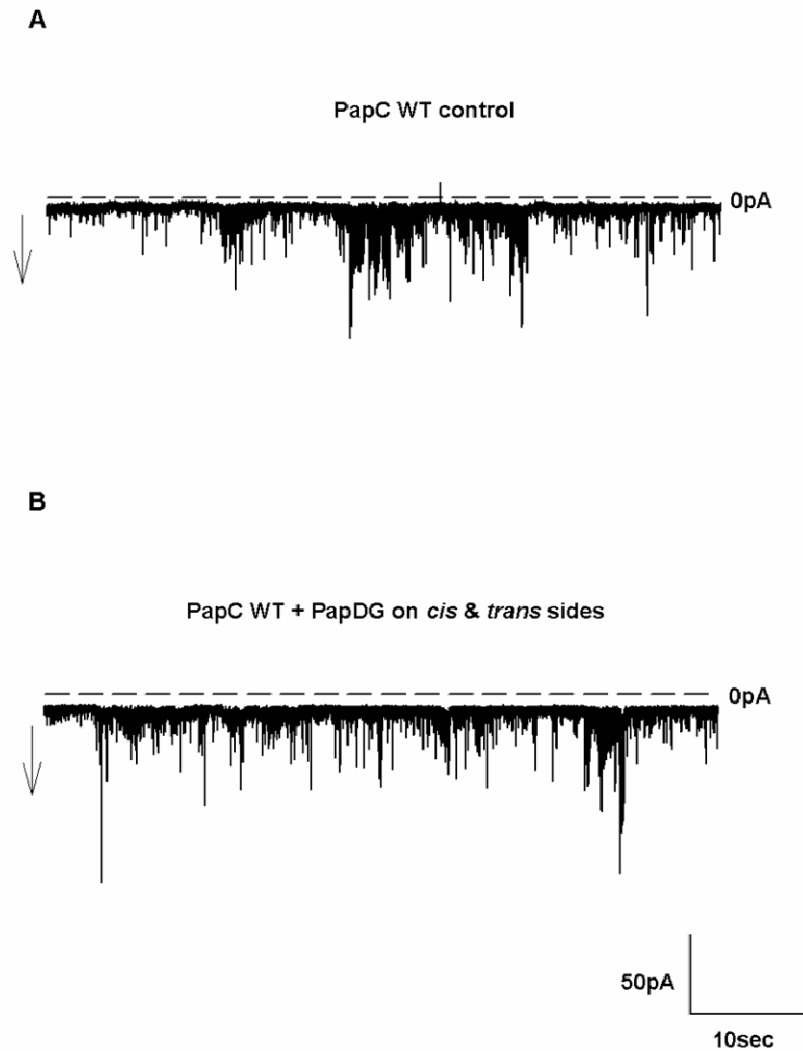


Fig 5.2 *PapDG* addition on both *cis* and *trans* sides does not show modulation effect on *PapC* usher channel behavior. Shown are representative traces before and after substrate addition from one selected experiment. **A.** Current recording of an inserted *PapC* WT channel before *PapDG* addition. The downward arrow shows the direction of opening events at negative voltage. **B.** Current recording of *PapC* channel after addition of *PapDG* complex on both *cis* and *trans* sides. The dashed lines mark the zero current level. All recordings were acquired in 150 mM KCl with a voltage of -50 mV applied.

PapA has the second highest affinity to the usher and is most abundant in the periplasm prior to biogenesis. However differential affinity ensures it does not out-compete the adhesin subunit in the recruitment to the usher (See table 5.1) [91, 129].

We decided to explore if any one of these subunits could potentially bind to the usher and modulate its channel behavior in our assay. A blend of PapDG, PapDF, PapDE, PapDK, and PapDA was made and added to the bilayer chamber and channel recordings acquired for comparison with the basal activity recording of the usher. Our ultimate aim was to pin-point the specific subunit(s) responsible for any observed effect, through subsequent exclusion of each chaperone-subunit complex from the mixture. In the bilayer chamber each chaperone-subunit complex had a final concentration that was equal or above its K_d to the usher (See table 5.1). For example for PapDG, the final protein concentration added to the bilayer was in the range of 57 – 570 nM. However, similar to the PapDG outcome, the chaperone-subunit complexes' mixture did not show a modulating effect on usher channel behavior. The recordings attained before and after substrate addition displayed similar character. In the representative traces shown in Fig 5.3A and 5.3B, the same closed channel behavior marked by downward opening transitions was observed at negative voltage. Despite having all the subunits present in the chamber, none of them was able affect the channel kinetics of the usher channel in this assay. Thus we could not demonstrate a modulating effect of any of the Pap chaperone-subunit complexes on the usher channel using electrophysiology.

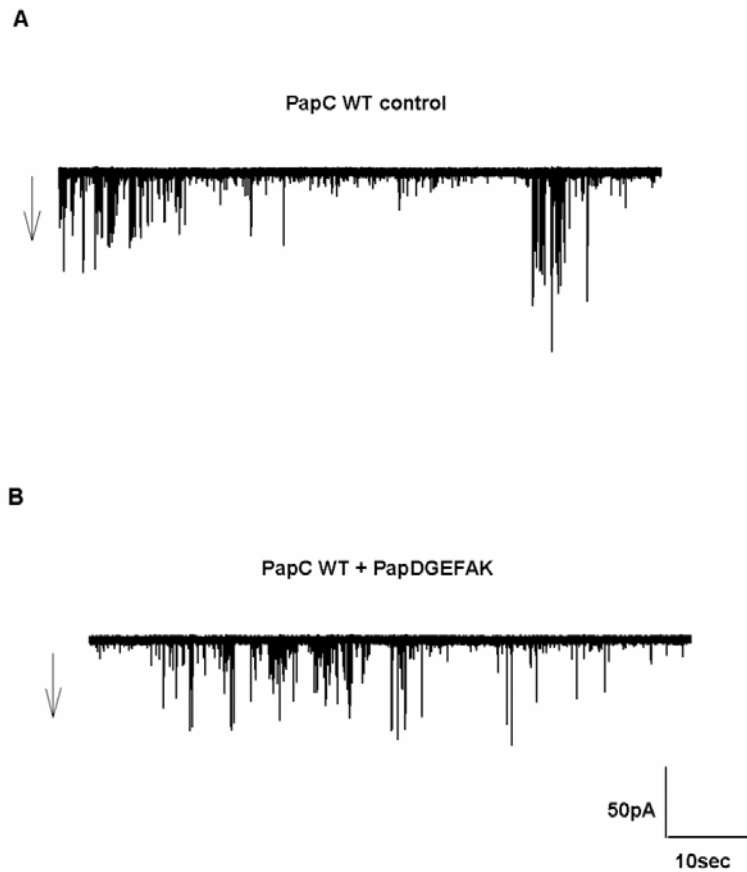


Fig 5.3 *PapD-GFEKA* chaperone-subunit complexes fail to modulate *PapC* usher channel activity. Shown are representative traces before and after substrate addition from one selected experiment. **A.** Current recording of an inserted *PapC* WT channel before *PapDG,F,E,K,A* mixture addition. The downward arrow shows the direction of opening events at negative voltage. **B.** Current recording of *PapC* channel after addition of *PapDG,F,E,K,A* complexes on the *cis* side. All recordings were acquired in 150mM KCl with a voltage of -50 mV applied.

5.2.3 Fim CH and FimCG chaperone-subunits do not show modulation effect on the FimD usher channel

Although we sought out to test and demonstrate chaperone-subunit modulation on the usher channel with the Pap system, the Fim system from Type 1 pili, is generally thought to be the one more likely to undergo chaperone-subunit induced activation that culminates in plug displacement [113]. Suggestions have been put forward that PapC might exist in an already activated state that does not require chaperone-subunit induced activation. We therefore sought to use the Fim system to test chaperone – subunit modulation of the usher channel in electrophysiology. This was done using the same experimental designs applied with PapC.

The adhesin subunit complex, FimCH was acquired and used in planar lipid bilayer experiments. FimD was initially characterized in 150 mM KCl before FimCH substrate was added to the *cis* side. Recordings of the usher channel after addition of substrate were attained and compared to the basal activity controls using the same qualitative approach applied to the Pap system. Similar with the Pap results, the recordings before and after FimCH addition showed no effect of the substrate on the usher channel kinetics. Both traces exhibited the closed channel behavior akin to PapC, with a well defined baseline close to the zero current level marked by downward current deflections that represent channel opening transitions at negative voltage. There was no indication of a gated open channel after addition of FimCH in planar lipid bilayer. We also tested the effect of the second Type 1 pili tip subunit FimG on usher channel activity using patch clamp. With

patch clamp substrate addition can be done in two ways. Substrate can be added in the pipette solution prior to locating the blister and making seals in buffer B. Substrates can also be perfused into the bath solution or added directly into the bath solution. FimD was reconstituted in liposomes and the basal activity recorded before purified FimCG chaperone-subunit complex was added to the bath side. Recordings attained before and after FimCG substrate addition were compared and did not show any distinct difference in channel behavior or kinetics (See Fig 5.5A and 5.5B). Both traces showed the typical closed channel activity, with a well defined baseline closest to zero current level, marked by downward channel opening transitions.

Various experimental designs were applied in probing the modulation effect of chaperone-subunit complexes on the usher. Table 5.2 shows a summary of all the various experiments attempted. In these experiments chaperone-subunits were added on one side or both sides of the bilayer. In planar lipid bilayer, substrates were added on either the *cis* side or both the *cis* and *trans* side after recording the WT behavior. With patch clamp, substrate additions on one side of the bilayer was done by either adding chaperone-subunit complexes into the pipette solution prior to making seals or to the bath solution after seals were made.

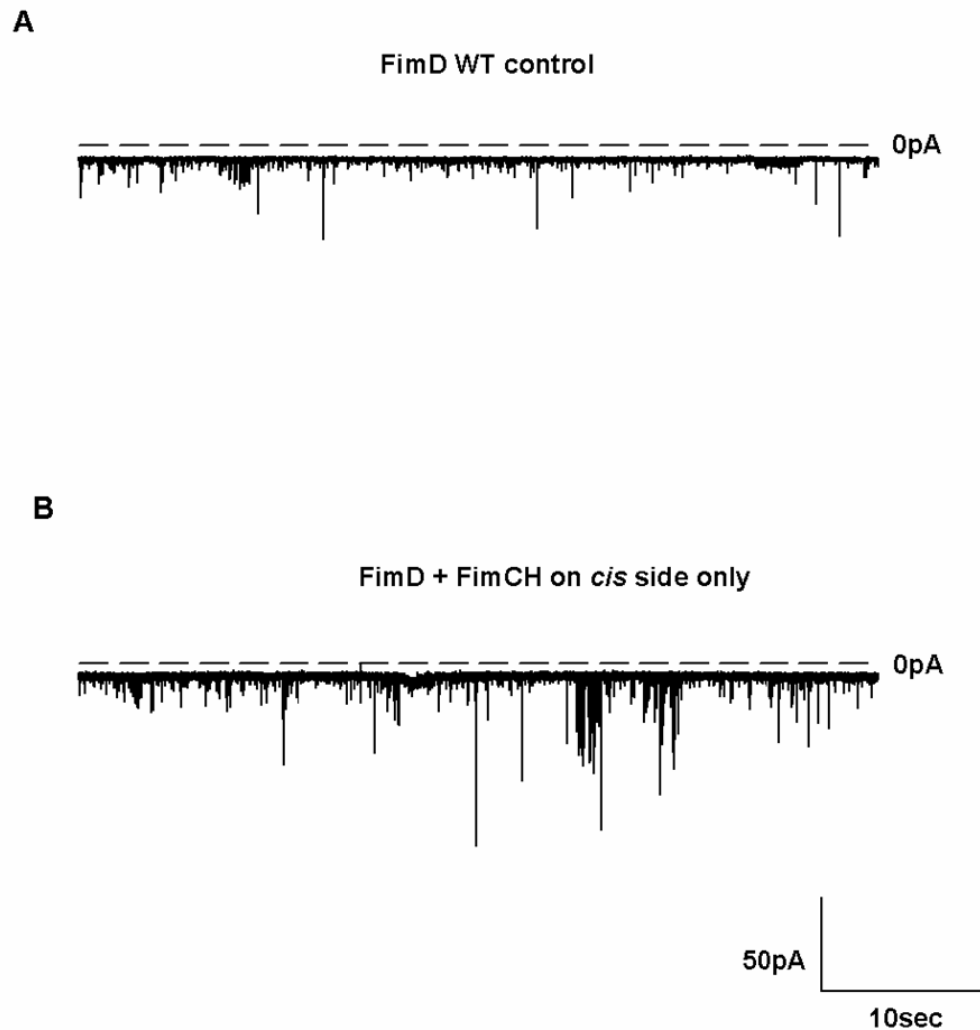


Fig 5.4 *FimCH* chaperone-subunit complex does not modulate *FimD* usher channel activity. Shown are representative traces before and after substrate addition from one selected experiment. **A.** Current recording of an inserted *FimD* usher channel before *FimCH* addition. **B.** Current recording of *FimD* usher channel after addition of *FimCH* chaperone subunit complex the *cis* side. The dashed lines mark the zero current level. All recordings were acquired in 150mM KCl with a voltage of -50 mV applied.

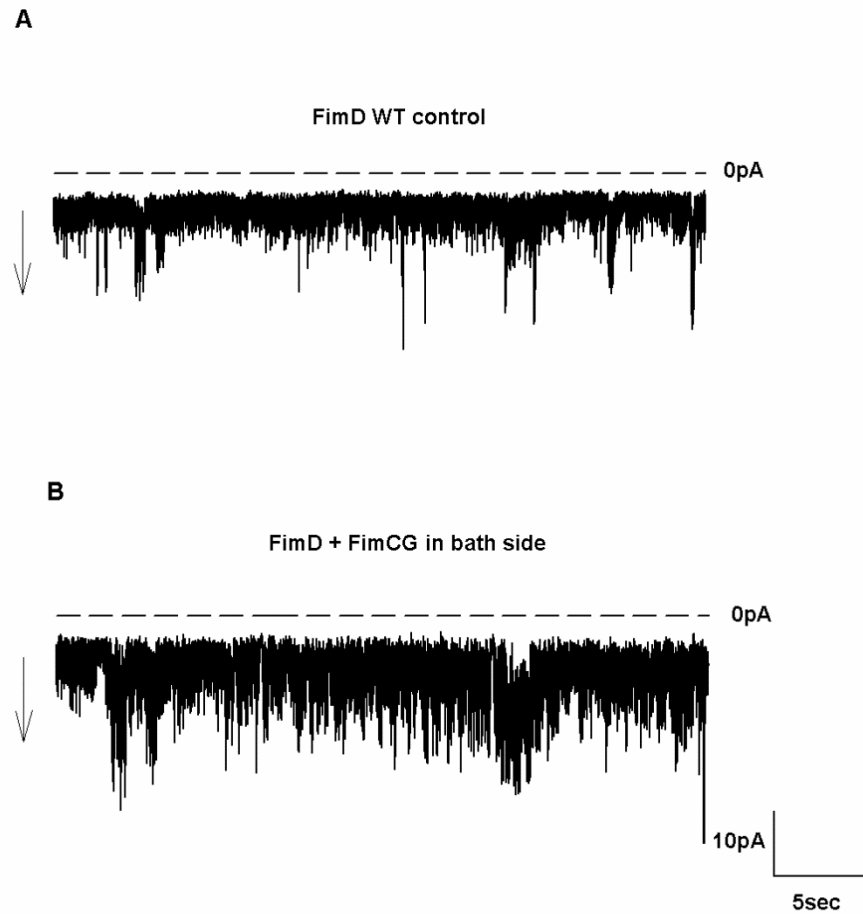


Fig 5.5 *FimCG* chaperone-subunit complex does not show a modulating effect on *FimD* usher channel activity. **A.** Patch clamp recording of liposome reconstituted *FimD* usher channel before addition of chaperone-subunit substrate. **B.** Patch clamp recording of the same *FimD* usher channel in (A), after addition of *FimCG* complex in the bath. The dashed lines represent the zero current level and the downward arrows show direction of opening transitions at negative voltage. All recordings were done in Buffer A (150 mM) with a -15 mV voltage applied.

	Planar lipid bilayer			Patch clamp		
	substrate added	on <i>cis</i> side only	on (<i>cis/trans</i>)	substrate added	in bath	in pipette
PapC	PapDG	(21)	(5)		(ND)	(ND)
	PapDGFEKA	(13)	(6)		(ND)	(ND)
	PapC and PapDG pre-incubated	(5) – no insertions	(3) – no insertions		(ND)	(ND)
FimD	FimCH	(4)	(0)	FimCH	(7)	(3)
	FimCG	(2)	(0)	FimCG	(11)	(4)
	FimCG/CH	(0)	(0)	FimCG/CH	(3)	(ND)
Δ Plug	Δ Plug + PapDG	(5)	(3)		(ND)	(ND)

Table 5.2 A summary of the various experimental designs applied to study usher modulation by the chaperone-subunit complexes. Patch clamp was used to study the Fim system and planar lipid bilayer used with both Fim and Pap systems. The number of experimental trials is shown as numerals in parenthesis with (0) meaning experiments were attempted but no high quality recordings were attained. (ND) denotes experiments that were not attempted.

5.3 Discussion

The binding of chaperone-subunits to the usher NTD is thought to activate the channel and gate the pore open through a conformational change that releases the plug from channel lumen and repositions it in the periplasm [45, 100]. This has been proposed in most models of pilus biogenesis and supported strongly by the co-crystal structure of the Type 1 pili FimD usher and its cognate substrate FimCH which shows the plug completely displaced to the periplasmic side [100]. While these data show strong evidence of plug displacement during pilus biogenesis, the precise details of this chaperone – subunit induced plug displacement remain unclear. Combined with our prior work on PapC and its domain deletion mutants, electrophysiology provides a unique real time single molecule analysis assay that can elucidate the dynamics involved in this chaperone-subunit induced conformational change. By studying channel ion flux patterns, conformational changes such as plug displacement can be reported in real time through changes to the basal channel kinetics pattern after introduction of a modulating substrate. Since PapC is a closed channel we hypothesized that chaperone – subunit complexes shown to bind to the usher in other *in vitro* assays would trigger opening of the channel through plug displacement resulting in open channel kinetics. The expectation was that if indeed, chaperone-subunit complexes activate the channel and primes it ready for pilus biogenesis by releasing the plug out of the channel lumen, open channel kinetics akin to the PapC Δ plug or PapC Δ helix would be acquired following substrate addition in our assay. However from a comprehensive set of diverse experimental designs (see table 5.2) we did not observe any distinct difference in the

channel behavior of PapC or FimD usher after addition of chaperone-subunit complexes. In most experiments, the usher channel behavior was similar before and after substrate addition. The usher retained the signature closed channel character with marked baseline nearest the zero current level, with frequent opening transitions to various current levels. We did not observe a shift of the current signal baseline to a higher conductance state in all of the various experiment designs with PapC or FimD ushers.

Our analysis of the current recordings before and after substrate addition was based on a qualitative approach. Due to the intrinsic dynamic nature of PapC, quantifying the frequency of opening events through amplitude histograms proved an unreliable tool. PapC channel has been shown to have behavior diversity with an inherent tendency to shift to various levels of activity over any given time (See chapter 3). Within a single recording, there can be variability in the frequency, size, and duration of opening events over time. This shifting in kinetics is completely random and shows no pattern or correlation to any specific factor. Therefore we limited our analysis to monitoring conductance states and general current fluctuation patterns before and after substrate addition without a quantitative analysis of the frequency of channel opening events. Nonetheless, because we did not observe a real time opening of the channel in both FimD and PapC, it is an open question if the chaperone-subunits are indeed binding to the usher. Our assays are limited in this regard as they do not give any indication of whether there is any interaction between the chaperone-subunit complex and the channel protein inserted in the lipid bilayer. While chaperone-subunit complex concentrations were kept at equal or in excess of K_d values we could not influence the probability of the protein

complex in chamber solution randomly targeting the site where the channel protein in the lipid bilayer is located. In some planar lipid bilayer experiments stirring was applied to increase the probability of interaction, but this also ran the risk of having more channel insertions into the lipid bilayer and was not pursued further. Nevertheless, another alternative explanation to our negative results was that interaction of the chaperone – subunit complex and the usher channels could occur, but was not causing any conformational changes that could be reported in our assays with either PapC or FimD. We therefore tested whether chaperone-subunit complexes could enter an open pore and plug it shut or transiently block the pore. We acquired recordings of before and after PapDG addition with the PapC Δ plug mutant. In tandem with previous WT usher results, we found no difference between the before and after PapDG addition recordings with the Δ plug mutant (data not shown). This therefore enhanced the notion that the chaperone-subunit complexes might not be interacting with the lipid bilayer inserted usher channel under our assay conditions. We attempted to attain recordings with the FimD:C:H quaternary complex in planar lipid bilayer, but we were not able to attain insertions. This indicated the complex might not be able to reconstitute in a planar lipid bilayer. This complex was then preliminarily characterized in patch clamp and showed promising results of an open FimD channel in one experiment (data not shown). However, we were not able to reproduce this result. Nevertheless, focus should now be centered on this complex and find ways to reconstitute it in planar lipid bilayers or liposomes. An alternative that might help in the reconstitution of the usher is reconstitution in native vesicles. It has been demonstrated that PapC *in vitro* pore activity is enhanced in a more native environment [88]. The use of patch clamp on PapC native vesicles and the

FimD:C:H complex should be explored in investigating the modulating effects of chaperone-subunit complexes on the usher.

Chapter 6

Concluding remarks

Urinary tract infections are one of the most common bacterial infectious diseases that plague the human population. This disease exerts an enormous economic and health burden. In the United States, health care costs attributed to UTI were estimated to be over \$2 billion in the year 2000 [11, 12]. UTI disproportionately affect women and nearly half of the female population will experience a UTI at least once in their life time [9, 10]. This is further compounded by the high risk of UTI recurrence following treatment. It has been reported that 20 – 30 % of individuals with an acute infection will suffer a recurrence of the infection within 3 – 4 months and some individuals will continue to struggle with recurrence over a whole lifetime. Although host genetic and lifestyle factors contribute to the occurrence of infections and their varying degrees of complication, an emerging concern is the increase antibiotic resistance in UPEC, the major causal agent of UTI. In the past, a simple antibiotic course had proven to be an effective regimen in treating bladder infections. However, there has been an increase in the prevalence of antibiotic resistant UPEC strains [130] which threatens to enhance the incidence of chronic and recurrent infections.

A major virulence factor in the colonization of the urinary tract is the pili. Type 1 and P pili mediate the attachment of bacterial cells to the epithelial surface of the bladder and kidney, respectively. Within the bladder type 1 pili-mediated binding to the urothelium elicits a host response that results in self-inflicted breach of the mucosal barrier, allowing UPEC to opportunistically invade the urothelium and establish IBCs and latent intracellular reservoirs [6]. With upper UTI, P pili are cardinal in the binding of UPEC to the kidney tissue epithelial surface prior to colonization. It is believed that Type 1 and P

pili act in synergy to colonize and persist within the kidney, where type 1 pili mediate bacterial cell-to-cell interaction.

The composite type 1 and P pili structures are assembled and secreted to the cell surface through the bi-component chaperone/usher system. The usher is the outer membrane transport protein, which performs the dual function of pilus assembly and simultaneous translocation across the OM. As such, considerable focus has been centered on understanding the usher's mechanism of pilus biogenesis. Since bacterial adhesion to host epithelial cells within the urinary tract is a critical step in bacterial colonization, understanding the mechanism of pilus biogenesis is the precursor in developing novel strategies to block UPEC adhesion. This offers the potential to develop new therapeutics that could directly target pilus assembly or the host – pathogen interface and help counter acute, chronic or recurrent infection.

The usher is the site of assembly and provides a translocation channel for the nascent pilus during biogenesis. Based on the crystal structure of PapC, the usher is occluded by a plug domain and is closed shut prior to activation by the first chaperone-subunit complex. In addition the crystal structure of the FimD:C:H complex provides a snapshot of pilus biogenesis and demonstrates that plug displacement occurs during pilus assembly. This has prompted inquiry on the gating mechanism of the usher and the precise molecular details of how this critical conformational change arises. Furthermore, another important source of inquiry, is understanding how the chaperone-subunit complexes activate the usher. This will help reveal the molecular choreography involved in gating the usher.

To date, a diverse and detailed bank of information on the PapC usher has been gathered over the last two decades. Genetic, biochemical, and structure studies (among others), have shared a wealth of information on the properties of the chaperone/usher pathway. However, the mechanistic details on the molecular steps involved in pilus biogenesis is lacking. The work presented in this dissertation has shed more insight on the mechanism of pilus biogenesis by studying the PapC usher channel in electrophysiology. As a result, the use of electrophysiology as an investigative tool represents a novel approach that was reported for the first time in 2009 [108]. Electrophysiology is a canonical technique in studying the properties of pore forming proteins. Unlike most *in vivo* assays, electrophysiology allows for a real-time single molecule analysis. The technique is an assay that measures the electrical activity of a pore/channel and each channel can generate a signature current signal pattern. By employing a structure function relationship study, we have used this assay to investigate the channel properties of PapC and engineered mutants to investigate the molecular details behind channel gating. We have also attempted to demonstrate the modulation of the usher by its cognate chaperone – subunit complexes.

Our data show that PapC forms an ion conducting pore. The WT channel was able to generate a current signal under voltage clamp conditions. In addition to prior studies done by other workers, my work lends support to the ascribed channel function for the usher. We have also found that PapC WT is mostly in closed state, but is highly dynamic. The closed state observation also supports previous assertions made by various authors that PapC requires some activation that primes it ready for pilus biogenesis. The dynamic

behavior found in PapC WT and the domain deletion mutants was attributed to the rapid, frequent, and random movement of various domains. Opening and closing transitions were observed for all PapC constructs investigated and point to a molecular machine that has an intrinsic flexibility and domains with high kinetic potential. And herein the advantage of electrophysiology is shown. Liposome swelling assays done on PapC only reveal the presence of pore/channel, but cannot report the channel dynamics as shown here. These conclusions shall lead to a greater appreciation of the dynamic nature of the usher translocation machinery.

Our most significant observation was that the plug domain gates the channel shut. The Δ plug mutant showed open channel behavior with an extremely high conductance, demonstrating that when the plug is removed, PapC forms an open pore that should be large enough to allow passage of the folded pilus subunits. The plug is located within the channel lumen but is also capable of occasional displacement without any catalyst. This conclusion was derived from the Δ helix mutant that initially showed closed channel behavior, but progressively went into open channel mode with a high conductance. We also found the same high conductance Δ plug-like openings in the WT recordings, indicating that the “molecular lock” that holds the plug in place might be easily loosened. This “molecular lock” is proposed to be the network of electrostatic interactions between residues on the β 5-6 hairpin, plug, α -helix and the barrel wall. Our data strongly suggest that indeed this network of residues constitute part of the usher gating mechanism. Recordings from the Δ helix mutant which showed opened channel behavior could be the result of a disruption to this network due to the deletion of the α -helix residue E467 that

forms part of this network. Site-directed mutagenesis of the D234 residue, further reinforced this notion. The D234C mutant showed opened channel behavior proving that disturbing the electrostatic network loosens the plug causing plug dislocation and the formation of a more open pore. My work projects this network of electrostatic interactions as a prominent aspect in the gating of the usher. We propose a greater focus on the residues that comprise this network through a comprehensive functional analysis of each residue.

In conclusion my work has demonstrated a novel application of electrophysiology to study the usher channel. Although, the experiments presented in this dissertation did not yield conclusive results, regarding the modulation of chaperone-subunit complexes on the usher. The data presented in this dissertation set the foundation for more structure function relationship studies on PapC using electrophysiology or other phenotypic assays. This approach will reveal the mechanistic molecular details behind the usher gating mechanism and shed further insight on pilus biogenesis.

References

1. Dhakal, B.K., R.R. Kulesus, and M.A. Mulvey, *Mechanisms and consequences of bladder cell invasion by uropathogenic Escherichia coli*. Eur J Clin Invest, 2008. **38 Suppl 2**: p. 2-11.
2. Bower, J.M., D.S. Eto, and M.A. Mulvey, *Covert operations of uropathogenic Escherichia coli within the urinary tract*. Traffic, 2005. **6**(1): p. 18-31.
3. Schilling, J.D., S.M. Martin, C.S. Hung, R.G. Lorenz, and S.J. Hultgren, *Toll-like receptor 4 on stromal and hematopoietic cells mediates innate resistance to uropathogenic Escherichia coli*. Proc Natl Acad Sci U S A, 2003. **100**(7): p. 4203-4208.
4. Haraoka, M., L. Hang, B. Frendeus, G. Godaly, M. Burdick, R. Strieter, and C. Svanborg, *Neutrophil recruitment and resistance to urinary tract infection*. J Infect Dis, 1999. **180**(4): p. 1220-1229.
5. Hang, L., M. Haraoka, W.W. Agace, H. Leffler, M. Burdick, R. Strieter, and C. Svanborg, *Macrophage inflammatory protein-2 is required for neutrophil passage across the epithelial barrier of the infected urinary tract*. J Immunol, 1999. **162**(5): p. 3037-3044.
6. Mulvey, M.A., J.D. Schilling, J.J. Martinez, and S.J. Hultgren, *Bad bugs and beleaguered bladders: interplay between uropathogenic Escherichia coli and innate host defenses*. Proc Natl Acad Sci U S A, 2000. **97**(16): p. 8829-8835.

7. Bien, J., O. Sokolova, and P. Bozko, *Role of uropathogenic Escherichia coli virulence factors in development of urinary tract infection and kidney damage*. Int J Nephrol, 2012. **2012**: p. 681-473.
8. Nicolle, L.E., *Urinary tract infection in geriatric and institutionalized patients*. Curr Opin Urol, 2002. **12**(1): p. 51-55.
9. Foxman, B., R. Barlow, H. D'Arcy, B. Gillespie, and J.D. Sobel, *Urinary tract infection: self-reported incidence and associated costs*. Ann Epidemiol, 2000. **10**(8): p. 509-515.
10. Foxman, B., *Epidemiology of urinary tract infections: incidence, morbidity, and economic costs*. Am J Med, 2002. **113 Suppl 1A**: p. 5S-13S.
11. Scholes, D., T.M. Hooton, P.L. Roberts, K. Gupta, A.E. Stapleton, and W.E. Stamm, *Risk factors associated with acute pyelonephritis in healthy women*. Ann Intern Med, 2005. **142**(1): p. 20-27.
12. Foxman, B., *Epidemiology of urinary tract infections: incidence, morbidity, and economic costs*. Dis Mon, 2003. **49**(2): p. 53-70.
13. Ronald, A., *The etiology of urinary tract infection: traditional and emerging pathogens*. Am J Med, 2002. **113 Suppl 1A**: p. 14S-19S.
14. Jacobsen, S.M., D.J. Stickler, H.L. Mobley, and M.E. Shirtliff, *Complicated catheter-associated urinary tract infections due to Escherichia coli and Proteus mirabilis*. Clin Microbiol Rev, 2008. **21**(1): p. 26-59.
15. Yan, F. and D.B. Polk, *Commensal bacteria in the gut: learning who our friends are*. Curr Opin Gastroenterol, 2004. **20**(6): p. 565-571.

16. Kaper, J.B., J.P. Nataro, and H.L. Mobley, *Pathogenic Escherichia coli*. Nat Rev Microbiol, 2004. **2**(2): p. 123-140.
17. Russo, T.A. and J.R. Johnson, *Proposal for a new inclusive designation for extraintestinal pathogenic isolates of Escherichia coli: ExPEC*. J Infect Dis, 2000. **181**(5): p. 1753-1754.
18. Marrs, C.F., L. Zhang, and B. Foxman, *Escherichia coli mediated urinary tract infections: are there distinct uropathogenic E. coli (UPEC) pathotypes?* FEMS Microbiol Lett, 2005. **252**(2): p. 183-190.
19. Wiles, T.J., R.R. Kulesus, and M.A. Mulvey, *Origins and virulence mechanisms of uropathogenic Escherichia coli*. Exp Mol Pathol, 2008. **85**(1): p. 11-19.
20. Russo, T.A., A. Stapleton, S. Wenderoth, T.M. Hooton, and W.E. Stamm, *Chromosomal restriction fragment length polymorphism analysis of Escherichia coli strains causing recurrent urinary tract infections in young women*. J Infect Dis, 1995. **172**(2): p. 440-445.
21. Hawn, T.R., D. Scholes, H. Wang, S.S. Li, A.E. Stapleton, M. Janer, A. Aderem, W.E. Stamm, L.P. Zhao, and T.M. Hooton, *Genetic variation of the human urinary tract innate immune response and asymptomatic bacteriuria in women*. PLoS One, 2009. **4**(12): p. e8300.
22. Dielubanza, E.J. and A.J. Schaeffer, *Urinary tract infections in women*. Med Clin North Am, 2011. **95**(1): p. 27-41.
23. Trautner, B.W., R.A. Hull, and R.O. Darouiche, *Escherichia coli 83972 inhibits catheter adherence by a broad spectrum of uropathogens*. Urology, 2003. **61**(5): p. 1059-1062.

24. Darouiche, R.O., W.H. Donovan, M. Del Terzo, J.I. Thornby, D.C. Rudy, and R.A. Hull, *Pilot trial of bacterial interference for preventing urinary tract infection*. *Urology*, 2001. **58**(3): p. 339-344.
25. Hull, R., D. Rudy, W. Donovan, C. Svanborg, I. Wieser, C. Stewart, and R. Darouiche, *Urinary tract infection prophylaxis using Escherichia coli 83972 in spinal cord injured patients*. *J Urol*, 2000. **163**(3): p. 872-877.
26. Sussman, M., *Molecular medical microbiology*. 2002, San Diego: Academic Press. 3 v. (xxii, 2223, lxx p.).
27. Kaijser, B. and S. Ahlstedt, *Protective capacity of antibodies against Escherichia coli and K antigens*. *Infect Immun*, 1977. **17**(2): p. 286-289.
28. Eden, C.S., L.A. Hanson, U. Jodal, U. Lindberg, and A.S. Akerlund, *Variable adherence to normal human urinary-tract epithelial cells of Escherichia coli strains associated with various forms of urinary-tract infection*. *Lancet*, 1976. **1**(7984): p. 490-492.
29. Lindberg, U., L.A. Hanson, U. Jodal, G. Lidin-Janson, K. Lincoln, and S. Olling, *Asymptomatic bacteriuria in schoolgirls. II. Differences in Escherichia coli causing asymptomatic bacteriuria*. *Acta Paediatr Scand*, 1975. **64**(3): p. 432-436.
30. Johnson, J.R., *Virulence factors in Escherichia coli urinary tract infection*. *Clin Microbiol Rev*, 1991. **4**(1): p. 80-128.
31. Emody, L., M. Kerenyi, and G. Nagy, *Virulence factors of uropathogenic Escherichia coli*. *Int J Antimicrob Agents*, 2003. **22 Suppl 2**: p. 29-33.

32. Buchanan, K., S. Falkow, R.A. Hull, and S.I. Hull, *Frequency among Enterobacteriaceae of the DNA sequences encoding type 1 pili*. J Bacteriol, 1985. **162**(2): p. 799-803.
33. Martinez, J.J., M.A. Mulvey, J.D. Schilling, J.S. Pinkner, and S.J. Hultgren, *Type 1 pilus-mediated bacterial invasion of bladder epithelial cells*. Embo J, 2000. **19**(12): p. 2803-2812.
34. Langermann, S., S. Palaszynski, M. Barnhart, G. Auguste, J.S. Pinkner, J. Burlein, P. Barren, S. Koenig, S. Leath, C.H. Jones, and S.J. Hultgren, *Prevention of mucosal Escherichia coli infection by FimH-adhesin-based systemic vaccination*. Science, 1997. **276**(5312): p. 607-611.
35. Arthur, M., C.E. Johnson, R.H. Rubin, R.D. Arbeit, C. Campanelli, C. Kim, S. Steinbach, M. Agarwal, R. Wilkinson, and R. Goldstein, *Molecular epidemiology of adhesin and hemolysin virulence factors among uropathogenic Escherichia coli*. Infect Immun, 1989. **57**(2): p. 303-313.
36. Svanborg Eden, C. and P. de Man, *Bacterial virulence in urinary tract infection*. Infect Dis Clin North Am, 1987. **1**(4): p. 731-750.
37. Mulvey, M.A., Y.S. Lopez-Boado, C.L. Wilson, R. Roth, W.C. Parks, J. Heuser, and S.J. Hultgren, *Induction and evasion of host defenses by type 1-piliated uropathogenic Escherichia coli*. Science, 1998. **282**(5393): p. 1494-1497.
38. Plos, K., H. Connell, U. Jodal, B.I. Marklund, S. Marild, B. Wettergren, and C. Svanborg, *Intestinal carriage of P fimbriated Escherichia coli and the susceptibility to urinary tract infection in young children*. J Infect Dis, 1995. **171**(3): p. 625-631.

39. Apodaca, G., *The uroepithelium: not just a passive barrier*. Traffic, 2004. **5**(3): p. 117-128.
40. Agace, W.W., S.R. Hedges, M. Ceska, and C. Svanborg, *Interleukin-8 and the neutrophil response to mucosal Gram-negative infection*. J Clin Invest, 1993. **92**(2): p. 780-785.
41. Hannan, T.J., M. Totsika, K.J. Mansfield, K.H. Moore, M.A. Schembri, and S.J. Hultgren, *Host-pathogen checkpoints and population bottlenecks in persistent and intracellular uropathogenic Escherichia coli bladder infection*. FEMS Microbiol Rev, 2012. **36**(3): p. 616-648.
42. Thanassi, D.G., E.T. Saulino, and S.J. Hultgren, *The chaperone/usher pathway: a major terminal branch of the general secretory pathway*. Curr Opin Microbiol, 1998. **1**(2): p. 223-231.
43. Bullitt, E. and L. Makowski, *Structural polymorphism of bacterial adhesion pili*. Nature, 1995. **373**(6510): p. 164-167.
44. Sauer, F.G., H. Remaut, S.J. Hultgren, and G. Waksman, *Fiber assembly by the chaperone-usher pathway*. Biochim Biophys Acta, 2004. **1694**(1-3): p. 259-267.
45. Remaut, H., C. Tang, N.S. Henderson, J.S. Pinkner, T. Wang, S.J. Hultgren, D.G. Thanassi, G. Waksman, and H. Li, *Fiber formation across the bacterial outer membrane by the chaperone/usher pathway*. Cell, 2008. **133**(4): p. 640-652.
46. Waksman, G. and S.J. Hultgren, *Structural biology of the chaperone-usher pathway of pilus biogenesis*. Nat Rev Microbiol, 2009. **7**(11): p. 765-774.

47. Kuehn, M.J., J. Heuser, S. Normark, and S.J. Hultgren, *P pili in uropathogenic E. coli are composite fibres with distinct fibrillar adhesive tips*. Nature, 1992. **356**(6366): p. 252-255.
48. Gong, M. and L. Makowski, *Helical structure of P pili from Escherichia coli. Evidence from X-ray fiber diffraction and scanning transmission electron microscopy*. J Mol Biol, 1992. **228**(3): p. 735-742.
49. Baga, M., M. Norgren, and S. Normark, *Biogenesis of E. coli Pap pili: papH, a minor pilin subunit involved in cell anchoring and length modulation*. Cell, 1987. **49**(2): p. 241-251.
50. Verger, D., E. Miller, H. Remaut, G. Waksman, and S. Hultgren, *Molecular mechanism of P pilus termination in uropathogenic Escherichia coli*. EMBO Rep, 2006. **7**(12): p. 1228-1232.
51. Lund, B., F. Lindberg, B.I. Marklund, and S. Normark, *The PapG protein is the alpha-D-galactopyranosyl-(1----4)-beta-D-galactopyranose-binding adhesin of uropathogenic Escherichia coli*. Proc Natl Acad Sci U S A, 1987. **84**(16): p. 5898-5902.
52. Jacob-Dubuisson, F., J. Heuser, K. Dodson, S. Normark, and S. Hultgren, *Initiation of assembly and association of the structural elements of a bacterial pilus depend on two specialized tip proteins*. Embo J, 1993. **12**(3): p. 837-847.
53. Hull, R.A., R.E. Gill, P. Hsu, B.H. Minshew, and S. Falkow, *Construction and expression of recombinant plasmids encoding type 1 or D-mannose-resistant pili from a urinary tract infection Escherichia coli isolate*. Infect Immun, 1981. **33**(3): p. 933-938.

54. Jones, C.H., J.S. Pinkner, R. Roth, J. Heuser, A.V. Nicholes, S.N. Abraham, and S.J. Hultgren, *FimH adhesin of type 1 pili is assembled into a fibrillar tip structure in the Enterobacteriaceae*. Proc Natl Acad Sci U S A, 1995. **92**(6): p. 2081-2085.
55. Silhavy, T.J., D. Kahne, and S. Walker, *The bacterial cell envelope*. Cold Spring Harb Perspect Biol, 2010. **2**(5): p. a000414.
56. Dwyer, M.A. and H.W. Hellinga, *Periplasmic binding proteins: a versatile superfamily for protein engineering*. Curr Opin Struct Biol, 2004. **14**(4): p. 495-504.
57. Felder, C.B., R.C. Graul, A.Y. Lee, H.P. Merkle, and W. Sadee, *The Venus flytrap of periplasmic binding proteins: an ancient protein module present in multiple drug receptors*. AAPS PharmSci, 1999. **1**(2): p. E2.
58. Spiess, C., A. Beil, and M. Ehrmann, *A temperature-dependent switch from chaperone to protease in a widely conserved heat shock protein*. Cell, 1999. **97**(3): p. 339-347.
59. Kamio, Y. and H. Nikaido, *Outer membrane of Salmonella typhimurium: accessibility of phospholipid head groups to phospholipase c and cyanogen bromide activated dextran in the external medium*. Biochemistry, 1976. **15**(12): p. 2561-2570.
60. Nikaido, H., *Molecular basis of bacterial outer membrane permeability revisited*. Microbiol Mol Biol Rev, 2003. **67**(4): p. 593-656.

61. Sankaran, K. and H.C. Wu, *Lipid modification of bacterial prolipoprotein. Transfer of diacylglyceryl moiety from phosphatidylglycerol*. J Biol Chem, 1994. **269**(31): p. 19701-19706.
62. Okuda, S. and H. Tokuda, *Lipoprotein sorting in bacteria*. Annu Rev Microbiol, 2011. **65**: p. 239-259.
63. Nikaido, H., *Multiple antibiotic resistance and efflux*. Curr Opin Microbiol, 1998. **1**(5): p. 516-523.
64. Raetz, C.R. and C. Whitfield, *Lipopolysaccharide endotoxins*. Annu Rev Biochem, 2002. **71**: p. 635-700.
65. Delcour, A.H., *Outer membrane permeability and antibiotic resistance*. Biochim Biophys Acta, 2009. **1794**(5): p. 808-816.
66. Heinrichs, D.E., J.A. Yethon, and C. Whitfield, *Molecular basis for structural diversity in the core regions of the lipopolysaccharides of Escherichia coli and Salmonella enterica*. Mol Microbiol, 1998. **30**(2): p. 221-232.
67. Kostakioti, M., C.L. Newman, D.G. Thanassi, and C. Stathopoulos, *Mechanisms of protein export across the bacterial outer membrane*. J Bacteriol, 2005. **187**(13): p. 4306-4314.
68. Ruiz, N., D. Kahne, and T.J. Silhavy, *Advances in understanding bacterial outer-membrane biogenesis*. Nat Rev Microbiol, 2006. **4**(1): p. 57-66.
69. Randall, L.L. and S.J. Hardy, *SecB, one small chaperone in the complex milieu of the cell*. Cell Mol Life Sci, 2002. **59**(10): p. 1617-1623.

70. Papanikou, E., S. Karamanou, and A. Economou, *Bacterial protein secretion through the translocase nanomachine*. Nat Rev Microbiol, 2007. **5**(11): p. 839-851.
71. Paetzel, M., A. Karla, N.C. Strynadka, and R.E. Dalbey, *Signal peptidases*. Chem Rev, 2002. **102**(12): p. 4549-4580.
72. Koronakis, V., A. Sharff, E. Koronakis, B. Luisi, and C. Hughes, *Crystal structure of the bacterial membrane protein TolC central to multidrug efflux and protein export*. Nature, 2000. **405**(6789): p. 914-919.
73. Touze, T., J. Eswaran, E. Bokma, E. Koronakis, C. Hughes, and V. Koronakis, *Interactions underlying assembly of the Escherichia coli AcrAB-TolC multidrug efflux system*. Mol Microbiol, 2004. **53**(2): p. 697-706.
74. Blight, M.A. and I.B. Holland, *Heterologous protein secretion and the versatile Escherichia coli haemolysin translocator*. Trends Biotechnol, 1994. **12**(11): p. 450-455.
75. Koronakis, V., J. Eswaran, and C. Hughes, *Structure and function of TolC: the bacterial exit duct for proteins and drugs*. Annu Rev Biochem, 2004. **73**: p. 467-489.
76. Korotkov, K.V., M. Sandkvist, and W.G. Hol, *The type II secretion system: biogenesis, molecular architecture and mechanism*. Nat Rev Microbiol, 2012. **10**(5): p. 336-351.
77. Nouwen, N., N. Ranson, H. Saibil, B. Wolpensinger, A. Engel, A. Ghazi, and A.P. Pugsley, *Secretin PulD: association with pilot PulS, structure, and ion-*

- conducting channel formation*. Proc Natl Acad Sci U S A, 1999. **96**(14): p. 8173-8177.
78. Galan, J.E. and A. Collmer, *Type III secretion machines: bacterial devices for protein delivery into host cells*. Science, 1999. **284**(5418): p. 1322-1328.
79. Alvarez-Martinez, C.E. and P.J. Christie, *Biological diversity of prokaryotic type IV secretion systems*. Microbiol Mol Biol Rev, 2009. **73**(4): p. 775-808.
80. Christie, P.J., *Structural biology: Translocation chamber's secrets*. Nature, 2009. **462**(7276): p. 992-994.
81. Chandran, V., R. Fronzes, S. Duquerroy, N. Cronin, J. Navaza, and G. Waksman, *Structure of the outer membrane complex of a type IV secretion system*. Nature, 2009. **462**(7276): p. 1011-1015.
82. Thanassi, D.G., C. Stathopoulos, A. Karkal, and H. Li, *Protein secretion in the absence of ATP: the autotransporter, two-partner secretion and chaperone/usher pathways of Gram-negative bacteria (review)*. Mol Membr Biol, 2005. **22**(1-2): p. 63-72.
83. Jacob-Dubuisson, F., R. Fernandez, and L. Coutte, *Protein secretion through autotransporter and two-partner pathways*. Biochim Biophys Acta, 2004. **1694**(1-3): p. 235-257.
84. Jacob-Dubuisson, F., C. El-Hamel, N. Saint, S. Guedin, E. Willery, G. Molle, and C. Locht, *Channel formation by FhaC, the outer membrane protein involved in the secretion of the Bordetella pertussis filamentous hemagglutinin*. J Biol Chem, 1999. **274**(53): p. 37731-37735.

85. Jacob-Dubuisson, F., V. Villeret, B. Clantin, A.S. Delattre, and N. Saint, *First structural insights into the TpsB/Omp85 superfamily*. Biol Chem, 2009. **390**(8): p. 675-684.
86. Klemm, P. and G. Christiansen, *The fimD gene required for cell surface localization of Escherichia coli type 1 fimbriae*. Mol Gen Genet, 1990. **220**(2): p. 334-338.
87. Holmgren, A. and C.I. Branden, *Crystal structure of chaperone protein PapD reveals an immunoglobulin fold*. Nature, 1989. **342**(6247): p. 248-251.
88. Thanassi, D.G., E.T. Saulino, M.J. Lombardo, R. Roth, J. Heuser, and S.J. Hultgren, *The PapC usher forms an oligomeric channel: implications for pilus biogenesis across the outer membrane*. Proc Natl Acad Sci U S A, 1998. **95**(6): p. 3146-3151.
89. Nikaido, H., K. Nikaido, and S. Harayama, *Identification and characterization of porins in Pseudomonas aeruginosa*. J Biol Chem, 1991. **266**(2): p. 770-779.
90. Sugawara, E. and H. Nikaido, *Pore-forming activity of OmpA protein of Escherichia coli*. J Biol Chem, 1992. **267**(4): p. 2507-2511.
91. Li, Q., T.W. Ng, K.W. Dodson, S.S. So, K.M. Bayle, J.S. Pinkner, S. Scarlata, S.J. Hultgren, and D.G. Thanassi, *The differential affinity of the usher for chaperone-subunit complexes is required for assembly of complete pili*. Mol Microbiol, 2010. **76**(1): p. 159-172.
92. Sauer, F.G., J.S. Pinkner, G. Waksman, and S.J. Hultgren, *Chaperone priming of pilus subunits facilitates a topological transition that drives fiber formation*. Cell, 2002. **111**(4): p. 543-551.

93. Zavialov, A.V., J. Berglund, A.F. Pudney, L.J. Fooks, T.M. Ibrahim, S. MacIntyre, and S.D. Knight, *Structure and biogenesis of the capsular F1 antigen from Yersinia pestis: preserved folding energy drives fiber formation*. Cell, 2003. **113**(5): p. 587-596.
94. Jacob-Dubuisson, F., R. Striker, and S.J. Hultgren, *Chaperone-assisted self-assembly of pili independent of cellular energy*. J Biol Chem, 1994. **269**(17): p. 12447-12455.
95. Dodson, K.W., F. Jacob-Dubuisson, R.T. Striker, and S.J. Hultgren, *Outer-membrane PapC molecular usher discriminately recognizes periplasmic chaperone-pilus subunit complexes*. Proc Natl Acad Sci U S A, 1993. **90**(8): p. 3670-3674.
96. Saulino, E.T., E. Bullitt, and S.J. Hultgren, *Snapshots of usher-mediated protein secretion and ordered pilus assembly*. Proc Natl Acad Sci U S A, 2000. **97**(16): p. 9240-9245.
97. Ng, T.W., L. Akman, M. Osisami, and D.G. Thanassi, *The usher N terminus is the initial targeting site for chaperone-subunit complexes and participates in subsequent pilus biogenesis events*. J Bacteriol, 2004. **186**(16): p. 5321-5331.
98. Nishiyama, M., R. Horst, O. Eidam, T. Herrmann, O. Ignatov, M. Vetsch, P. Bettendorff, I. Jelesarov, M.G. Grutter, K. Wuthrich, R. Glockshuber, and G. Capitani, *Structural basis of chaperone-subunit complex recognition by the type I pilus assembly platform FimD*. Embo J, 2005. **24**(12): p. 2075-2086.
99. Nishiyama, M., M. Vetsch, C. Puorger, I. Jelesarov, and R. Glockshuber, *Identification and characterization of the chaperone-subunit complex-binding*

- domain from the type 1 pilus assembly platform FimD*. J Mol Biol, 2003. **330**(3): p. 513-525.
100. Phan, G., H. Remaut, T. Wang, W.J. Allen, K.F. Pirker, A. Lebedev, N.S. Henderson, S. Geibel, E. Volkan, J. Yan, M.B. Kunze, J.S. Pinkner, B. Ford, C.W. Kay, H. Li, S.J. Hultgren, D.G. Thanassi, and G. Waksman, *Crystal structure of the FimD usher bound to its cognate FimC-FimH substrate*. Nature, 2011. **474**(7349): p. 49-53.
101. Volkan, E., B.A. Ford, J.S. Pinkner, K.W. Dodson, N.S. Henderson, D.G. Thanassi, G. Waksman, and S.J. Hultgren, *Domain activities of PapC usher reveal the mechanism of action of an Escherichia coli molecular machine*. Proc Natl Acad Sci U S A, 2012. **109**(24): p. 9563-9568.
102. St Geme, J.W., 3rd and S. Grass, *Secretion of the Haemophilus influenzae HMW1 and HMW2 adhesins involves a periplasmic intermediate and requires the HMWB and HMWC proteins*. Mol Microbiol, 1998. **27**(3): p. 617-630.
103. Duret, G., M. Szymanski, K.J. Choi, H.J. Yeo, and A.H. Delcour, *The TpsB translocator HMW1B of haemophilus influenzae forms a large conductance channel*. J Biol Chem, 2008. **283**(23): p. 15771-15778.
104. Huang, Y., B.S. Smith, L.X. Chen, R.H. Baxter, and J. Deisenhofer, *Insights into pilus assembly and secretion from the structure and functional characterization of usher PapC*. Proc Natl Acad Sci U S A, 2009. **106**(18): p. 7403-7407.
105. Grant, S.G., J. Jessee, F.R. Bloom, and D. Hanahan, *Differential plasmid rescue from transgenic mouse DNAs into Escherichia coli methylation-restriction mutants*.

- 10.1073/pnas.87.12.4645. Proceedings of the National Academy of Sciences, 1990.
87(12): p. 4645-4649.
106. Prilipov, A., P.S. Phale, P. Van Gelder, J.P. Rosenbusch, and R. Koebnik, *Coupling site-directed mutagenesis with high-level expression: large scale production of mutant porins from E. coli*. FEMS Microbiol Lett, 1998. **163**(1): p. 65-72.
107. Li, H., L. Qian, Z. Chen, D. Thibault, G. Liu, T. Liu, and D.G. Thanassi, *The outer membrane usher forms a twin-pore secretion complex*. J Mol Biol, 2004. **344**(5): p. 1397-1407.
108. Mappingire, O.S., N.S. Henderson, G. Duret, D.G. Thanassi, and A.H. Delcour, *Modulating effects of the plug, helix, and N- and C-terminal domains on channel properties of the PapC usher*. J Biol Chem, 2009. **284**(52): p. 36324-36333.
109. Chiu, J., D. Tillett, I.W. Dawes, and P.E. March, *Site-directed, Ligase-Independent Mutagenesis (SLIM) for highly efficient mutagenesis of plasmids greater than 8kb*. J Microbiol Methods, 2008. **73**(2): p. 195-198.
110. Dombkowski, A.A., *Disulfide by Design: a computational method for the rational design of disulfide bonds in proteins*. Bioinformatics, 2003. **19**(14): p. 1852-1853.
111. Dani, V.S., C. Ramakrishnan, and R. Varadarajan, *MODIP revisited: re-evaluation and refinement of an automated procedure for modeling of disulfide bonds in proteins*. Protein Eng, 2003. **16**(3): p. 187-193.
112. Henderson, N.S., S.S. So, C. Martin, R. Kulkarni, and D.G. Thanassi, *Topology of the outer membrane usher PapC determined by site-directed fluorescence labeling*. J Biol Chem, 2004. **279**(51): p. 53747-53754.

113. Saulino, E.T., D.G. Thanassi, J.S. Pinkner, and S.J. Hultgren, *Ramifications of kinetic partitioning on usher-mediated pilus biogenesis*. *Embo J*, 1998. **17**(8): p. 2177-2185.
114. Jones, C.H., P.N. Danese, J.S. Pinkner, T.J. Silhavy, and S.J. Hultgren, *The chaperone-assisted membrane release and folding pathway is sensed by two signal transduction systems*. *Embo J*, 1997. **16**(21): p. 6394-6406.
115. Montal, M. and P. Mueller, *Formation of bimolecular membranes from lipid monolayers and a study of their electrical properties*. *Proc Natl Acad Sci U S A*, 1972. **69**(12): p. 3561-3566.
116. Delcour, A.H., B. Martinac, J. Adler, and C. Kung, *Modified reconstitution method used in patch-clamp studies of Escherichia coli ion channels*. *Biophys J*, 1989. **56**(3): p. 631-636.
117. Roberts, J.A., B.I. Marklund, D. Ilver, D. Haslam, M.B. Kaack, G. Baskin, M. Louis, R. Mollby, J. Winberg, and S. Normark, *The Gal(alpha 1-4)Gal-specific tip adhesin of Escherichia coli P-fimbriae is needed for pyelonephritis to occur in the normal urinary tract*. *Proc Natl Acad Sci U S A*, 1994. **91**(25): p. 11889-11893.
118. Lindberg, F., J.M. Tennent, S.J. Hultgren, B. Lund, and S. Normark, *PapD, a periplasmic transport protein in P-pilus biogenesis*. *J Bacteriol*, 1989. **171**(11): p. 6052-6058.
119. Norgren, M., M. Baga, J.M. Tennent, and S. Normark, *Nucleotide sequence, regulation and functional analysis of the papC gene required for cell surface*

- localization of Pap pili of uropathogenic Escherichia coli.* Mol Microbiol, 1987. **1**(2): p. 169-178.
120. Ford, B., A.T. Rego, T.J. Ragan, J. Pinkner, K. Dodson, P.C. Driscoll, S. Hultgren, and G. Waksman, *Structural homology between the C-terminal domain of the PapC usher and its plug.* J Bacteriol, 2010. **192**(7): p. 1824-1831.
121. Brok, R., P. Van Gelder, M. Winterhalter, U. Ziese, A.J. Koster, H. de Cock, M. Koster, J. Tommassen, and W. Bitter, *The C-terminal domain of the Pseudomonas secretin XcpQ forms oligomeric rings with pore activity.* J Mol Biol, 1999. **294**(5): p. 1169-1179.
122. Burghout, P., R. van Boxtel, P. Van Gelder, P. Ringler, S.A. Muller, J. Tommassen, and M. Koster, *Structure and electrophysiological properties of the YscC secretin from the type III secretion system of Yersinia enterocolitica.* J Bacteriol, 2004. **186**(14): p. 4645-4654.
123. Bitter, W., *Secretins of Pseudomonas aeruginosa: large holes in the outer membrane.* Arch Microbiol, 2003. **179**(5): p. 307-314.
124. Capitani, G., O. Eidam, R. Glockshuber, and M.G. Grutter, *Structural and functional insights into the assembly of type I pili from Escherichia coli.* Microbes Infect, 2006. **8**(8): p. 2284-2290.
125. Sauer, F.G., K. Futterer, J.S. Pinkner, K.W. Dodson, S.J. Hultgren, and G. Waksman, *Structural basis of chaperone function and pilus biogenesis.* Science, 1999. **285**(5430): p. 1058-1061.
126. Basle, A., R. Iyer, and A.H. Delcour, *Subconductance states in OmpF gating.* Biochim Biophys Acta, 2004. **1664**(1): p. 100-107.

127. Kobashi, K., *Catalytic oxidation of sulfhydryl groups by o-phenanthroline copper complex*. Biochim Biophys Acta, 1968. **158**(2): p. 239-245.
128. Thanassi, D.G., C. Stathopoulos, K. Dodson, D. Geiger, and S.J. Hultgren, *Bacterial outer membrane ushers contain distinct targeting and assembly domains for pilus biogenesis*. J Bacteriol, 2002. **184**(22): p. 6260-6269.
129. So, S.S. and D.G. Thanassi, *Analysis of the requirements for pilus biogenesis at the outer membrane usher and the function of the usher C-terminus*. Mol Microbiol, 2006. **60**(2): p. 364-375.
130. Gupta, K., T.M. Hooton, and W.E. Stamm, *Increasing antimicrobial resistance and the management of uncomplicated community-acquired urinary tract infections*. Ann Intern Med, 2001. **135**(1): p. 41-50.